*Response to Reviewer 4

Chemical Engineering Journal
Manuscript Draft

Manuscript Number: CEJ-D-19-16168

Title: Modeling persulfate activated by iron and heat: removal in water of contaminants of emerging concern

Article Type: Research Paper

Section/Category: Environmental Chemical Engineering

Keywords: carbamazepine, microcontaminants, tertiary treatment, kinetics, wastewater

Abstract: A semi-empirical model of the heat-activated and iron-activated persulfate processes applied to the removal of carbamazepine in water at low concentration (0.0025 mM) has been proposed and validated. In the heat-activation experimental series that was carried out at pH 3 varying temperature from 25°C to 65°C, acid-activation of persulfate showed an important initial role in the process. For the iron-activated experimental series in which iron concentration was changed from 0.5 mg/L to 10 mg/L and two temperatures were also studied (25°C and 35°C), heat-activation was negligible with iron being the main activation mechanism and acid-activation showing also an important initial effect on process performance. The model prediction capability for both carbamazepine degradation and persulfate decomposition profiles was high in each cases. Finally, the model was validated including supplementary experiments based on Fe(II) additions (1 mg/L each at 0, 10 and 20 min) and persulfate additions (0.17 mM each at 0, 10 and 20 min) throughout the treatment. The developed model is a powerful predictive tool for the application of persulfate in the removal of contaminants of emerging concern in water.

Summary of Comments on CEJ-D-19-16168 annotated.pdf

This page contains no comments

Graphical Abstract

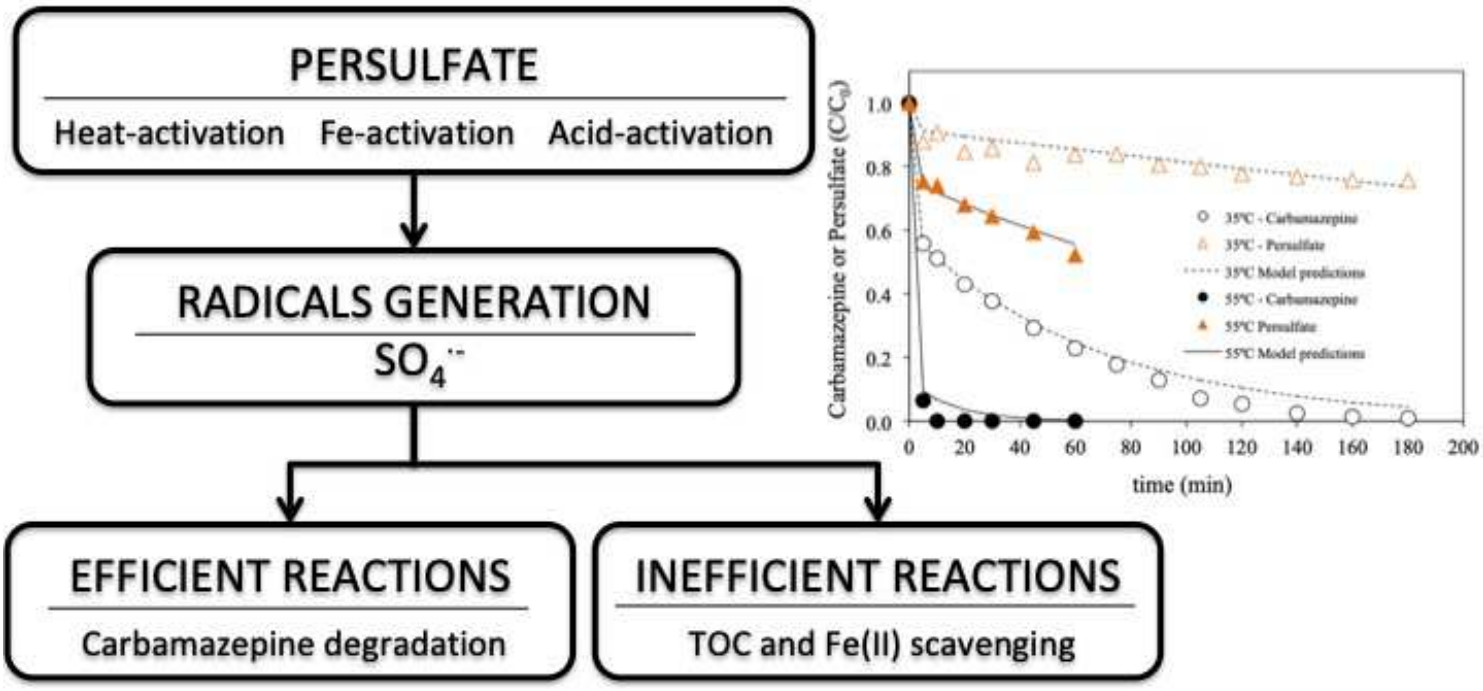

This page contains no comments

Highlights

- A semi-empirical model of heat and iron activation of persulfate was developed
- Persulfate acid activation showed an important role at the begining of the process
- An excess of iron favoured radicals scavenging
- Good agreement between experimental data and model predictions was always obtained
- Model was validated with additional assays based on iron and persulfate additions

This page contains no comments

Modeling persulfate activated by iron and heat: removal in water of contaminants of emerging concern

Cabrera-Reina, A.[1], Miralles-Cuevas, S.[2,3], Oller, I.[3,4], Sánchez-Pérez, J.A.[2,3], Malato, S.[3,4]

[1] Engineering Faculty, University of Tarapacá, Avda. General Velásquez, Arica, Chile
[2] Chemical Engineering Department, University of Almería, Ctra. Sacramento s/n, Almería, Spain
[3] CIESOL, Joint Centre of the University of Almería-CIEMAT, Ctra. Sacramento s/n, Almería Spain
[4] Plataforma Solar de Almeria-CIEMAT, Carretera de Senés, km 4, Tabernas, Spain

Corresponding authors: Cabrera-Reina, A. (acabrera@limza.cl)

Oller, I. (isabel.oller@psa.es)

Abstract

A semi-empirical model of the heat-activated and iron-activated persulfate processes applied to the removal of carbamazepine in water at low concentration (0.0025 mM) has been proposed and validated. In the heat-activation ~~experimental series~~ [1] that ~~was~~ [2] carried out at pH 3 varying temperature from 25ºC to 65ºC, acid-activation of persulfate showed an important initial role in the process. For the iron-activated experimental series in which iron concentration was changed from 0.5 mg/L to 10 mg/L ~~and~~ [4] two temperatures [5] [3] ~~were also studied~~ (25ºC and 35ºC), heat-activation was negligible with iron being the main activation mechanism and acid-activation showing also an important initial effect on process performance. The model prediction capability for both carbamazepine degradation and persulfate decomposition profiles was high in each cases. Finally, the model was validated including supplementary experiments based on Fe(II) additions (1 mg/L each at 0, 10 and 20 min) and $S_2O_8^{2-}$ additions (0.17 mM each at 0, 10 and 20 min) throughout the treatment. The developed model is a powerful predictive tool for the application of persulfate in the removal of contaminants of emerging concern in water.

Keywords: carbamazepine, microcontaminants, tertiary treatment, kinetics, wastewater

Page: 4

Number: 1 Author: Subject: Inserted Text Date: 1/2/20, 10:40:44 AM
systems

Status
AlexCabrera Completed 1/28/20, 11:39:54 PM

Number: 2 Author: Subject: Inserted Text Date: 1/2/20, 10:40:44 AM
were

Status
AlexCabrera Completed 1/28/20, 11:39:50 PM

Number: 3 Author: Alejandro Cabrera Reina Subject: Cross-Out Date: Indeterminate

Status
AlexCabrera Completed 1/28/20, 11:39:44 PM

Number: 4 Author: Subject: Inserted Text Date: 1/2/20, 10:40:44 AM
at

Status
AlexCabrera Completed 1/28/20, 11:41:44 PM

Number: 5 Author: Subject: Inserted Text Date: 1/2/20, 10:40:44 AM
different

Status
AlexCabrera Completed 1/28/20, 11:41:49 PM

1. Introduction

Contaminants of emerging concern (CECs) are unregulated substances that enter the environment at low concentrations, among others, through municipal wastewater treatment plants (MWWTP) because biological systems were not designed for their removal [1]. Their properties make CECs highly risky for the environment and human health as they are bio-accumulative substances, very persistent in the environment and, at the same time, show a great capacity for transformation, generating intermediate products, such as metabolites, which, in many occasions, are more toxic than the parent compounds [2]. Personal care products, antiseptics, detergents and their metabolites, gasoline additives and industrial agents, among others, are considered as CECs [3]. Nevertheless, the ones that are possibly causing the greatest concern are the pharmaceutical products and, in particular, antibiotics [4]. The use of pharmaceutical products in European Union countries has been estimated of thousands of tons per year, and the majority of the most consumed, including antibiotics, are used in amounts similar to those of pesticides. Indeed, the presence of more than 3,000 pharmaceuticals in the aquatic environment has been already reported by Roig 2010 [5]. In this study, the carbamazepine was selected as CEC model because it is a bio-recalcitrant microcontaminant that is not efficiently removed by MWWTPs and usually reaches water bodies. According to Zhang et al. 2008 [6], carbamazepine has been detected in MWWTP effluents and surface waters around the world, as happens in Germany where it has been found at concentrations of around 3 µg/L in MWWTP effluents and 0.5 µg/L in surface waters. Moreover, according to several researchers, this pollutant is frequently detected in surface water, groundwater and even in drinking water at ng/L- µg/L levels [3, 7-10]. Therefore, it is a good indicator for following the performance of an advanced tertiary treatment to polish the effluent from conventional MWWTPs.

Page: 5

Number: 1 Author: Subject: Inserted Text Date: 1/2/20, 10:40:44 AM

CBZ was also considered as typical pharmaceutical active ingredient by some researchers for degradation through AOPs systems using improved methods such as ultrasonication in combination with iron particles and hydrogen peroxide [ref]
ref
Degradation of aqueous carbamazepine in ultrasonic/Fe0/H2O2 systems
Chemical Engineering Journal 172 (1), 18-27 2011

Status
AlexCabrera Completed 1/28/20, 11:42:01 PM

Author: AlexCabrera Subject: Nota adhesiva Date: 1/29/20, 2:19:20 PM

Done

To prevent the entry of these CECs into the environment and also to achieve good water-reuse quality, an advanced tertiary treatment must be proposed and carried out as a final step in the treatment of MWWTP effluents. In recent years, sulfate radical-based advanced oxidation processes ($SO_4^{\bullet-}$-AOPs) applied to the removal of CECs are being investigated as an alternative to AOPs only based on the generation of hydroxyl radicals [11]. Sulfate radical has a high oxidation potential (E°=2.6 V), similar to hydroxyl radical (E°=2.8 V), is very efficient to CECs degradation at low concentrations and environmentally friendly [12-14]. Persulfate activation to form highly reactive species can be achieved by many different mechanisms: UV light [15], thermal energy [16], acidic and alkaline conditions [17] or transition metals such as silver, iron, copper, zinc [18]. In this way, the feasibility of $SO_4^{\bullet-}$-AOPs for CEC abatement has already been proven, furthermore, several investigations about kinetics, degradation mechanism of different contaminants and the effect of water matrix on process performance have been reported [14, 19-21]. In this context, research should move forward to applications at pilot plant scale and, consequently, modelling studies are needed. Few studies about persulfate modelling can be found in the literature. Kusic et al. 2011 [22] developed a first principle mathematical model to predict decolorization of Reactive Red 45 and mineralization using persulfate activated via zerovalent iron and ferrous sulfate both under dark and UV light conditions. Besides, persulfate was compared to H_2O_2 addition using 80 mg/L of Reactive Red 45 as initial pollutant load (≈32 mg/L of total organic carbon -TOC-). The reaction scheme included 12 bulk Fenton reactions, 14 surface Fenton reactions, 11 inorganic bulk reactions related to H_2O_2, 3 bulk iron/persulfate reactions, 5 surface iron/persulfate reactions, 6 inorganic bulk reactions related to $S_2O_8^{2-}$, 6 photo-induced reactions and 8 pollutant degradation reactions. Selecting the corresponding reactions from this group, different models for direct UV

Page: 6

Number: 1 Author: Subject: Comment on Text Date: 1/2/20, 10:40:44 AM

references should more focus on pharmaceuticals rather than pesticides as this paper is for the removal and degradation of carbamazepine. Some suggested references to consider on pharmaceuticals degradation:
UV light
Contribution of persulfate in UV-254 nm activated systems for complete degradation of chloramphenicol antibiotic in water
Chemical Engineering Journal 317, 1012-1025 2017
Degradation of theophylline in a UV254/PS system: Matrix effect and application to a factory effluent
Chemical Engineering Journal 380, 122478 2020

Status
AlexCabrera Completed 1/28/20, 11:42:08 PM

Author: AlexCabrera Subject: Nota adhesiva Date: 1/28/20, 10:41:12 PM

Following the reviewer suggestion, new references focused on pharmaceuticals have been included in the document.

Number: 2 Author: Subject: Comment on Text Date: 1/2/20, 10:40:44 AM

same comment as before
suggested references to consider for the application of persulfate heat systems on pharmaceutical removal:
A comparative study of the common persulfate activation techniques for the complete degradation of an NSAID: The case of Ketoprofen
Chemical Engineering Journal 350, 395-410 39 2018
Naproxen abatement by thermally activated persulfate in aqueous systems
Chemical Engineering Journal 279, 861-873 2015
Ibuprofen removal by heated persulfate in aqueous solution: a kinetics study
Chemical engineering journal 197, 483-492 2012
Oxidation of bisoprolol in heated persulfate/H2O systems: kinetics and products
Chemical Engineering Journal 183, 162-171 2012

Status
AlexCabrera Completed 1/28/20, 11:42:16 PM

Author: AlexCabrera Subject: Nota adhesiva Date: 1/28/20, 10:43:08 PM

As suggested by the Reviewer, new references for each PS activation mechanism in which pharmaceuticals have been used as model pollutant have included in the manuscript.

Number: 3 Author: Subject: Inserted Text Date: 1/2/20, 10:40:44 AM

in homogeneous as well as in heterogeneous media.

Status
AlexCabrera Completed 1/28/20, 11:42:23 PM

Author: AlexCabrera Subject: Nota adhesiva Date: 1/29/20, 2:19:47 PM

Done

Number: 4 Author: Subject: Inserted Text Date: 1/2/20, 10:40:44 AM

based

Status
AlexCabrera Completed 1/28/20, 11:42:32 PM

Number: 5 Author: Subject: Inserted Text Date: 1/2/20, 10:40:44 AM

in the form of dissolved salts in solution or zero valent metals being monometallic or bi/trimetallics iron based systems. Those are commercial or scrap waste collected from the car industry.
references to consider
zero valent iron
Degradation of sulfamethoxazole by persulfate assisted micrometric Fe0 in aqueous solution
Chemical Engineering Journal 228, 1168-1181 2013
Assessment of bimetallic and trimetallic iron-based systems for persulfate activation: application to sulfamethoxazole degradation
Chemical Engineering Journal 256, 280-292 2014
Ranitidine abatement in chemically activated persulfate systems: assessment of industrial iron waste for sustainable applications
Chemical Engineering Journal 288, 276-288 2016

Status
AlexCabrera Completed 1/28/20, 11:42:44 PM

Author: AlexCabrera Subject: Nota adhesiva Date: 1/29/20, 2:20:01 PM

Done

Number: 6 Author: Subject: Inserted Text Date: 1/2/20, 10:40:44 AM

e.g.

Status
AlexCabrera Completed 1/28/20, 11:42:53 PM

photolysis, UV/ H_2O_2, UV/$S_2O_8^{2-}$, Fe^{2+}/H_2O_2, UV/Fe^{2+}/H_2O_2, Fe^0/H_2O_2, UV/Fe^0/H_2O_2, UV/$Fe^{2+}/S_2O_8^{2-}$, $Fe^{2+}/S_2O_8^{2-}$, $Fe^0/S_2O_8^{2-}$ and UV/$Fe^0/S_2O_8^{2-}$ were proposed. Bu et al., 2017 [23] reported the modelling of Fe(II)-activated persulfate for the removal of atrazine at different initial concentrations. A first principle model based on 26 reactions including the influence of tertiary butanol, methanol and natural organic matter on process performance was used. Lominchar et al. 2018 [19] proposed a simplified reaction mechanism to model phenol abatement by alkaline-activated (pH 12) persulfate. Good agreement between experimental data and model simulations was found, being the model able to accurately predict the evolution of phenol, persulfate, hydroquinone and catechol. Another modelling work was carried out by Rodriguez et al. 2017 [24], who studied the removal of diuron, caffeine and ibuprofen at concentrations in the range from 0.086 mM to 0.129 mM by zerovalent iron-activated persulfate. An interesting semi-empirical modelling approach based on only 7 general reactions was proposed, capable of describing the evolution of pollutant, oxidant agent, iron concentrations and mineralization. All the reported studies considered an extremely higher concentration of target pollutants compared to the actual concentration of microcontaminants that can be found in MWWTP effluents.

The aim of the present work was to develop a general mathematical model under a semi-empirical approach of the heat-activated and iron-activated persulfate processes when these are applied to the removal of CECs. In this sense, carbamazepine dissolved in water at very low concentration (0.0025 mM), closer to actual conditions, was used as model pollutant. In a first experimental series, a heat-activation persulfate model was proposed for a temperature range from 25ºC to 65ºC. In the second part of the study, a complementary model was implemented for persulfate activated by iron in concentrations from 0.009 mM

This page contains no comments

to 0.18 mM at 25ºC and 35ºC. Finally, the model was validated including supplementary experiments based on iron and persulfate additions carried out throughout the treatment.

2. Materials and Methods

2.1 Chemicals and reagents

Carbamazepine (standard quality, 99%), acetonitrile (HPLC-grade), ferrous sulfate heptahydrate ($FeSO_4 \cdot 7H_2O$), 1,10-phenantroline (99% w/w), acetic acid (99.7% w/v), ascorbic acid (99%, w/w), formic acid (95%, w/v) were supplied by Sigma-Aldrich. Sodium persulfate, $Na_2S_2O_8$ was provided by Merck Millipore (Darmstadt, Germany). Ultrapure water was produced with a Millipore (Direct-Q® Ultrapure Water System, Bedford, MA, USA).

2.2 Analytical methods

Carbamazepine concentration was quantified by ultra-performance liquid chromatography (UPLC, Agilent 1260) coupled to UV/DAD detector. The column selected was C18 (1.8 µm, 50 x 4.6 mm). The initial conditions of 10% AcN and 90% of Milli-Q water acidified with formic acid (25mM w/v) progressed to 100% AcN in 15 min. 3 min post-time was selected: time elapsed before the next injection for the method to stabilize in the selected initial condition. Flow rate was 1 mL/min and the injection volume was 100 µL. Wavelength for carbamazepine quantification was 267 nm. Each sample was previously filtered (0.22 µm – Milipore). Additionally, the filter was washed with AcN, added to the sample so that proportion between sample and AcN was the same than the one of the HPLC solvents at the start of the method (10% AcN – 90% sample).

Persulfate concentration was quantified evaluating the sulfate anion concentration generated during the reaction by Ion chromatography with a Metrohm 872 Extension

Page: 8

Number: 1 Author: Subject: Comment on Text Date: 1/2/20, 10:40:44 AM

Number: 2 Author: Subject: Inserted Text Date: 1/2/20, 10:40:44 AM

did you encounter any problem for the quantification of sulfate anions in samples where iron was present? it happened that quantification of anions on Metrohm 872 showed lot of interferences on column in the presence of dissolved iron in solution. pls check and clarify.

Status

AlexCabrera Completed 1/28/20, 11:43:12 PM

Author: AlexCabrera Subject: Nota adhesiva Date: 1/29/20, 10:38:07 PM

In general, our experience with this quantification method is good. Ion chromatography has been also used in previous works and most of the results have been coherent. In any case, the samples were doubly checked using also the spectrophotometric method developed by Liang et al. 2008 [1].

[1] Chenju Liang, Chiu-Fen Huang, Nihar Mohanty, Rama Mohan Kurakalva, A rapid spectrophotometric determination of persulfate anion in ISCO, Chemosphere, Volume 73, Issue 9, 2008, Pages 1540-1543.

Module 1 and 2 ion chromatograph (IC) system configured for gradient analysis. To determine the total iron concentration, the 1,10-phentranoline method was used (ISO 6332).

2.3 Experimental procedure

Experiments were carried out in an opaque-wall reaction vessel (1L) placed under dark conditions. Temperature was manually controlled using a heater that also provided agitation in order to work under perfect mixing conditions. In a typical run, pH of the deionized water was adjusted to 2.7-2.9, then carbamazepine (0.0025 mM equivalent to 500 µg/L) was added and, finally, persulfate was added marking the start of the experiment. ~~Carbamazepine~~ stock solution (4 g/L) was prepared in methanol so that 0.125 mL of stock solution was added per liter of reactor, providing 37 mg/L of total organic carbon (TOC) to the solution. This amount is similar to the natural organic content found in MWWTP effluents. In the iron-activation experimental series, Fe(II) (as $FeSO_4 \cdot 7H_2O$) was added before persulfate.

2.4 Reaction kinetic model

In this work, the processes are represented by 3 groups of reactions: (i) related to persulfate activation for sulfate radicals production, (ii) related to efficient sulfate radicals consumption in which the pollutant is oxidized and (iii) related to non-efficient consumption of sulfate radicals, i.e. scavenging interactions. Semi-empirical dynamic model is based on mass balances of the most relevant components of the process obtained under batch mode operation and considering perfect mixing conditions.

In the case of heat-activated persulfate process, the model assumes 4 reactions and 5 model components (Table 1), these being $S_2O_8^{2-}$ (PS), $SO_4^{\bullet-}$ (~~RAD~~), H^+ (H), carbamazepine (~~CARB~~) and TOC. With respect to reactions, the activation of ~~persulfate~~ by heat (Reaction 1) and acidic conditions (Reaction 2), ~~carbamazepine~~ oxidation (Reaction 5) and

Page: 9

Number: 1 Author: Subject: Comment on Text Date: 1/2/20, 10:40:44 AM

use abbreviation throughout the manuscript as CBZ

Status

AlexCabrera Completed 1/28/20, 11:43:19 PM

Author: AlexCabrera Subject: Nota adhesiva Date: 1/29/20, 2:24:09 PM

Done

Number: 2 Author: Subject: Inserted Text Date: 1/2/20, 10:40:44 AM

CBZ

Status

AlexCabrera Completed 1/28/20, 11:43:44 PM

Number: 3 Author: Subject: Comment on Text Date: 1/2/20, 10:40:44 AM

pls use abbreviation as PS for the whole manuscript

Status

AlexCabrera Completed 1/28/20, 11:43:53 PM

Author: AlexCabrera Subject: Nota adhesiva Date: 1/23/20, 6:33:03 PM

Author: AlexCabrera Subject: Nota adhesiva Date: 1/29/20, 2:24:21 PM

Done

Number: 4 Author: Subject: Cross-Out Date: 1/2/20, 10:40:44 AM

Status

AlexCabrera Completed 1/28/20, 11:44:04 PM

Number: 5 Author: Subject: Inserted Text Date: 1/2/20, 10:40:44 AM

SRs

Status

AlexCabrera Completed 1/28/20, 11:44:11 PM

Author: AlexCabrera Subject: Nota adhesiva Date: 1/29/20, 2:24:28 PM

Done

Number: 6 Author: Subject: Cross-Out Date: 1/2/20, 10:40:44 AM

Status

AlexCabrera Completed 1/28/20, 11:44:18 PM

Number: 7 Author: Subject: Inserted Text Date: 1/2/20, 10:40:44 AM

Z

Status

AlexCabrera Completed 1/28/20, 11:44:31 PM

Number: 8 Author: Subject: Inserted Text Date: 1/2/20, 10:40:44 AM

PS

Status

AlexCabrera Completed 1/28/20, 11:44:36 PM

Number: 9 Author: Subject: Inserted Text Date: 1/2/20, 10:40:44 AM

CBZ

Status

AlexCabrera Completed 1/28/20, 11:44:46 PM

mineralization (Reaction 6) are the interactions between model components considered. As no equilibrium reactions were included in the model, in order to follow the parsimony principle, the acid-activation reaction was only considered within the first 5 minutes of the process.

In the iron-activated persulfate process, the model assumes 7 reactions and model components (Table 1), including the 5 components of the heat-activated persulfate process plus Fe(II) and Fe(III). With respect to reactions, Reactions 1, 2, 5 and 6 are complemented with the activation of persulfate by Fe(II) (Reaction 3), Fe(III) (Reaction 4) and the oxidation of Fe(II) by sulfate radicals (Reaction 7).

A summary of reactions and the corresponding kinetics equations are presented in Table 1.

Table 1. Reactions and kinetics equations included in the semi-empirical model proposed.

Reaction		Rate law equation	
$PS + heat \rightarrow 2\ RAD$	(Reaction 1)	$r_1 = k_1\ [PS]$	(Equation 1)
$PS + H \rightarrow RAD$	(Reaction 2)	$r_2 = k_2\ [PS]\ [H]$	(Equation 2)
$PS + Fe(II) \rightarrow RAD + Fe(III)$	(Reaction 3)	$r_3 = k_3\ [PS]\ [Fe(II)]$	(Equation 3)
$PS + Fe(III) \rightarrow RAD + Fe(II)$	(Reaction 4)	$r_4 = k_4\ [PS]\ [Fe(III)]$	(Equation 4)
$CARB + RAD \rightarrow Products$	(Reaction 5)	$r_5 = k_5\ [CARB]\ [RAD]$	(Equation 5)
$TOC + RAD \rightarrow Products$	(Reaction 6)	$r_6 = k_6\ [TOC]\ [RAD]$	(Equation 6)
$Fe(II) + RAD \rightarrow Fe(III)$	(Reaction 7)	$r_7 = k_7\ [Fe(II)]\ [RAD]$	(Equation 7)

2.5. Numerical issues and assays

The experiments carried out in this study were divided into two groups for parameter identification and model validation. One experiment from the heat-activation experimental series and two experiments from the iron-activated experimental series were used for model validation plus another two specific assays, one based on iron additions (0.018 mM) and another based on persulfate additions (0.17 mM).

Page: 10

Number: 1 Author: Subject: Cross-Out Date: 1/2/20, 10:40:44 AM

Status
AlexCabrera Completed 1/28/20, 11:45:07 PM

Number: 2 Author: Subject: Inserted Text Date: 1/2/20, 10:40:44 AM
PS

Status
AlexCabrera Completed 1/28/20, 11:45:25 PM

Number: 3 Author: Subject: Inserted Text Date: 1/2/20, 10:40:44 AM
PS

Status
AlexCabrera Completed 1/28/20, 11:45:35 PM

Number: 4 Author: Subject: Inserted Text Date: 1/2/20, 10:40:44 AM
SRs

Status
AlexCabrera Completed 1/28/20, 11:45:44 PM

Number: 5 Author: Subject: Comment on Text Date: 1/2/20, 10:40:44 AM
pls substitute in the table for more clarity and wording familiar to PS-AOP based processes:
RAD = SRs
CARB = CBZ otherwise CARB is used as abbreviation for carbohydrates.

Status
AlexCabrera Completed 1/28/20, 11:45:52 PM

Author: AlexCabrera Subject: Nota adhesiva Date: 1/29/20, 12:12:41 AM
The Table 1 has been modified according to the Reviewer comment (PAGE 8 of the document)

In a first step of the model calibration procedure, only ~~persulfate~~ decomposition data was taken into account in the construction of the objective function, so that the kinetic constants of the ~~persulfate~~ activation reactions could be obtained. The remaining parameters were obtained in a second step where the objective function was augmented with ~~carbamazepine~~ oxidation profiles. The searching procedure was carried out until trapped in local minima for some combinations of kinetic parameters with no improvement of the defined objective function.

The model parameters were obtained by implementing a Monte Carlo approach in MATLAB® in which the objective was the minimization of the function presented in Equation 8.

$$J = \sum_{n} \left[\sum_{m} \frac{\left| X_{e,n,m} - X_{p,n,m} \right|}{X_{e,m}} \right] \qquad \text{(Equation 8)}$$

Where the subscript "e" represents the experimental measurement and the subscript "p" the model prediction of the variable X (~~carbamazepine~~ and/or ~~persulfate~~ concentrations); being the subscript "m" the total number of samples of the "n" experiments carried out.

When only model fine-tuning was carried out, MATLAB® optimization toolbox with a weighted quadratic objective function was used.

3. Results and discussion

3.1 Heat-activation of ~~persulfate~~

~~Persulfate~~ can form two $SO_4^{\bullet-}$ through scission of the peroxide bond as a result of heat energy absorption [25]. In this part of the study, the degradation of ~~carbamazepine~~ (0.0025 mM) by using ~~persulfate~~ (1mM) as oxidant agent at temperatures in the range from 25ºC to

Page: 11

Number: 1 Author: Subject: Inserted Text Date: 1/2/20, 10:40:44 AM
PS

Status
AlexCabrera Completed 1/28/20, 11:46:11 PM

Number: 2 Author: Subject: Inserted Text Date: 1/2/20, 10:40:44 AM
PS

Status
AlexCabrera Completed 1/28/20, 11:46:25 PM

Number: 3 Author: Subject: Inserted Text Date: 1/2/20, 10:40:44 AM
CBZ

Status
AlexCabrera Completed 1/28/20, 11:46:35 PM

Number: 4 Author: Subject: Inserted Text Date: 1/2/20, 10:40:44 AM
CBZ

Status
AlexCabrera Completed 1/28/20, 11:46:51 PM

Number: 5 Author: Subject: Inserted Text Date: 1/2/20, 10:40:44 AM
PS

Status
AlexCabrera Completed 1/28/20, 11:46:56 PM

Number: 6 Author: Subject: Inserted Text Date: 1/2/20, 10:40:44 AM
PS

Status
AlexCabrera Completed 1/28/20, 11:47:07 PM

Number: 7 Author: Subject: Inserted Text Date: 1/2/20, 10:40:44 AM
PS

Status
AlexCabrera Completed 1/28/20, 11:47:20 PM

Number: 8 Author: Subject: Inserted Text Date: 1/2/20, 10:40:44 AM
CBZ

Status
AlexCabrera Completed 1/28/20, 11:47:31 PM

Number: 9 Author: Subject: Inserted Text Date: 1/2/20, 10:40:44 AM
PS

Status
AlexCabrera Completed 1/28/20, 11:47:40 PM

65ºC and pH 3 was evaluated (Figure 1). This pH was selected in order to know heat-activation contribution when ~~persulfate~~ is also activated by dissolved iron (notice that acidic pH is needed to keep iron in solution). At the lowest temperature (25ºC), about 30% ~~carbamazepine~~ degradation was achieved after 20 min remaining the pollutant concentration almost constant from this moment until the end of the assay (180 min). From 35ºC, the complete removal of carbamazepine was always achieved. Increasing the temperature always resulted in faster kinetics till attaining complete polluant removal in less than 5 min at 65ºC. These results show that there is an initial degradation non-related to heat-activation, as the latter should be characterized by a continuous decomposition of persulfate, as occurs at 35ºC (see Figure 1a). This phenomenom could be caused by acid-catalyzed decomposition of persulfate, which has been reported by several authors [21, 26].

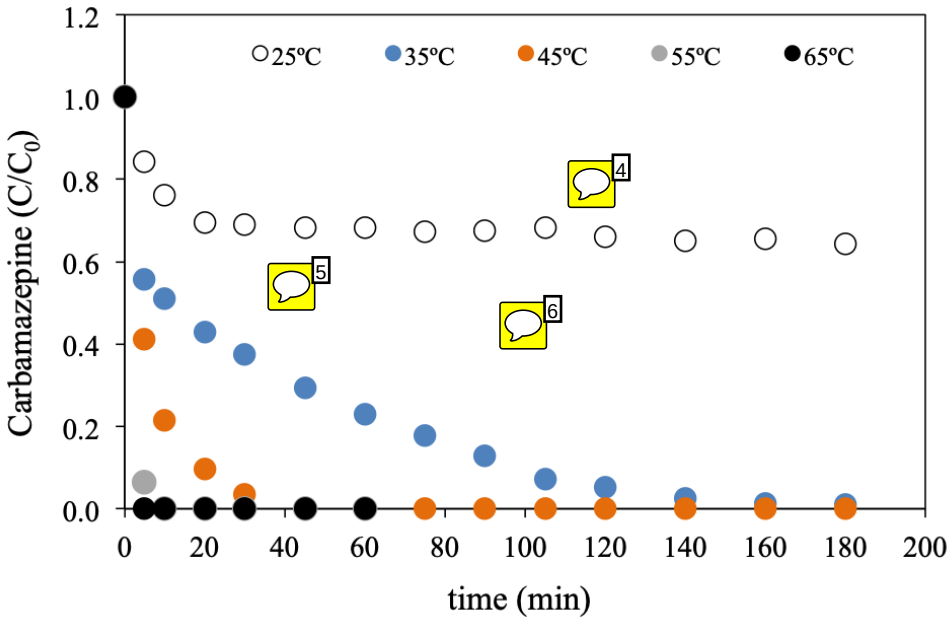

(a)

Page: 12

Number: 1 Author: Subject: Inserted Text Date: 1/2/20, 10:40:44 AM

PS

Status

AlexCabrera Completed 1/28/20, 11:47:52 PM

Number: 2 Author: Subject: Inserted Text Date: 1/2/20, 10:40:44 AM

CBZ

Status

AlexCabrera Completed 1/28/20, 11:48:02 PM

Number: 3 Author: AlexCabrera Subject: Texto insertado Date: 1/27/20, 8:48:07 AM

C

Status

AlexCabrera Completed 1/28/20, 11:48:07 PM

Number: 4 Author: Subject: Sticky Note Date: 1/2/20, 10:40:44 AM

%RSE is missing. An inset in the form of histograms can be used here to show the %RSE. Consider an average RSE or a specific reaction time before PS depletion in solution.

Status

AlexCabrera Completed 1/28/20, 11:48:12 PM

Author: AlexCabrera Subject: Nota adhesiva Date: 1/27/20, 8:51:21 AM

As suggested by the Reviewer, the average RSE for each experiment has been calculated and inserted in the Figure. Further information about RSE can be found below.

Number: 5 Author: Subject: Sticky Note Date: 1/2/20, 10:40:44 AM

a steady state is reached at 25oC

Status

AlexCabrera Completed 1/28/20, 11:48:23 PM

Author: AlexCabrera Subject: Nota adhesiva Date: 1/28/20, 11:12:57 PM

There is no activation of PS at this temperature or the activation is extremely low. Probably, there is an initial activation of persulfate by acidic conditions and, then, the process is stopped so that steady state is reached.

Number: 6 Author: Subject: Sticky Note Date: 1/2/20, 10:40:44 AM

error bars and uncertainties should appear on the plots

Status

AlexCabrera Rejected 1/29/20, 1:59:38 AM

Author: AlexCabrera Subject: Sticky Note Date: 2/3/20, 3:40:43 PM

The authors agree with the Reviewer about the importance of errors in plots, nevertheless, errors are already considered during model calibration and these are implicitly included in the kinetic constants (model parameters), which are presented with the corresponding error value (see comment below). In our opinion, to include the errors in the Figures does not provide important information in this particular case because the main output of this work is the model.

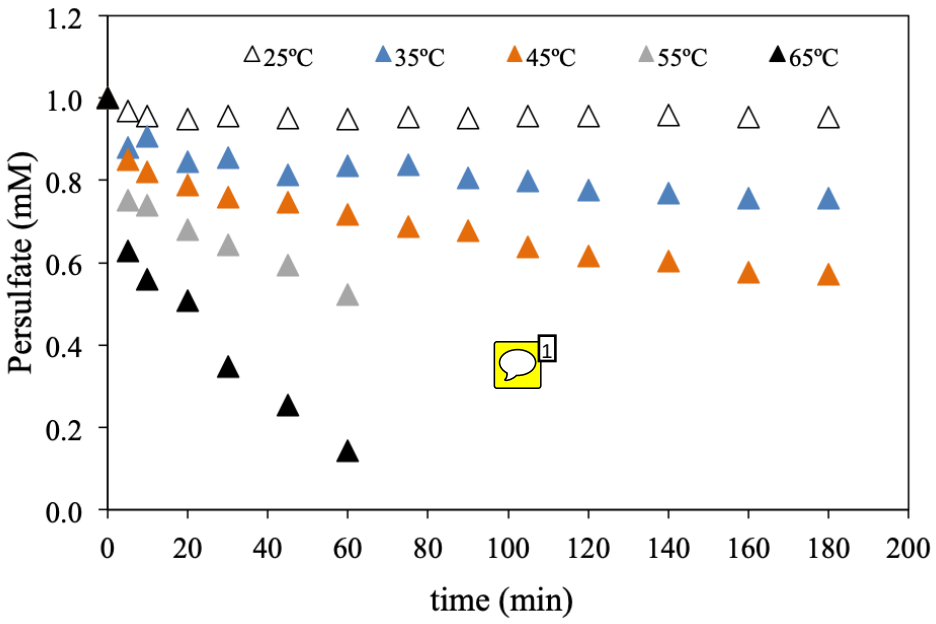

(b)

Figure 1. Carbamazepine removal (0.0025 mM initial concentration) (a) and persulfate decomposition (1 mM initial concentration) (b) profiles along the heat-activation experimental series.

The above explanation is also in accordance with model structure resulting from calibration process. If only heat-activation of ~~persulfate~~ is considered in the model, the agreement between experimental data and model prediction profiles is good only for 45, 55 and 65ºC experiments, i.e. once temperature is high enough to be the main activation mechanism. Including acid-catalyzed decomposition of ~~persulfate~~ in the reaction mechanism improved model accuracy allowing also an accurate prediction of the low temperature experiments. Another important aspect to enhance model predictions was to include a radical scavenging reaction, as the pollutant stock solution was prepared in methanol, which provides additional TOC (37 mg/L) in the reaction bulk affecting process performance. This situation is similar to the one found in natural surface waters and municipal WWTP

Page: 13

Number: 1 Author: Subject: Sticky Note Date: 1/2/20, 10:40:44 AM
error bars and uncertainties should appear on the plots

Status
AlexCabrera None 1/29/20, 2:25:39 PM

Number: 2 Author: Subject: Comment on Text Date: 1/2/20, 10:40:44 AM
Authors are required to calculate here the reaction stoichiometric efficiency which is the number of moles of CBZ degraded over the number of moles of PS consumed. A comparative study can then be done with published data on Thermally activated persulfate (TAP) systems and chemically activated persulfate (CAP) systems. for example, TAP systems showed greater RSE than CAP systems and in some cases RSE reached 70% while in other cases in CAP systems it dropped to less than 5%.
This parameter in important to consider for a better validation of the current model.
references that can help for the determination of the %RSE and its correlation with the TOC as well.

ref
A comparative study of the common persulfate activation techniques for the complete degradation of an NSAID: The case of Ketoprofen
Chemical Engineering Journal 350, 395-410 39 2018
Contribution of persulfate in UV-254 nm activated systems for complete degradation of chloramphenicol antibiotic in water
Chemical Engineering Journal 317, 1012-1025 79 2017
Naproxen abatement by thermally activated persulfate in aqueous systems
Chemical Engineering Journal 279, 861-873 2015
Ibuprofen removal by heated persulfate in aqueous solution: a kinetics study
Chemical engineering journal 197, 483-492 2012

Status
AlexCabrera Completed 1/28/20, 11:48:54 PM

Author: AlexCabrera Subject: Nota adhesiva Date: 1/29/20, 2:26:49 PM
The discussion has been improved by including the RSE.

The average RSE for each experiment was calculated resulting in values from 0.7% to 1.7%. As explained in the new text, the important difference with reported RSE results can be justified by (i) acidic conditions, which are known to decrease the RSE, and (ii) initial pollutant concentration, which is much lower in our study because it is focused on CECs removal. In this sense, the importance of RSE parameter is probably lower when the pollutant concentration is in the range of micrograms per liter. Instead, other process parameters such as the reaction rate or the reaction time needed to reach the treatment goal should be optimized. (PAGE 10 of the document)

Number: 3 Author: Subject: Inserted Text Date: 1/2/20, 10:40:44 AM
PS

Status
AlexCabrera Completed 1/28/20, 11:49:10 PM

Number: 4 Author: Subject: Inserted Text Date: 1/2/20, 10:40:44 AM
PS

Status
AlexCabrera Completed 1/28/20, 11:49:20 PM

secondary effluents, where similar TOC values are also found in the matrix. Mineralization was not selected as prediction objective because it is not a concern when dealing with CECs dissolved in real aqueous matrices, in which TOC concentration is in the order of several tens of mg/L, while the concentration of CECs is typically in the order of µg/L. Therefore, the mineralization of CECs cannot be detected in actual wastewater treatment conditions [27] and degradation of harmless TOC is not an objective of any advanced tertiary treatment designed to polish the effluent from conventional WWTPs [28].

As it can be seen in Figure 2, very good agreement between experimental results and model predictions were obtained both for ~~carbamazepine and persulfate~~ time-concentration profiles for the complete range of temperatures studied. The kinetic parameters of the proposed model are shown in Table 2. The slowest reactions were those responsible of radical production (Reactions 1 and 2) being the lowest values obtained for ~~persulfate~~ heat-activation reaction (Reaction 1). The corresponding activation energy obtained for this reaction (105.2 kJ/mol) is in the range of the reported values at acid pH (110-116 kJ/mol) [29]. On the contrary, the ~~carbamazepine~~ degradation reaction (Reactions 5) resulted in the highest kinetic parameters.

Page: 14

Number: 1 Author: Subject: Inserted Text Date: 1/2/20, 10:40:44 AM
CBZ and PS

Status
AlexCabrera Completed 1/28/20, 11:49:30 PM

Number: 2 Author: Subject: Inserted Text Date: 1/2/20, 10:40:44 AM
PS

Status
AlexCabrera Completed 1/28/20, 11:49:41 PM

Number: 3 Author: Subject: Inserted Text Date: 1/2/20, 10:40:44 AM
CBZ

Status
AlexCabrera Completed 1/28/20, 11:49:51 PM

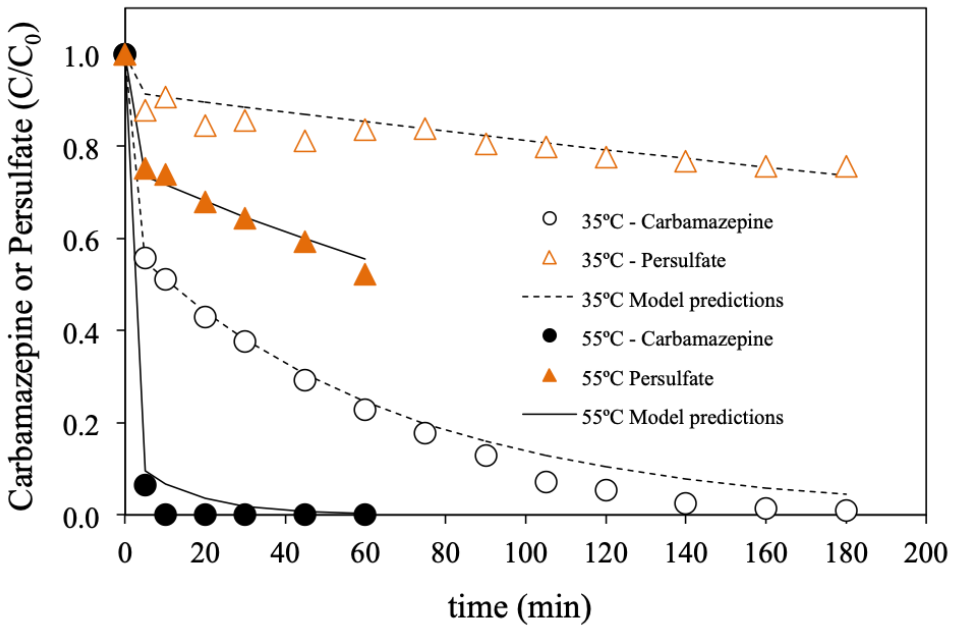

Figure 2. Comparison between experimental data (dots) and model predictions (lines) for the heat-activation experiments carried out at 35ºC and 55ºC.

Table 2. Kinetic parameters resulting from the calibration of the heat-activated ~~persulfate~~ model at the different temperatures and the corresponding activation energy of the Arrhenius fitting.

		25ºC	35ºC	45ºC	55ºC	65ºC	E_a kJ/mol	r^2
k_1	min^{-1}	$(0.1\pm0.1)\cdot10^{-3}$	$(1.2\pm0.1)\cdot10^{-3}$	$(3.0\pm0.1)\cdot10^{-3}$	$(5.1\pm0.2)\cdot10^{-3}$	$(25.2\pm0.8)\cdot10^{-3}$	105.2	0.9496
k_2	$mM^{-1}min^{-1}$	0.069±0.001	0.089±0.002	0.147±0.006	0.326±0.014	0.404±0.026	40.4	0.9608
k_5	$mM^{-1}min^{-1}$	1.99±0.10	3.30±0.13	4.14±0.39	5.38±0.57	-	26.1	0.9722
k_6	$mM^{-1}min^{-1}$	0.141±0.006	0.150±0.007	0.156±0.011	0.159±0.005	-	3.2	0.9477

Page: 15

Number: 1 Author: Subject: Inserted Text Date: 1/2/20, 10:40:44 AM

PS

Status

AlexCabrera Completed 1/28/20, 11:50:01 PM

Number: 2 Author: Subject: Sticky Note Date: 1/2/20, 10:40:44 AM

How uncertainties were calculated? did you use LINEST of excel or something else? pls clarify.

Status

AlexCabrera Completed 1/28/20, 11:50:15 PM

Author: AlexCabrera Subject: Nota adhesiva Date: 1/29/20, 2:27:29 PM

The uncertainities were determined in MATLAB®. Using the errors of PS and CBZ measurement methods and the experimental data, 5 new sets of "simulated experiments" were randonmly generated. For each data set, model fine tunning procedure was carried out and a new group of kinetic constants obtained. Finally, the standard deviation for each kinetic constant was calculated using the 5 values previously obtained.

This information has been included in the manuscript (PAGE 9 of the document)

Number: 3 Author: AlexCabrera Subject: Resaltado Date: 1/27/20, 10:11:52 AM

Status

AlexCabrera Completed 1/28/20, 11:50:25 PM

Number: 4 Author: Subject: Comment on Text Date: 1/2/20, 10:40:44 AM

These values are for which temperature? how do these values compare with existing Ea for other pharmaceutical compounds as for example Ibuprofen, Ketoprofen, Naproxen, Ranitidine, Chloramphenicol, etc. values for these compounds are in the suggested references above on thermal activation of PS in pharmaceuticals fed solutions.

Status

AlexCabrera Completed 1/28/20, 11:51:15 PM

Author: AlexCabrera Subject: Nota adhesiva Date: 1/29/20, 1:30:39 AM

The Ea values were calculated from the Arrhenius plot using the whole range of temperatures studied.

As proposed by the Reviewer, the Ea of CBZ was compared to the Ea of some other pharmaceuticals (PAGE 13 of the document).

3.2 Iron-activation of persulfate

Sulfate radical can also be formed through the reaction of persulfate and metals in which one electron is transferred [30]. In this context, the use of iron has been widely studied because it presents low toxicity and low cost [13]. Based on the above considerations, in the next part of the study, the removal of carbamazepine (0.0025 mM) by Fe(II)-activated persulfate (1mM) under six different iron concentrations in the range from 0.009 mM to 0.18 mM (equivalent to 0.5 - 10 mg/L) at constant temperature (25ºC) was evaluated and modeled. In general, an important initial degradation of the pollutant is again observed and later the process is extremely slowed down due to the formation of Fe(III) (Figure 3). After 2 hours, the complete carbamazepine removal was not achieved in any case though, when 5 mg/L of Fe(II) or higher concentrations were used, about 90% oxidation was obtained within the first 5 min. Negligible differences in terms of carbamazepine removal were found between the experiments carried out with 5, 7.5 and 10 mg/L of Fe(II). This behavior, in which there is fast pollutant degradation at initial stages but, subsequently, asymptotic values of pollutant and oxidant agent are observed, is in agreement with some other published works. Rodriguez et al. 2017 [24] reported similar process performance. Additionally, the authors indicated that an undesired reaction occurs that consumes both Fe(II) and $S_2O_8^{2-}$ if iron excess is added in the reaction bulk, which can justify the similarity between the experiments above 5 mg/L of iron. Minimizing this undesirable reaction (Reaction 7) is required to increase the efficiency of the oxidant, which could be obtained for instance by employing zero valent iron that allows a slow release of Fe(II). Slight differences were also found between the experiments carried out with 0.5 and 1 mg/L of Fe(II). For both concentrations, about 60% initial degradation was observed. Under these

Page: 16

Number: 1 Author: Subject: Inserted Text Date: 1/2/20, 10:40:44 AM
SRs

Status
AlexCabrera Completed 1/28/20, 11:51:37 PM

Number: 2 Author: Subject: Inserted Text Date: 1/2/20, 10:40:44 AM
PS

Status
AlexCabrera Completed 1/28/20, 11:51:45 PM

Number: 3 Author: Subject: Comment on Text Date: 1/27/20, 12:00:05 PM
pls add the following: in addition of its use in its zero valent form in monometallic and multimetallic heterogeneous systems presenting advantages on homogeneous systems mainly improving the reaction stoichiometric efficiency with less iron sludge generation.
ref
A comparative study of the common persulfate activation techniques for the complete degradation of an NSAID: The case of Ketoprofen
M Amasha, A Baalbaki, A Ghauch
Chemical Engineering Journal 350, 395-410 2018
Ranitidine abatement in chemically activated persulfate systems: assessment of industrial iron waste for sustainable applications
Chemical Engineering Journal 288, 276-288 2016
Assessment of bimetallic and trimetallic iron-based systems for persulfate activation: application to sulfamethoxazole degradation
Chemical Engineering Journal 256, 280-292 2014

Status
AlexCabrera Completed 1/28/20, 11:51:50 PM

Author: AlexCabrera Subject: Nota adhesiva Date: 1/29/20, 1:31:20 AM
Following the suggestion of the Reviewer, this information has been added in the text (PAGE 14 of the document)

Number: 4 Author: Subject: Inserted Text Date: 1/2/20, 10:40:44 AM
CBZ

Status
AlexCabrera Completed 1/28/20, 11:52:06 PM

Number: 5 Author: Subject: Inserted Text Date: 1/2/20, 10:40:44 AM
PS

Status
AlexCabrera Completed 1/28/20, 11:52:15 PM

Number: 6 Author: Subject: Cross-Out Date: 1/2/20, 10:40:44 AM

Status
AlexCabrera Completed 1/28/20, 11:52:21 PM

Number: 7 Author: Subject: Inserted Text Date: 1/2/20, 10:40:44 AM
CBZ

Status
AlexCabrera Completed 1/28/20, 11:52:33 PM

Number: 8 Author: Subject: Inserted Text Date: 1/2/20, 10:40:44 AM
CBZ

Status
AlexCabrera Completed 1/28/20, 11:52:41 PM

Number: 9 Author: Subject: Comment on Text Date: 1/27/20, 12:08:23 PM
This was also found by Ghauch and co-workers who demonstrated the superiority of ZVI particles in activating PS while keeping high performance of the system especially that reaction was accompanied with pH slight decrease favoring the continuous generation of iron species and iron corrosion products helping PS activation in a controlled manner for sulfametoxazole degradation.
ref:
Degradation of sulfamethoxazole by persulfate assisted micrometric Fe0 in aqueous solution
Chemical Engineering Journal 228, 1168-1181 2013
Assessment of bimetallic and trimetallic iron-based systems for persulfate activation: application to sulfamethoxazole degradation
Chemical Engineering Journal 256, 280-292 2014

Status
AlexCabrera Completed 1/28/20, 11:52:51 PM

Author: AlexCabrera Subject: Nota adhesiva Date: 1/29/20, 3:41:00 PM
This information has been added in the manuscript (PAGE 15 of the document)

conditions, the process is probably mainly initiated by the above-mentioned acid-activation mechanism instead of Fe-activation.

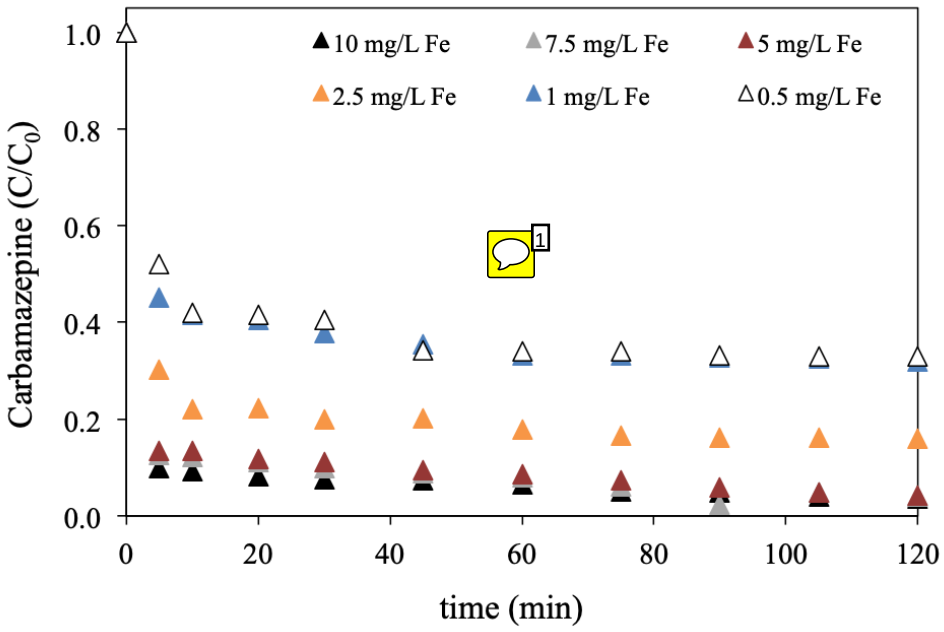

(a)

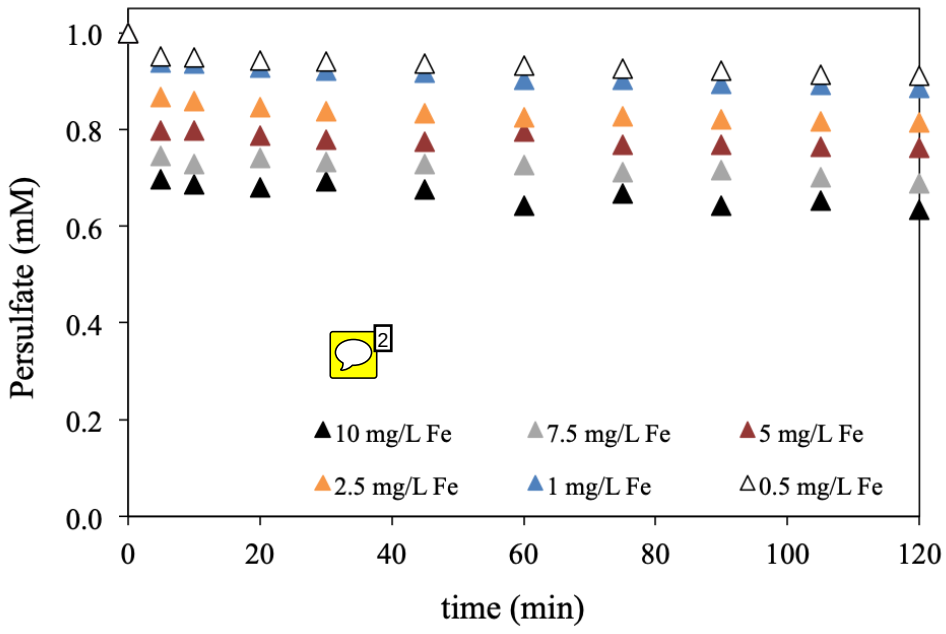

(b)

Page: 17

Number: 1 Author: Subject: Sticky Note Date: 1/2/20, 10:40:44 AM

error bars should be added

Status

AlexCabrera None 1/29/20, 10:39:41 PM

Number: 2 Author: Subject: Sticky Note Date: 1/2/20, 10:40:44 AM

error bars should be added

Status

AlexCabrera None 1/29/20, 10:39:35 PM

Figure 3. Carbamazepine degradation (0.0025 mM initial concentration) (a) and persulfate decomposition (b) curves for the experiments carried out with 0.5, 2.5 and 10 mg/L of iron at 25ºC.

In the next experimental series, the same iron concentrations were used but increasing the operation temperature to 35ºC (Figure 4). In all the cases, reaction kinetics improved with respect to the previous experimental series carried out at 25ºC. The complete degradation of ~~carbamazepine~~ was achieved in approximately 40 min when iron concentrations of 5 mg/L or higher were used. Again, negligible differences between the experiments with 5, 7.5 and 10 mg/L of iron were found. In the case of the experiment with 2.5 mg/L of iron, the pollutant could be also completely degraded after 100 min. In contrast, 1 and 0.5 mg/L of iron assays only allowed reaching 80% and 70% degradation, respectively, after 120 min.

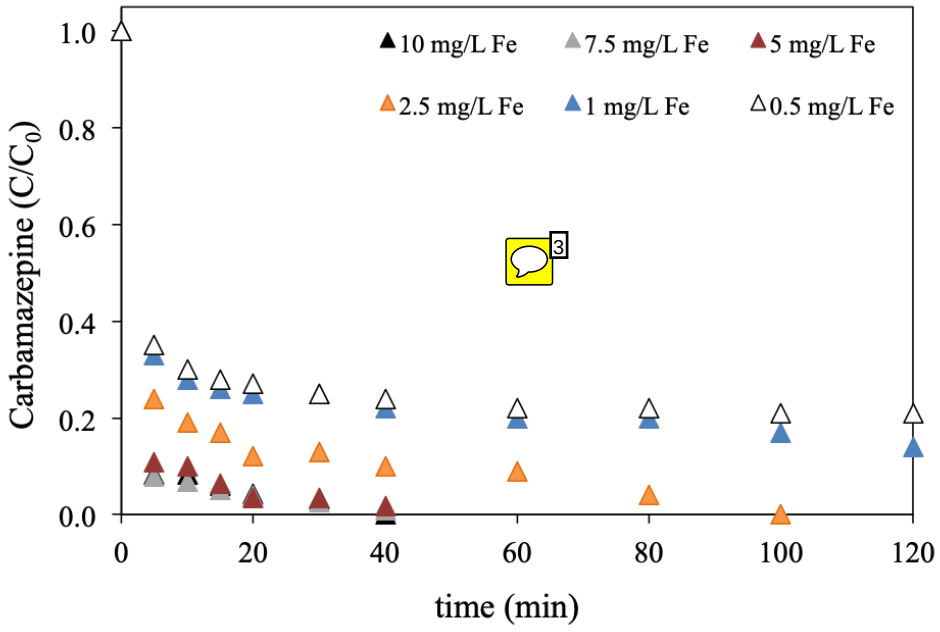

(a)

Page: 18

Number: 1 Author: Subject: Comment on Text Date: 1/2/20, 10:40:44 AM

Authors should definitely considered the molar ratio PS:Fe and discuss result with some comparison to existing data on experiments performed with similar ratios. It happened that a molar ratio if 1:1 is the best for higher RSE. example can be taken from Ranitidine paper, Sulfamethoxazole paper and Theophylline paper by Ghauch group.

Status

AlexCabrera Completed 1/28/20, 11:53:49 PM

Author: AlexCabrera Subject: Nota adhesiva Date: 1/29/20, 3:41:52 PM

Following the Reviewer suggestion, the Fe:PS ratio was calculated for each experiment and the results discussed considering the existing data on literature. In this case, the discussion was focused on the pollutant final degradation level instead of RSE, as this parameter seems to be less important when PS is used to remove CECs. (PAGE 15 of the document)

Number: 2 Author: Subject: Inserted Text Date: 1/2/20, 10:40:44 AM

CBZ

Status

AlexCabrera Completed 1/28/20, 11:54:00 PM

Number: 3 Author: Subject: Sticky Note Date: 1/2/20, 10:40:44 AM

error bars are missing

Status

AlexCabrera None 1/29/20, 10:40:12 PM

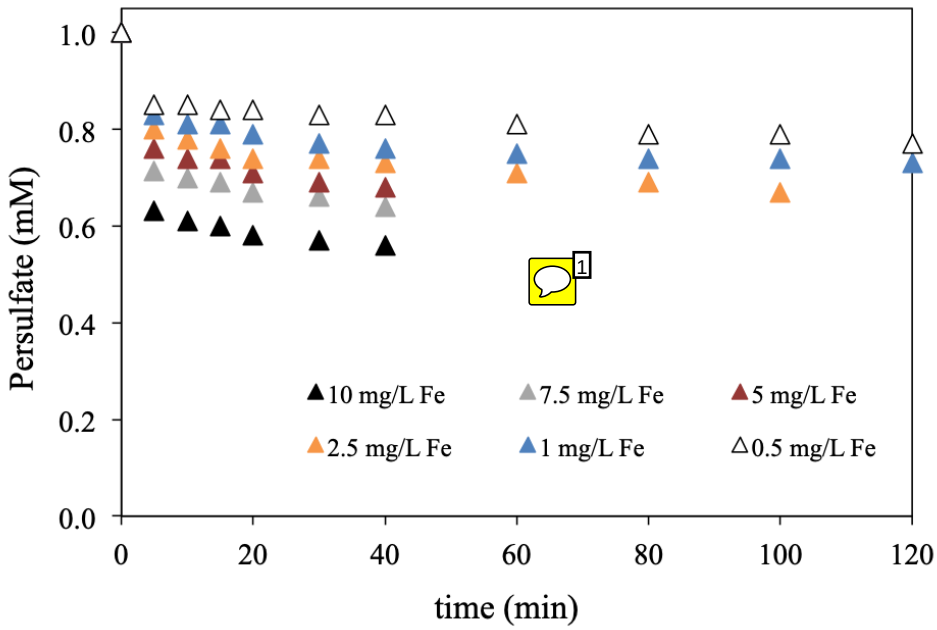

(b)

Figure 4. ~~Carbamazepine~~ degradation (0.0025 mM) (a) and ~~persulfate~~ decomposition (b) curves for the experiments carried out with 0.5, 2.5 and 10 mg/L of iron at 35ºC.

The semi-empirical model proposed in the previous section was modified in order to include the activation of ~~persulfate~~ by iron species. In this way, Fe(II) and Fe(III) activation reactions (Reactions 3 and 4) were added in the mechanism and the model was again calibrated. In the first calibration step, only ~~persulfate~~ decomposition data was used to determine the kinetic constants of both Fe(II) and Fe(III) activation reactions, using the already obtained model parameters in the temperature experimental series (Table 3) for acid and heat activation (k_1 and k_2). This option left to acceptable predictions, however, a better agreement between simulated and experimental profiles of ~~persulfate~~ decomposition was obtained after model fine-tuning. The calibration process showed that, in the range from 25ºC to 35ºC, the model prediction capability improves if heat-activation kinetic parameter comes to zero. Probably, this is due to its small effect can be implicitly included in the iron-

Page: 19

Number: 1 Author: Subject: Sticky Note Date: 1/2/20, 10:40:44 AM
error bars are missing

Status
AlexCabrera None 1/29/20, 10:40:21 PM

Number: 2 Author: Subject: Comment on Text Date: 1/2/20, 10:40:44 AM
molar ratios PS:Fe should be considered

Status
AlexCabrera Completed 1/28/20, 11:54:34 PM

Author: AlexCabrera Subject: Nota adhesiva Date: 1/29/20, 1:33:26 AM
Again, the results were analyzed considering the Fe:PS molar ratio. A brief explanation has been included in the document because the same conclusion than for the previous experimental serie was found (PAGE 18 of the document).

Number: 3 Author: Subject: Inserted Text Date: 1/2/20, 10:40:44 AM
CBZ

Status
AlexCabrera Completed 1/28/20, 11:54:40 PM

Number: 4 Author: Subject: Inserted Text Date: 1/2/20, 10:40:44 AM
PS

Status
AlexCabrera Completed 1/28/20, 11:54:44 PM

Number: 5 Author: Subject: Inserted Text Date: 1/2/20, 10:40:44 AM
PS

Status
AlexCabrera Completed 1/28/20, 11:54:55 PM

Number: 6 Author: Subject: Inserted Text Date: 1/2/20, 10:40:44 AM
PS

Status
AlexCabrera Completed 1/28/20, 11:55:04 PM

Number: 7 Author: Subject: Inserted Text Date: 1/2/20, 10:40:44 AM
PS

Status
AlexCabrera Completed 1/28/20, 11:55:13 PM

Number: 8 Author: Subject: Comment on Text Date: 1/2/20, 10:40:44 AM
?

Status
AlexCabrera Completed 1/28/20, 11:55:20 PM

Author: AlexCabrera Subject: Nota adhesiva Date: 1/29/20, 1:34:34 AM
This sentence has been modified in order to improve the explanation (PAGE 19 of the document).

activation reactions. On the contrary, this did not happen with acid-activation, which still showed an important effect on process performance. The next step was to include ~~carbamazepine~~ oxidation and scavenging reactions into the model and to simulate also the pollutant degradation profile. In addition, Fe(II) scavenging of radicals reaction (Reaction 7) was also included in the model to describe the negative effect of iron excess on process performance. Again, the values of the kinetic constants already available from the temperature experimental series (k_5 and k_6) were initially used determining only the kinetic parameter of Fe(II) scavenging reaction. As in the previous calibration stage, although model prediction was acceptable, it improved after model fine-tuning. The comparison between experimental data and model predictions for the assays carried out with 5 mg/L of iron at 25ºC and 35ºC is shown in Fig~~ure~~ . As it can be seen in the simulated profiles, the model prediction capability is high in both cases.

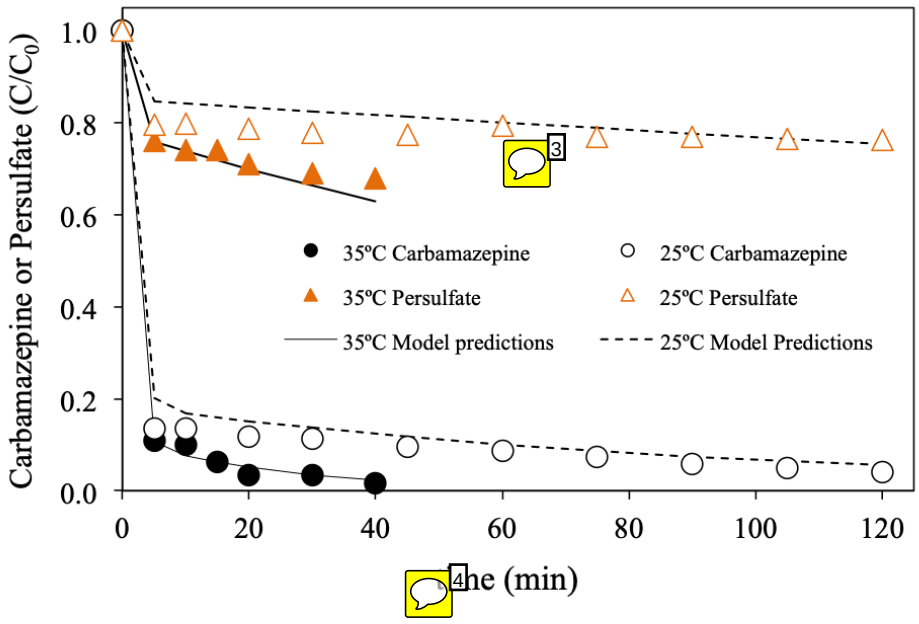

Page: 20

Number: 1 Author: Subject: Inserted Text Date: 1/2/20, 10:40:44 AM

CBZ

Status

AlexCabrera Completed 1/28/20, 11:55:31 PM

Number: 2 Author: Subject: Inserted Text Date: 1/2/20, 10:40:44 AM

.

Status

AlexCabrera Completed 1/28/20, 11:56:20 PM

Number: 3 Author: Subject: Sticky Note Date: 1/2/20, 10:40:44 AM

error bars are missing

Status

AlexCabrera None 1/29/20, 10:40:30 PM

Author: AlexCabrera Subject: Nota adhesiva Date: 1/27/20, 3:20:16 PM

Number: 4 Author: Subject: Sticky Note Date: 1/2/20, 10:40:44 AM

Reaction Time / [min]
use for all graphs

Status

AlexCabrera Completed 1/28/20, 11:56:32 PM

Figure 5. Comparison between experimental data (carbamazepine –dots- and persulfate –triangles-) and model simulations (lines) for the experiments carried out with 1 mg/L of iron at 25ºC and 35ºC.

Therefore, the final proposed model includes 3 reactions related to radical formation and 3 reactions related to radical consumption. ~~Persulfate~~ can be activated to produce ~~sulfate radicals~~ by acid conditions (Reaction 2), Fe(II) (Reaction 3) and Fe(III) (Reaction 4). With respect to heat-activation, it is not necessary to implicitly consider this mechanism in the model because it seems to be included through iron-activation reactions. With respect to radicals consumption, their reactions with ~~carbamazepine~~ organic matter and Fe(II) were considered. The kinetic parameters obtained by model fitting are presented in Table 3. This table shows that Fe(II) is the main responsible ~~of persulfate~~ activation with a small contribution of acid-activation. After the oxidation of Fe(II) to Fe(III), there is also ~~persulfate~~ activation by Fe(III), although it is extremely slow. The fastest reaction of the whole model was ~~carbamazepine~~ oxidation followed by Fe(II) oxidation by ~~sulfate radical~~. Again, Fe(II)-activation of ~~persulfate~~ as the most important activation mechanism, with an initial contribution of acid-activation that has to be considered in the model and a very slow Fe(III) impact.

Page: 21

Number: 1 Author: Subject: Comment on Text Date: 1/2/20, 10:40:44 AM
use ratios PS:FE

Status
AlexCabrera Completed 1/28/20, 11:56:44 PM

Number: 2 Author: Subject: Inserted Text Date: 1/2/20, 10:40:44 AM
PS

Status
AlexCabrera Completed 1/28/20, 11:57:00 PM

Number: 3 Author: Subject: Inserted Text Date: 1/2/20, 10:40:44 AM
SRs

Status
AlexCabrera Completed 1/28/20, 11:57:06 PM

Number: 4 Author: Subject: Inserted Text Date: 1/2/20, 10:40:44 AM
CBZ

Status
AlexCabrera Completed 1/28/20, 11:57:14 PM

Number: 5 Author: Subject: Cross-Out Date: 1/2/20, 10:40:44 AM

Status
AlexCabrera Completed 1/28/20, 11:57:26 PM

Number: 6 Author: Subject: Inserted Text Date: 1/2/20, 10:40:44 AM
for PS

Status
AlexCabrera Completed 1/28/20, 11:57:31 PM

Number: 7 Author: Subject: Inserted Text Date: 1/2/20, 10:40:44 AM
in

Status
AlexCabrera Completed 1/28/20, 11:57:34 PM

Number: 8 Author: Subject: Inserted Text Date: 1/2/20, 10:40:44 AM
PS

Status
AlexCabrera Completed 1/28/20, 11:57:43 PM

Number: 9 Author: Subject: Inserted Text Date: 1/2/20, 10:40:44 AM
CBZ

Status
AlexCabrera Completed 1/28/20, 11:58:01 PM

Number: 10 Author: Subject: Inserted Text Date: 1/2/20, 10:40:44 AM
SR

Status
AlexCabrera Completed 1/28/20, 11:58:07 PM

Number: 11 Author: Subject: Inserted Text Date: 1/2/20, 10:40:44 AM
PS

Status
AlexCabrera Completed 1/28/20, 11:58:21 PM

Table 3. Kinetic parameters for the iron concentration experimental series resulting from model fine-tuning.

	k_2	k_3	k_4	k_5	k_6	k_7
	$mM^{-1}\ min^{-1}$					
25ºC	2.04±0.16	0.0056±0.0009	0.016±0.008	16.42±0.96	0.46±0.11	8.25±0.92
35ºC	5.37±0.87	0.030±0.008	0.037±0.010	23.01±1.34	0.77±0.20	18.92±2.3

3.3 Model Validation

One assay from each experimental series (heat-activation, Fe(II)-activation at 25 and 35ºC) was not used for model calibration so that these could be used for model validation. In the case of the heat-activation experimental series, the assay carried out at 45ºC was the one selected for model validation. As it can be observed in Figure 6a, good agreement between experimental data and model simulations was obtained for both ~~carbamazepine~~ oxidation and ~~persulfate~~ decomposition profiles, validating the model proposed, which includes heat-activation plus acid-activation. In the case of the Fe(II)-activation model, the validation experiments are presented in Figure 6b. Again, the model showed great prediction accuracy validating the semi-empirical approach in which only Fe(II)-activation and acid-activation are considered.

Page: 22

Number: 1 Author: Subject: Sticky Note Date: 1/2/20, 10:40:44 AM

pls explain how uncertainties were calculated

Status

AlexCabrera Completed 1/28/20, 11:58:26 PM

Author: AlexCabrera Subject: Nota adhesiva Date: 1/28/20, 11:23:55 PM

This issue has been already clarified in a previous comment.

Number: 2 Author: Subject: Inserted Text Date: 1/2/20, 10:40:44 AM

CBZ

Status

AlexCabrera Completed 1/28/20, 11:58:36 PM

Number: 3 Author: Subject: Inserted Text Date: 1/2/20, 10:40:44 AM

PS

Status

AlexCabrera Completed 1/28/20, 11:58:47 PM

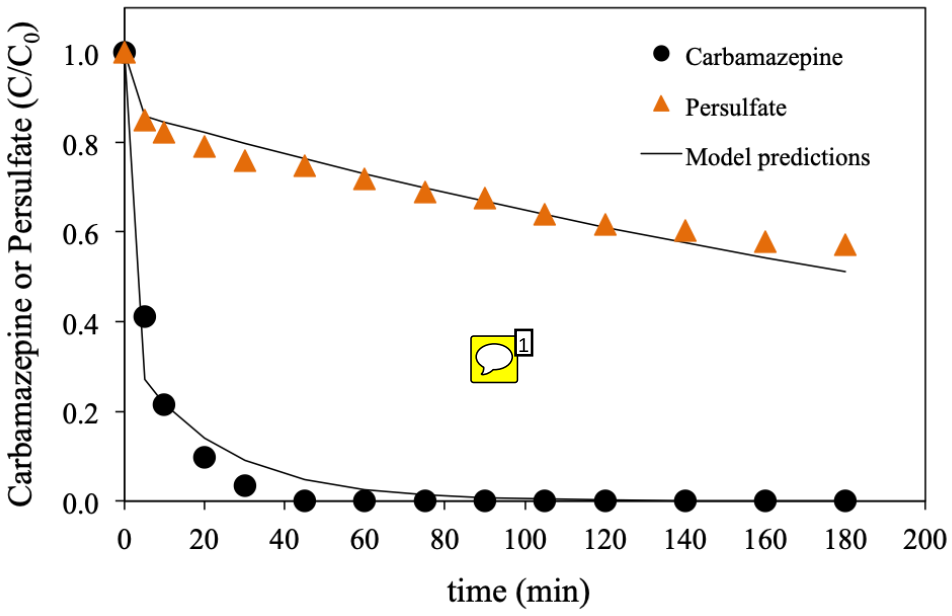

(a)

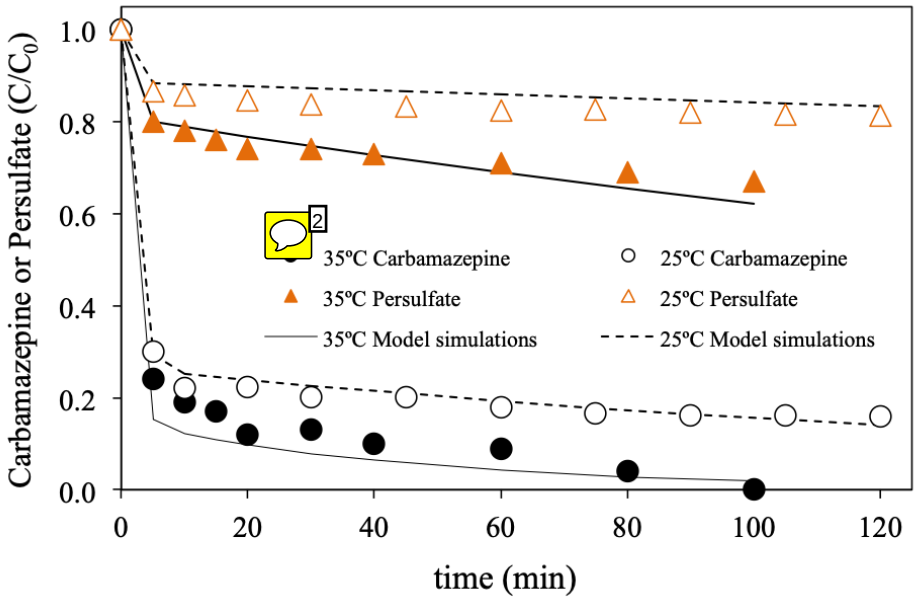

(b)

Figure 6. Comparison between experimental data (dots) and model predictions (lines) for the validation heat-activation experiment carried out at 45ºC (a) and the Fe-activation experiments carried out with 2.5 mg/L of iron at 25ºC and 35ºC (b).

Page: 23

Number: 1 Author: Subject: Sticky Note Date: 1/2/20, 10:40:44 AM

error bars are missing

Status

AlexCabrera None 1/29/20, 10:40:56 PM

Number: 2 Author: Subject: Sticky Note Date: 1/2/20, 10:40:44 AM

error bars are missing

Status

AlexCabrera None 1/29/20, 10:41:01 PM

Finally, two new validation experiments were carried out. In the first one, the removal of carbamazepine (0.0025 mM) using persulfate (1 mM) activated by different and low Fe(II) additions (0.018 mM each at 0, 10 and 20 min) was studied. Three steps can be clearly identified in the decontamination process corresponding to each one of the iron additions (Figure 7a). Initially, an important degradation is produced and, then, the process is almost stopped. The carbamazepine oxidation steps diminished with each one of the iron additions resulting in 60%, 20% and 10%. The model adequately predicts this process behavior; nevertheless, the prediction capability for carbamazepine removal diminished after the first addition. The initial carbamazepine concentration in all the experimental series used to develop the model was constant at 0.0025 mM. Consequently, the model has not been trained for concentrations lower than 0.0025 mM, as ≈0.001 mM and ≈0.0005 mM, concentrations measured when the second and third additions were done. A similar trend can be observed for persulfate decomposition. While the simulation for the first addition is adequate, in the second and third ones the persulfate concentration is overestimated. In the last validation experiment, the removal of carbamazepine (0.0025 mM) using 0.089 mM of Fe(II) and three $S_2O_8^{2-}$ additions (0.17 mM each at 0, 10 and 20 min) was studied. In this case, it is difficult to identify the additions in the carbamazepine oxidation curve, which is indeed extremely similar to the curves obtained in the Fe(II)-activation experimental series. After the first addition, almost 60% carbamazepine oxidation was obtained, then, 5% oxidation was achieved in the second one and, finally, the third addition resulted in only 2% degradation. This process behavior is well predicted by the model, indeed, model simulation shows that almost all the Fe(II) present initially in solution is already oxidized to Fe(III) (see Figure 7b) after the first persulfate addition. Consequently it can be said that the

Number: 1 Author: Subject: Inserted Text Date: 1/2/20, 10:40:44 AM
CBZ

Status
AlexCabrera Completed 1/28/20, 11:59:21 PM

Number: 2 Author: Subject: Inserted Text Date: 1/2/20, 10:40:44 AM
PS

Status
AlexCabrera Completed 1/28/20, 11:59:25 PM

Number: 3 Author: Subject: Inserted Text Date: 1/2/20, 10:40:44 AM
CBZ

Status
AlexCabrera Completed 1/28/20, 11:59:34 PM

Number: 4 Author: Subject: Inserted Text Date: 1/2/20, 10:40:44 AM
CBZ

Status
AlexCabrera Completed 1/28/20, 11:59:45 PM

Number: 5 Author: Subject: Inserted Text Date: 1/2/20, 10:40:44 AM
CBZ

Status
AlexCabrera Completed 1/28/20, 11:59:53 PM

Number: 6 Author: Subject: Inserted Text Date: 1/2/20, 10:40:44 AM
PS

Status
AlexCabrera Completed 1/29/20, 12:00:04 AM

Number: 7 Author: Subject: Comment on Text Date: 1/2/20, 10:40:44 AM
Here authors used molar concentration for all species in solution in contrast to previous data where mg was used.
authors should convert all concentrations to mM for more consistency and better comparison with existing published data especially that molar ratio optimization was very well studied by many authors.

Status
AlexCabrera Completed 1/29/20, 12:00:13 AM

Author: AlexCabrera Subject: Nota adhesiva Date: 1/27/20, 11:27:03 PM
As suggested by the Reviewer, all concentrations have been expressed in mM.

Number: 8 Author: Subject: Inserted Text Date: 1/2/20, 10:40:44 AM
PS

Status
AlexCabrera Completed 1/29/20, 12:00:23 AM

Number: 9 Author: Subject: Inserted Text Date: 1/2/20, 10:40:44 AM
CBZ

Status
AlexCabrera Completed 1/29/20, 12:00:32 AM

Number: 10 Author: Subject: Inserted Text Date: 1/2/20, 10:40:44 AM
CBZ

Status
AlexCabrera Completed 1/29/20, 12:00:51 AM

Number: 11 Author: Subject: Inserted Text Date: 1/2/20, 10:40:44 AM
CBZ

Status
AlexCabrera Completed 1/29/20, 12:01:02 AM

Number: 12 Author: Subject: Inserted Text Date: 1/2/20, 10:40:44 AM
PS

Status
AlexCabrera Completed 1/29/20, 12:01:12 AM

model is able to successfully simulate both ~~carbamazepine~~ oxidation process and ~~persulfate~~ decomposition, showing that it can be used as a predictive tool.

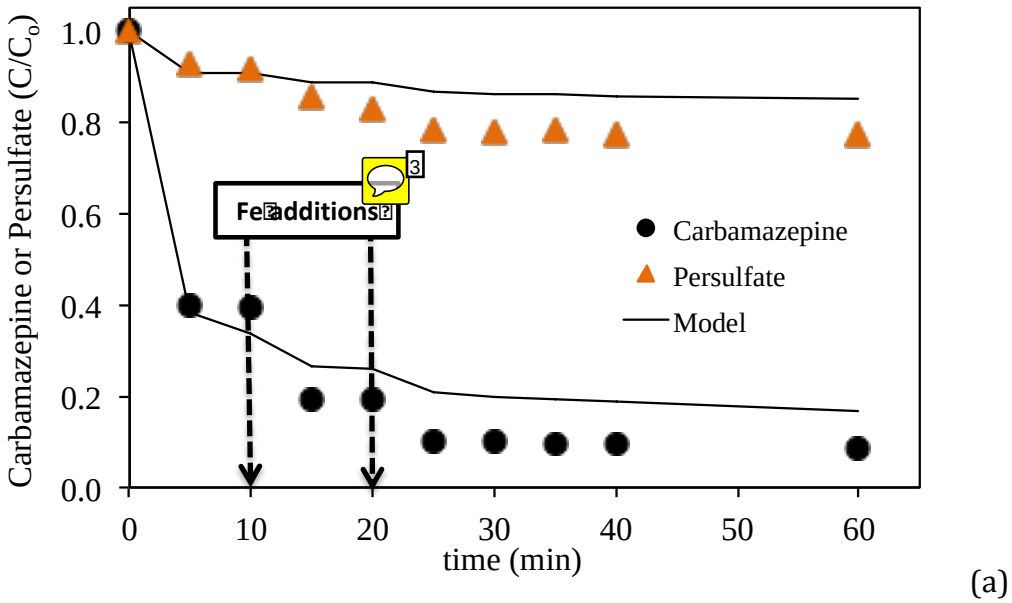

(a)

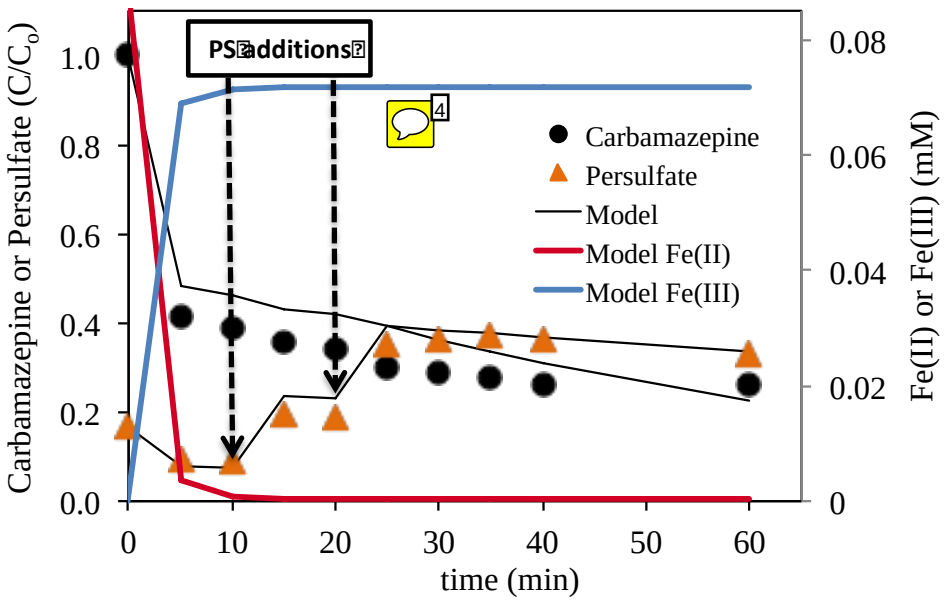

(b)

Figure 7. Comparison between experimental data (dots) and model predictions (lines) for ~~the validation experiment~~ carried out with iron additions (a) and persulfate additions (PS) (b).

Page: 25

Number: 1 Author: Subject: Inserted Text Date: 1/2/20, 10:40:44 AM

CBZ

Status

AlexCabrera Completed 1/29/20, 12:01:28 AM

Number: 2 Author: Subject: Inserted Text Date: 1/2/20, 10:40:44 AM

PS

Status

AlexCabrera Completed 1/29/20, 12:01:34 AM

Number: 3 Author: Subject: Sticky Note Date: 1/2/20, 10:40:44 AM

? to remove

Status

AlexCabrera Completed 1/29/20, 12:01:41 AM

Number: 4 Author: Subject: Sticky Note Date: 1/2/20, 10:40:44 AM

? to remove

Status

AlexCabrera Completed 1/29/20, 12:01:46 AM

Number: 5 Author: Subject: Cross-Out Date: 1/2/20, 10:40:44 AM

Status

AlexCabrera Completed 1/29/20, 12:01:51 AM

Number: 6 Author: Subject: Comment on Text Date: 1/2/20, 10:40:44 AM

concentrations of all species should be mentioned in the figure captions as experimental conditions: ....

Status

AlexCabrera Completed 1/29/20, 12:02:09 AM

Author: AlexCabrera Subject: Nota adhesiva Date: 1/29/20, 3:42:52 PM

Experimental conditions have been included in each figure caption.

Number: 7 Author: Subject: Inserted Text Date: 1/2/20, 10:40:44 AM

experiment validation

Status

AlexCabrera Completed 1/29/20, 12:02:18 AM

4. Conclusions

A semi-empirical mathematical model of the heat-activated and iron-activated ~~persulfate~~ processes applied to the removal of CECs in water using ~~carbamazepine~~ as model pollutant has been proposed and validated.

In the heat-activated experimental series, the selected temperature range was 25ºC-65ºC. The ~~carbamazepine~~ degradation reached 20% at 25ºC after 120 min while, from 35ºC; the complete degradation of the pollutant was always achieved. Kinetics always improved with temperature. The highest prediction capability was obtained when heat and acid activation of ~~persulfate~~ were considered in the model reaction mechanism, which included also ~~carbamazepine~~ degradation reaction and TOC scavenging reaction. Very good agreement between experimental results and model predictions were obtained both for ~~carbamazepine~~ and ~~persulfate~~ time-concentration profiles for the complete range of temperatures studied.

In the next experimental series, six different Fe(II) concentrations in the range from 0.5 to 10 mg/L at 25ºC and 35ºC were evaluated. At the lowest temperature, the complete ~~carbamazepine~~ removal was not achieved in any case, although about 90% degradation in the first 5 min was obtained when 5 mg/L of Fe(II) or higher concentrations were used. The fast pollutant degradation at initial stages and the asymptotic values of pollutant and oxidant agent obtained subsequently suggest that undesired reactions that consume both Fe(II) and $S_2O_8^{2-}$ are favored if iron excess is added in the reaction bulk. At 35ºC, the complete degradation of ~~carbamazepine~~ was obtained in about 40 min when Fe(II) concentration was 5 mg/L or higher, finding again negligible differences between the experiments with 5, 7.5 and 10 mg/L of Fe(II). With respect to model reaction mechanism for this part of the study, the calibration process showed that the model prediction capability improves if heat-activation kinetic parameter comes to ~~c~~ero. Probably, this is due

Page: 26

Number: 1 Author: Subject: Inserted Text Date: 1/2/20, 10:40:44 AM
PS

Status
AlexCabrera Completed 1/29/20, 12:02:39 AM

Number: 2 Author: Subject: Inserted Text Date: 1/2/20, 10:40:44 AM
CBZ

Status
AlexCabrera Completed 1/29/20, 12:02:50 AM

Number: 3 Author: Subject: Inserted Text Date: 1/2/20, 10:40:44 AM
CBZ

Status
AlexCabrera Completed 1/29/20, 12:03:01 AM

Number: 4 Author: Subject: Inserted Text Date: 1/2/20, 10:40:44 AM
PS

Status
AlexCabrera Completed 1/29/20, 12:03:14 AM

Number: 5 Author: Subject: Inserted Text Date: 1/2/20, 10:40:44 AM
CBZ

Status
AlexCabrera Completed 1/29/20, 12:03:24 AM

Number: 6 Author: Subject: Inserted Text Date: 1/2/20, 10:40:44 AM
CBZ

Status
AlexCabrera Completed 1/29/20, 12:03:35 AM

Number: 7 Author: Subject: Inserted Text Date: 1/2/20, 10:40:44 AM
PS

Status
AlexCabrera Completed 1/29/20, 12:03:44 AM

Number: 8 Author: Subject: Inserted Text Date: 1/2/20, 10:40:44 AM
CBZ

Status
AlexCabrera Completed 1/29/20, 12:03:55 AM

Number: 9 Author: Subject: Comment on Text Date: 1/2/20, 10:40:44 AM
Here you should consider adding the %RSE obtained and compare results for different experimental conditions.

Status
AlexCabrera Completed 1/29/20, 12:04:03 AM

Author: AlexCabrera Subject: Nota adhesiva Date: 1/29/20, 1:36:03 AM
New conclusions related to RSE and Fe:PS molar ratio have been included in the document as suggested by the Reviewer (PAGES 25 and 26 of the document, respectively).

Number: 10 Author: Subject: Inserted Text Date: 1/2/20, 10:40:44 AM
CBZ

Status
AlexCabrera Completed 1/29/20, 12:04:17 AM

to its small effect can be implicitly included in the iron-activation reactions. On the contrary, this did not happen with acid-activation, which still showed an important effect on process performance. Thus, the model reaction mechanism that showed the highest prediction accuracy includes: acid, Fe(II) and Fe(III) ~~persulfate~~ activation, ~~carbamazepine~~ degradation and both TOC and Fe(II) scavenging reactions.

Finally, the model was validated using one assay from each experimental series (heat-activation, Fe(II)-activation at 25 and 35ºC) and two additional assays, one using Fe(II) additions (0.018 mM each at 0, 10 and 20 min) and another one using $S_2O_8^{2-}$ additions (0.17 mM each at 0, 10 and 20 min) with satisfactory results.

In conclusion, a predictive tool for the use of ~~persulfate~~ in the removal of contaminants of emerging concern has been developed. This type of studies are needed in order to get the process closer to actual application, as models allow simulating the process, optimizing operation conditions or scaling-up reactors, among other. Further studies are needed in order to improve the model so that the effect of some other important variables such as sun-light and matrix content can be also considered.

5. Acknowledgments

A. Cabrera wants to thank FONDECYT 11160680 for the financial support of his research stay at Plataforma Solar de Almería and SERC Chile (FONDAP 15110019). The authors wish to thank CONICYT (International Cooperation Program, REDES 180149), FONDECYT 11170122 and the Spanish Ministry of Science, Innovation and Universities for funding under the CalypSol Project (Reference: RTI2018-097997-B-C32)

Page: 27

Number: 1 Author: Subject: Inserted Text Date: 1/2/20, 10:40:44 AM
that

Status
AlexCabrera Completed 1/29/20, 12:04:57 AM
Author: AlexCabrera Subject: Nota adhesiva Date: 1/29/20, 1:36:37 AM
This sentence has been modified (PAGE 26 of the document).

Number: 2 Author: Subject: Inserted Text Date: 1/2/20, 10:40:44 AM
PS

Status
AlexCabrera Completed 1/29/20, 12:05:12 AM
Number: 3 Author: Subject: Inserted Text Date: 1/2/20, 10:40:44 AM
CBZ

Status
AlexCabrera Completed 1/29/20, 12:05:18 AM
Number: 4 Author: Subject: Inserted Text Date: 1/2/20, 10:40:44 AM
PS

Status
AlexCabrera Completed 1/29/20, 12:05:31 AM

6. References

[1] Krzeminski, P., Tomei, M.C., Karaolia, P., Langenhoff, A., Almeida, C.M.A., Felis, E., Gritten, F., Andersen, H.R., Fernandes, T., Manaia, C.M., Rizzo, L., Fatta-Kassinos, D., Performance of secondary wastewater treatment methods for the removal of contaminants of emerging concern implicated in crop uptake and antibiotic resistance spread: a review. Sci. Total Environ. Volume 648, (2019) Pages 1052–1081

[2] Petrie, B., Barden, R., Kasprzyk-Hordern B., A review on emerging contaminants in wastewaters and the environment: Current knowledge, understudied areas and recommendations for future monitoring, Water Res., Volume 72, (2015) Pages 3-27, https://doi.org/10.1016/j.watres.2014.08.053

[3] Sousa J.C.G., Ribeiro, A.R., Barbosa, M., Pereira, F., Silva, A.M.T., A review on environmental monitoring of water organic pollutants identified by EU guidelines, J. Hazard., Volume 344, (2018) Pages 146-162, https://doi.org/10.1016/j.jhazmat.2017.09.058

[4] Grassi, M., Rizzo, L., Farina, A., Endocrine disruptors compounds, pharmaceuticals and personal care products in urban wastewater: implications for agricultural reuse and their removal by adsorption process. Environ. Sci. Pollut. R., Volume 20, (2013) Pages 3616-3628, https://doi.org/10.1007/s11356-013-1636-7

[5] Roig, B., Pharmaceuticals in the Environment: Current knowledge and need assessment to reduce presence and impact, IWA Publishing, (2010) ISBN: 9781843393146

[6] Zhang, Y., Geiben, S., Gal, C., Carbamazepine and diclofenac: Removal in wastewater treatment plants and occurrence in water bodies, Chemosphere, 73 (2008) 1151-1161

[7] Yang, Y., Sik Ok, Y., Kim, K., Kwon, E.E., Fai Tsang, Y., Occurrences and removal of pharmaceuticals and personal care products (PPCPs) in drinking water and water/sewage

This page contains no comments

treatment plants: A review, Sci. Total Environ., Volumes 596–597, (2017) Pages 303-320, https://doi.org/10.1016/j.scitotenv.2017.04.102

[8] Wood, T.P., Duvenage, C.S.J., Rohwer, E., The occurrence of anti-retroviral compounds used for HIV treatment in South African surface water, Environ. Pollut., Volume 199, (2015) Pages 235-243, https://doi.org/10.1016/j.envpol.2015.01.030

[9] Hernando, M.D., Mezcua, M., Fernández-Alba, A.R., Barceló, D., Environmental risk assessment of pharmaceutical residues in wastewater effluents, surface waters and sediments, Talanta, Volume 69, Issue 2, (2006) Pages 334-342, https://doi.org/10.1016/j.talanta.2005.09.037

[10] Kleywegt, S., Pileggi, V., Chunyan Hao, P.Y., Zhao, X., Rocks, C., Thach, S., Cheung, P., Whitehead, B., Pharmaceuticals, hormones and bisphenol A in untreated source and finished drinking water in Ontario, Canada — Occurrence and treatment efficiency, Sci. Total Environ., Volume 409, Issue 8, (2011) Pages 1481-1488, https://doi.org/10.1016/j.scitotenv.2011.01.010

[11] Wacławek, S., Lutze, H.V., Grübel, K., Padil, V.V.T., Černík, M., Dionysiou, D.D., Chemistry of persulfates in water and wastewater treatment: A review, Chem. Eng. J., Volume 330, (2017) Pages 44-62, https://doi.org/10.1016/j.cej.2017.07.132

[12] Miralles-Cuevas, S., Darowna, D., Wanag, A., Mozia, S., Malato, S., Oller, I., Comparison of UV/H_2O_2, UV/$S_2O_8^{2-}$, solar/Fe(II)/H_2O_2 and solar/Fe(II)/$S_2O_8^{2-}$ at pilot plant scale for the elimination of micro-contaminants in natural water: An economic assessment, Chem. Eng. J., Volume 310, Part 2, (2017) Pages 514-524, https://doi.org/10.1016/j.cej.2016.06.121

This page contains no comments

[13] Matzek, L., Carter, K.E., Activated persulfate for organic chemical degradation: A review, Chemosphere, Volume 151, (2016) Pages 178-188, https://doi.org/10.1016/j.chemosphere.2016.02.055

[14] Rodriguez, S., Vasquez, L., Costa, D., Romero, A., Santos, A. Oxidation of Orange G by persulfate activated by Fe(II), Fe(III) and zero valent iron (ZVI) (2014) Chemosphere, 101, pp. 86-92

[15] Zhang, R., Sun, P., Boyer, T.H., Zhao, L., Huang, C.-H. Degradation of pharmaceuticals and metabolite in synthetic human urine by UV, UV/H2O2, and UV/PDS (2015) Environ. Sci. Technol., 49 (5), pp. 3056-3066. DOI: 10.1021/es504799n

[16] Chaoqun Tan, Naiyun Gao, Yang Deng, Na An, Jing Deng, Heat-activated persulfate oxidation of diuron in water, Chem. Eng. J., Volume 203, (2012) Pages 294-300, https://doi.org/10.1016/j.cej.2012.07.005

[17] Yuefei Ji, Changxun Dong, Deyang Kong, Junhe Lu, Quansuo Zhou, Heat-activated persulfate oxidation of atrazine: Implications for remediation of groundwater contaminated by herbicides, Chem. Eng. J., Volume 263, (2015) Pages 45-54, https://doi.org/10.1016/j.cej.2014.10.097

[18] Zhao, L., Hou, H., Fujii, A., Hosomi, M., Li, F. Degradation of 1,4-dioxane in water with heat- and Fe2+-activated persulfate oxidation, (2014) Environ. Sci. Pollut. R., 21 (12), pp. 7457-7465. DOI: 10.1007/s11356-014-2668-3

[19] Lominchar, M.A., Rodríguez, S., Lorenzo, D., Santos, N., Romero, A., Santos, A. Phenol abatement using persulfate activated by nZVI, H2O2 and NaOH and development of a kinetic model for alkaline activation, (2018) Environ. Techn. (United Kingdom), 39 (1), pp. 35-43 doi:10.1080/09593330.2017.1294203

This page contains no comments

[20] Vicente, F., Santos, A., Romero, A., Rodriguez, S. Kinetic study of diuron oxidation and mineralization by persulphate: Effects of temperature, oxidant concentration and iron dosage method (2011) Chem. Eng. J., 170 (1), pp. 127-135

[21] Ji, Y., Ferronato, C., Salvador, A., Yang, X., Chovelon, J.-M. Degradation of ciprofloxacin and sulfamethoxazole by ferrous-activated persulfate: Implications for remediation of groundwater contaminated by antibiotics (2014) Sci. Total Environ., 472, pp. 800-808

[22] Kusic, H., Peternel, I., Ukic, S., Koprivanac, N., Bolanca, T., Papic, S., Loncaric Bozic, A. Modeling of iron activated persulfate oxidation treating reactive azo dye in water matrix. Chem. Eng. J., 172 (2011) 109– 121

[23] Bu, L., Shi, Z., Zhou, S., Modeling of Fe(II)-activated persulfate oxidation using atrazine as a target contaminant. Separation and Purification Technology 169 (2016) 59–65

[24] Rodriguez, S., Santos, A., Romero, A., Oxidation of priority and emerging pollutants with persulfate activated by iron: Effect of iron valence and particle size, Chem. Eng. J., Volume 318, 2017, Pages 197-205, https://doi.org/10.1016/j.cej.2016.06.057

[25] Kolthoff, I.M., Miller, I.K., 1951. The chemistry of persulfate 1. The kinetics and mechanism of the decomposition of the persulfate ion in aqueous medium. J. Am. Chem. Soc., Volume 73, (1951), Pages 3055-3059, https://doi.org/10.1021/ja01151a024

[26] Liang, C., Wang Z-S., Bruell, C.J., Influence of pH on persulfate oxidation of TCE at ambient temperatures, Chemosphere, Volume 66, Issue 1, 2007, Pages 106-113, https://doi.org/10.1016/j.chemosphere.2006.05.026

[27] Soriano-Molina, P., García Sánchez, J.L., Malato, S., Plaza-Bolaños, P., Agüera, A., Sánchez Pérez, J.A., On the design and operation of solar photo-Fenton open reactors for

This page contains no comments

the removal of contaminants of emerging concern from WWTP effluents at neutral pH, Appl. Catal. B Environ., Volume 256, (2019) 117801

[28] Bourgin, M., Beck, B., Boehler, M., Borowska, E., Fleiner, J., Salhi, E., Teichler, R., von Gunten, U., Siegrist, H., McArdell, C.S., Evaluation of a full-scale wastewater treatment plant upgraded with ozonation and biological post-treatments: abatement of micropollutants, formation of transformation products and oxidation by-products. Water Res. (2018) Volume 129, Pages 486–498

[29] House, D.A., Kinetics and mechanism of oxidations by peroxydisulfate. Chem. Rev. 1962, Volume 62, Issue 3, Pages 185-203, https://doi.org/10.1021/cr60217a001

[30] Zhang, M., Chen, X., Zhou, H., Murugananthan, M., Zhang, Y., Degradation of p-nitrophenol by heat and metal ions co-activated persulfate, Chem. Eng. J., Volume 264, 2015a, Pages 39-47, https://doi.org/10.1016/j.cej.2014.11.060

This page contains no comments

Graphical Abstract

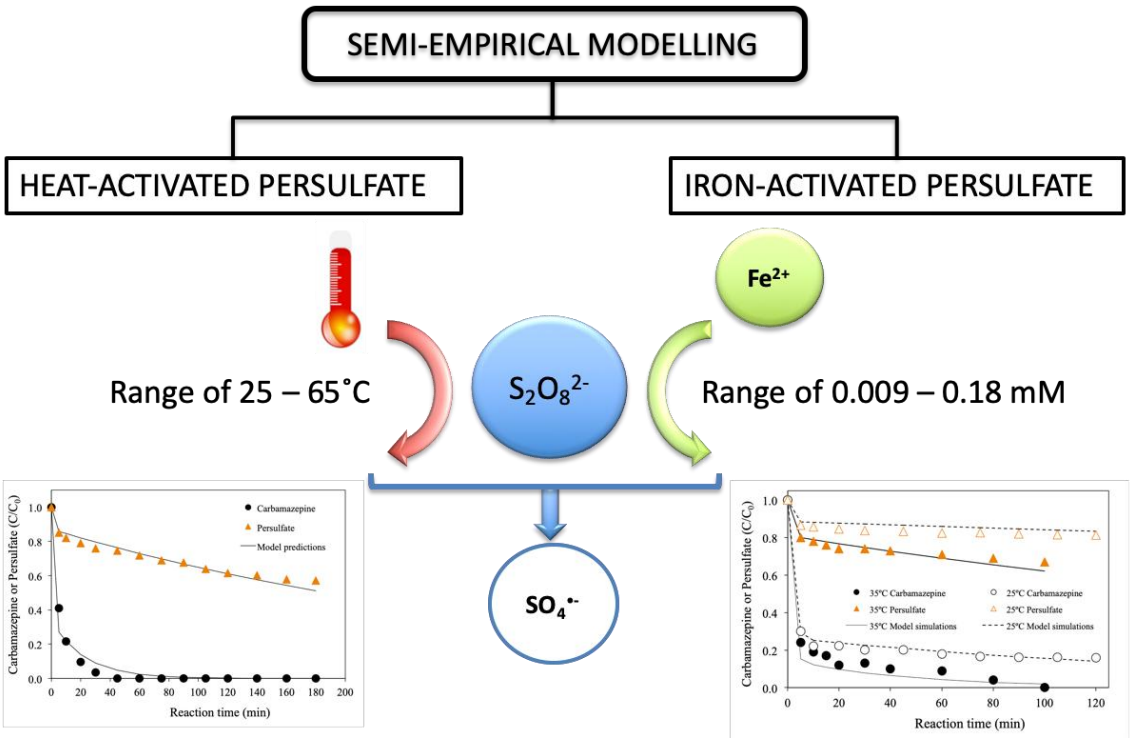

Highlights

- A semi-empirical model of heat and iron activation of persulfate was developed.
- Persulfate acid activation showed an important role at the begining of the process.
- An excess of iron favoured radicals scavenging.
- Good agreement between experimental data and model predictions was always obtained.
- Model was validated with additional assays based on iron and persulfate additions.

Modeling persulfate activation by iron and heat for the removal of contaminants of emerging concern using carbamazepine as model pollutant

Cabrera-Reina, A.[1], Miralles-Cuevas, S.[2,3], Oller, I.[3,4], Sánchez-Pérez, J.A.[2,3], Malato, S.[3,4]

[1] Engineering Faculty, University of Tarapacá, Avda. General Velásquez, Arica, Chile
[2] Chemical Engineering Department, University of Almería, Ctra. Sacramento s/n, Almería, Spain
[3] CIESOL, Joint Centre of the University of Almería-CIEMAT, Ctra. Sacramento s/n, Almería Spain
[4] Plataforma Solar de Almeria-CIEMAT, Carretera de Senés, km 4, Tabernas, Spain

Corresponding authors: Cabrera-Reina, A. (acabrera@limza.cl)

Oller, I. (isabel.oller@psa.es)

Abstract

A semi-empirical model of heat-activated and iron-activated persulfate (PS) processes applied to the removal of carbamazepine (CBZ) in water at low concentration (0.0025 mM) has been proposed and validated. In heat-activation systems, carried out at pH 3, temperature was varied from 25ºC to 65ºC, and acid-activation of PS showed an important initial role in the process. In iron-activated experimental series, iron concentration was changed from 0.009 mM to 0.18 mM at two different temperatures (25ºC and 35ºC), heat-activation was negligible with iron being the main activation mechanism and acid-activation showing also an important initial effect on process performance. High model prediction capability for both CBZ degradation and PS decomposition profiles was obtained in each case. Finally, the model was validated including supplementary experiments based on Fe(II) additions (0.018 mM each) and PS additions (0.17 mM) throughout the treatment. Developed model in this work is a powerful predictive tool for the application of PS in the removal of contaminants of emerging concern in water.

Keywords: modelling, microcontaminants, tertiary treatment, kinetics, wastewater

1. Introduction

Contaminants of emerging concern (CECs) are unregulated substances that enter the environment at low concentrations, among others, through municipal wastewater treatment plants (MWWTP) because biological systems were not designed for their removal [1]. Their properties make CECs highly risky for the environment and human health as they are bio-accumulative substances, very persistent in the environment and, at the same time, show a great capacity for transformation, generating intermediate products, such as metabolites, which, in many occasions, are more toxic than the parent compounds [2]. Personal care products, antiseptics, detergents and their metabolites, gasoline additives and industrial agents, among others, are considered as CECs [3]. Nevertheless, the ones that are possibly causing the greatest concern are the pharmaceutical products and, in particular, antibiotics [4]. The use of pharmaceutical products in European Union countries has been estimated of thousands of tons per year, and the majority of the most consumed, including antibiotics, are used in amounts similar to those of pesticides. Indeed, the presence of more than 3,000 pharmaceuticals in the aquatic environment has been already reported by Roig 2010 [5]. In this study, the carbamazepine (CBZ) was selected as CEC model because it is a bio-recalcitrant microcontaminant that is not efficiently removed by MWWTPs and usually reaches water bodies. According to Zhang et al. 2008 [6], CBZ has been detected in MWWTP effluents and surface waters around the world, as happens in Germany where it has been found at concentrations of around 3 µg/L in MWWTP effluents and 0.5 µg/L in surface waters. Moreover, according to several researchers, this pollutant is frequently detected in surface water, groundwater and even in drinking water at ng/L- µg/L levels [3, 7-10]. Therefore, it is a good indicator for following the performance of an advanced tertiary treatment to polish the effluent from conventional MWWTPs and it has been

widely used for AOPs applications research, e.g. in solar photo-Fenton [11], PS/TiO_2 [12] or improved methods such as the combination of ultrasonication, zero valent iron and hydrogen peroxide [13].

To prevent the entry of these CECs into the environment and also to achieve good water-reuse quality, an advanced tertiary treatment must be proposed and carried out as a final step in the treatment of MWWTP effluents. In recent years, sulfate radical-based advanced oxidation processes ($SO_4^{\bullet-}$-AOPs) applied to the removal of CECs are being investigated as an alternative to AOPs only based on the generation of hydroxyl radicals [14]. Sulfate radical, which has an oxidation potential similar to the one of hydroxyl radical, is very efficient to degrade CECs at low concentrations and environmentally friendly [15-17]. PS activation to form highly reactive species can be achieved by many different mechanisms in homogeneous as well as in heterogeneous media: UV light [18-20], thermal energy [21-23], acidic and alkaline conditions [24] or transition metals, e.g. silver, iron, copper, zinc. These transition metals can be in the form of dissolved salts in solution [25, 26] or zero valent metals being monometallic or bi/trimetallics iron based systems (commercial or scrap waste collected from the car industry) [27-29]. The feasibility of $SO_4^{\bullet-}$ based-AOPs for CECs abatement has already been proven, furthermore, several investigations about kinetics, degradation mechanism of different contaminants and the effect of water matrix on process performance have been reported [17, 30-32]. Therefore, considering that the basic knowledge of the PS oxidation process is high, new research focused on pilot plant scale studies, economic assessments, modelling, etc. is needed in order to favor the appearance of PS actual applications. Few studies about PS modelling can be found in the literature. Kusic et al. 2011 [33] developed a first principle mathematical model to predict decolorization of Reactive Red 45 and mineralization using PS activated via zerovalent iron

and ferrous sulfate both under dark and UV light conditions. Besides, PS was compared to H_2O_2 addition using 80 mg/L of Reactive Red 45 as initial pollutant load (≈32 mg/L of total organic carbon -TOC-). The reaction scheme included 12 bulk Fenton reactions, 14 surface Fenton reactions, 11 inorganic bulk reactions related to H_2O_2, 3 bulk iron/PS reactions, 5 surface iron/PS reactions, 6 inorganic bulk reactions related to PS, 6 photo-induced reactions and 8 pollutant degradation reactions. Selecting the corresponding reactions from this group, different models for direct UV photolysis, UV/H_2O_2, UV/$S_2O_8^{2-}$, Fe^{2+}/H_2O_2, UV/Fe^{2+}/H_2O_2, Fe^0/H_2O_2, UV/Fe^0/H_2O_2, UV/Fe^{2+}/$S_2O_8^{2-}$, Fe^{2+}/$S_2O_8^{2-}$, Fe^0/$S_2O_8^{2-}$ and UV/Fe^0/$S_2O_8^{2-}$ were proposed. Bu et al., 2017 [34] reported the modelling of Fe(II)-activated PS for the removal of atrazine at different initial concentrations. A first principle model based on 26 reactions including the influence of tertiary butanol, methanol and natural organic matter on process performance was used. Lominchar et al. 2018 [30] proposed a simplified reaction mechanism to model phenol abatement by alkaline-activated (pH 12) PS. Good agreement between experimental data and model simulations was found, being the model able to accurately predict the evolution of phenol, PS, hydroquinone and catechol. Another modelling work was carried out by Rodriguez et al. 2017 [35], who studied the removal of diuron, caffeine and ibuprofen at concentrations in the range from 0.086 mM to 0.129 mM by zerovalent iron-activated PS. An interesting semi-empirical modelling approach based only on 7 general reactions was proposed, capable of describing the evolution of pollutant, oxidant agent, iron concentrations and mineralization. All the reported studies considered an extremely higher concentration of target pollutants compared to the actual concentration of microcontaminants that can be found in MWWTP effluents.

The aim of the present work was to develop a general mathematical model under a semi-empirical approach of the heat-activated and iron-activated PS processes when these are applied to the removal of CECs. In this sense, CBZ dissolved in water at very low concentration (0.0025 mM), closer to actual conditions, was used as model pollutant. In a first experimental series, a heat-activation PS model was proposed for a temperature range from 25ºC to 65ºC. In the second part of the study, a complementary model was implemented for PS activated by iron in concentrations from 0.009 mM to 0.18 mM at 25ºC and 35ºC. Finally, the model was validated including supplementary experiments based on iron and PS additions carried out throughout the treatment.

2. Materials and Methods

2.1 Chemicals and reagents

CBZ (standard quality, 99%), acetonitrile (HPLC-grade), ferrous sulfate heptahydrate ($FeSO_4 \cdot 7H_2O$), 1,10-phenantroline (99% w/w), acetic acid (99.7% w/v), ascorbic acid (99%, w/w), formic acid (95%, w/v) were supplied by Sigma-Aldrich. Sodium persulfate, $Na_2S_2O_8$ was provided by Merck Millipore (Darmstadt, Germany). Ultrapure water was produced with a Millipore (Direct-Q® Ultrapure Water System, Bedford, MA, USA).

2.2 Analytical methods

CBZ concentration was quantified by ultra-performance liquid chromatography (UPLC, Agilent 1260) coupled to UV/DAD detector. The column selected was C18 (1.8 µm, 50 x 4.6 mm). The initial conditions of 10% AcN and 90% of Milli-Q water acidified with formic acid (25mM w/v) progressed to 100% AcN in 15 min. 3 min post-time was selected: time elapsed before the next injection for the method to stabilize in the selected initial condition. Flow rate was 1 mL/min and the injection volume was 100 µL. Wavelength for CBZ quantification was 267 nm. Each sample was previously filtered (0.22 µm –

Milipore). Additionally, the filter was washed with AcN, added to the sample so that proportion between sample and AcN was the same than the one of the HPLC solvents at the start of the method (10% AcN – 90% sample). The AcN addition also allows quenching the radicals present in the samples.

PS concentration was quantified by evaluating the sulfate anion concentration generated during the reaction by ion chromatography with a Metrohm 872 Extension Module 1 and 2 ion chromatograph (IC) system configured for gradient analysis. Samples stability was confirmed after long time storing. To determine the total iron concentration, the 1,10-phentranoline method was used (ISO 6332).

2.3 Experimental procedure

Experiments were carried out in an opaque-wall reaction vessel (1L) placed under dark conditions. Temperature was manually controlled using a heater that also provided agitation in order to work under perfect mixing conditions. In a typical run, pH of the deionized water was adjusted to 2.7-2.9, then CBZ (0.0025 mM equivalent to 500 µg/L) was added and, finally, PS was added marking the start of the experiment. CBZ stock solution (4 g/L) was prepared in methanol. To achieve the initial concentration, 0.125 mL of stock solution was added to the reactor providing 37 mg/L of total organic carbon (TOC) to the solution due to methanol content. This amount is similar to the natural organic content found in MWWTP effluents. In the iron-activation experimental series, Fe(II) (as $FeSO_4 \cdot 7H_2O$) was added before PS.

2.4 Reaction kinetic model

To develop a PS model (first principle model) considering all the possible interactions between CECs, inorganic salts, natural organic matter (NOM) and oxidizing species present in actual MWWTP effluents is not possible. The opposite approach relies on a completely

empirical view of the process and the use of response surface platform. This option is simpler, however, it is only valid under exactly the same conditions applied for model development. Thus, its application is also very limited. To face up these problems, this work proposes an intermediate solution, semi-empirical modelling. With this aim, PS oxidation process is described by means of a small group of simple reactions (usually known as "pseudo-reactions") where each one represents what is actually occurring through many elementary steps.

In this work, PS reaction mechanism is represented in the model by a limited number of reactions that can be grouped in three classes: (i) PS activation reactions, which are related to radicals production, (ii) reactions in which radicals are efficiently consumed, i.e. reactions related to CBZ oxidation and (iii)reactions in which radicals are inefficiently consumed, i.e. reactions related to mineralization (total organic carbon degradation) which is not the objective of tertiary treatments. Therefore, although the proposed model is simple due to the low number of reactions used, it still represents the overall process. Semi-empirical dynamic model is based on mass balances of the most relevant components of the process obtained under batch mode operation and considering perfect mixing conditions in the reactor.

In the case of heat-activated PS process, the model assumes 4 reactions and 5 model components (Table 1), these being $S_2O_8^{2-}$ (PS), $SO_4^{\bullet-}$ (SRs), H^+ (H), carbamazepine (CBZ) and TOC. With respect to reactions, the activation of PS by heat (Reaction 1) and acidic conditions (Reaction 2), CBZ oxidation (Reaction 5) and mineralization (Reaction 6) are the interactions between model components considered. As no equilibrium reactions were included in the model in order to follow the parsimony principle, the acid-activation reaction was only considered within the first 5 min of the process.

In the iron-activated PS process, the model assumes 7 reactions and model components (Table 1), including the 5 components of the heat-activated PS process plus Fe(II) and Fe(III). With respect to reactions, Reactions 1, 2, 5 and 6 are complemented with the activation of PS by Fe(II) (Reaction 3) and Fe(III) (Reaction 4) and the oxidation of Fe(II) by SRs (Reaction 7).

A summary of the reactions and the corresponding kinetics equations are presented in Table 1.

Table 1. Reactions and kinetics equations included in the semi-empirical model proposed.

Reaction		Rate law equation	
$PS + heat \rightarrow 2\,SRs$	(Reaction 1)	$r_1 = k_1\,[PS]$	(Equation 1)
$PS + H \rightarrow SRs$	(Reaction 2)	$r_2 = k_2\,[PS]\,[H]$	(Equation 2)
$PS + Fe(II) \rightarrow SRs + Fe(III)$	(Reaction 3)	$r_3 = k_3\,[PS]\,[Fe(II)]$	(Equation 3)
$PS + Fe(III) \rightarrow SRs + Fe(II)$	(Reaction 4)	$r_4 = k_4\,[PS]\,[Fe(III)]$	(Equation 4)
$CBZ + SRs \rightarrow Products$	(Reaction 5)	$r_5 = k_5\,[CBZ]\,[SRs]$	(Equation 5)
$TOC + SRs \rightarrow Products$	(Reaction 6)	$r_6 = k_6\,[TOC]\,[SRs]$	(Equation 6)
$Fe(II) + SRs \rightarrow Fe(III)$	(Reaction 7)	$r_7 = k_7\,[Fe(II)]\,[SRs]$	(Equation 7)

2.5. Numerical issues and assays

The experiments carried out in this study were divided into two groups for parameter identification and model validation. One experiment from the heat-activation experimental series and two experiments from the iron-activated experimental series were used for model validation plus another two specific assays, one based on iron additions (0.018 mM) and another based on PS additions (0.17 mM).

In a first step of the model calibration procedure, only PS decomposition data was taken into account in the construction of the objective function, so that the kinetic constants of the PS activation reactions could be obtained. The remaining parameters were obtained in a

second step where the objective function was augmented with CBZ oxidation profiles. The searching procedure was carried out until trapped in local minima for some combinations of kinetic parameters with no improvement of the defined objective function.

The model parameters were obtained by implementing a Monte Carlo approach in MATLAB® in which the objective was the minimization of the function presented in Equation 8.

$$J = \sum_{n} \left[\sum_{m} \frac{|X_{e,n,m} - X_{p,n,m}|}{X_{e,m}} \right] \quad \text{(Equation 8)}$$

Where the subscript "e" represents the experimental measurement and the subscript "p" the model prediction of the variable X (CBZ and/or PS concentrations); being the subscript "m" the total number of samples of the "n" experiments carried out.

When only model fine-tuning was carried out, MATLAB® optimization toolbox with a weighted quadratic objective function was used.

In order to calculate uncertainties of the kinetic constants, new groups of simulated experiments were generated by random modification of the experimental data based on the errors of PS and CBZ measurement methods. For each new data set, model fine-tuning procedure was carried out so that a new group of model parameters was obtained. Finally, the standard deviation of each model parameter was calculated.

3. Results and discussion

3.1 Heat-activation of PS

PS can form two $SO_4^{\bullet-}$ through scission of the peroxide bond as a result of heat energy absorption [36]. In this part of the study, the degradation of CBZ (0.0025 mM) by using PS

(1mM) as oxidant agent at temperatures in the range from 25ºC to 65ºC and pH 3 was evaluated (Figure 1). This pH was selected in order to know heat-activation contribution when PS is also activated by dissolved iron (notice that acidic pH is needed to keep iron in solution). At the lowest temperature (25ºC), about 30% CBZ degradation was achieved after 20 min remaining the pollutant concentration almost constant from this moment until the end of the assay (180 min). From 35ºC, the complete removal of CBZ was always achieved. Increasing the temperature always resulted in faster kinetics till attaining complete polluant removal in less than 5 min at 65ºC. These results show that there is an initial degradation non-related to heat-activation, as the latter should be characterized by a continuous decomposition of PS, as occurs at 35ºC (see Figure 1a). This phenomenom could be caused by acid-catalyzed decomposition of PS, which has been reported by several authors [32, 37]. At this point, the number of CBZ moles degraded over the number of PS moles consumed was calculated for each experiment. This parameter is known as the reaction stoichiometric efficiency (RSE). As it can be seen in the inset of Figure 1a, RSE decreased with temperature from 0.017 at 25ºC to 0.007 at 65ºC. These values are rather low in comparison to the ones reported in similar works related to heat activation of PS. Gauch et al. 2015 [23], who studied Naproxen degradation at circumneutral pH, obtained RSE values ≈0.70 when working at 70ºC. This important difference seems to be mainly caused by pH. Gauch et al. 2012 [38] reported that the RSE value for the removal of ibuprofen by PS heat activation decreases from 0.65 at pH 7 to 0.25 at pH 9 and to 0.09 at pH 4. Although this RSE value for acidic pH is still higher than the range of values obtained in this work, this difference can be justified since the ibuprofen initial concentration (20.3 μM equivalent to ≈4 mg/L) was considerably higher than the CBZ initial concentration used in this research (2.5 μM equivalent to ≈0.5 mg/L). Such low

concentration of contaminant favors the appearance of reactions different from pollutant degradation such as radical-to-radical reactions or reaction between radicals and organic matter and so, RSE diminishes.

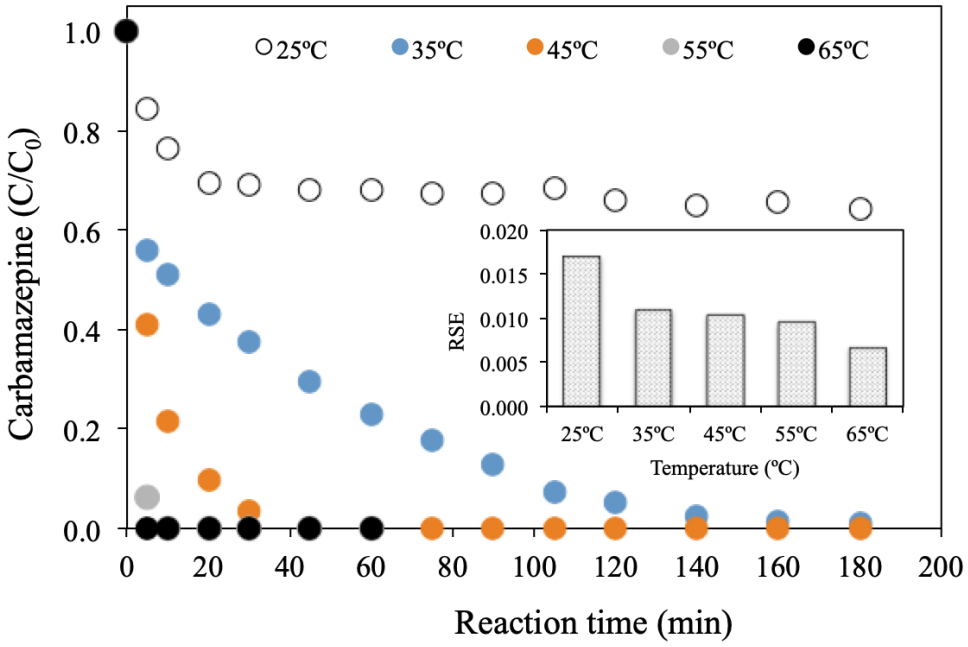

(a)

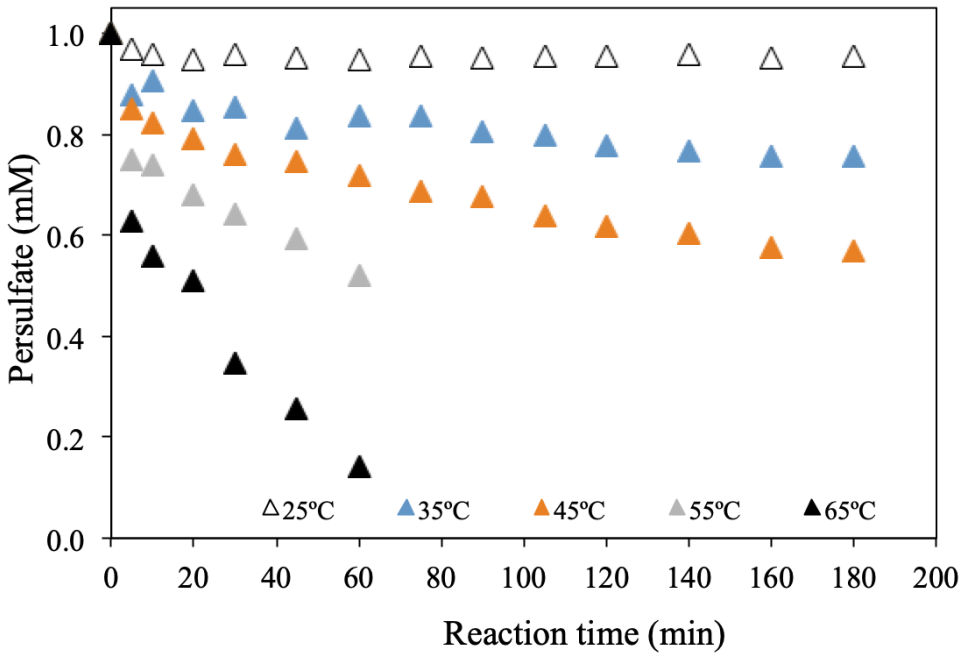

(b)

Figure 1. Effect of temperature on CBZ degradation (a) and PS decomposition (b). Experimental conditions: $[CBZ]_0$= 0.0025 mM, $[PS]_0$= 1 mM and T=25ºC/35ºC/45ºC/55ºC/65ºC.

The above explanation is also in accordance with model structure resulting from calibration process. If only heat-activation of PS is considered in the model, the agreement between experimental data and model prediction profiles is good only for 45, 55 and 65ºC experiments, i.e. once temperature is high enough to be the main activation mechanism. Including acid-catalyzed decomposition of PS in the reaction mechanism improved model accuracy allowing also an accurate prediction of the low temperature experiments. Another important aspect to enhance model predictions was to include a radical scavenging reaction, as the CBZ stock solution was prepared in methanol, which provides additional TOC (37 mg/L) in the reaction bulk affecting process performance. This situation is similar to the one found in natural surface waters and municipal WWTP secondary effluents, where similar TOC values are also found in the matrix. Mineralization was not selected as prediction objective because it is not a concern when dealing with CECs dissolved in real aqueous matrices, in which TOC concentration is in the order of several tens of mg/L, while the concentration of CECs is typically in the order of µg/L. Therefore, the mineralization of CECs cannot be detected in actual wastewater treatment conditions [39] and degradation of harmless TOC is not an objective of any advanced tertiary treatment designed to polish the effluent from conventional WWTPs [40].

As it can be seen in Figure 2, very good agreement between experimental results and model predictions were obtained both for CBZ and PS time-concentration profiles for the complete range of temperatures studied. The kinetic parameters of the proposed model are

shown in Table 2. The slowest reactions were those responsible of radical production (Reactions 1 and 2) being the lowest values obtained for PS heat-activation reaction (Reaction 1). The corresponding activation energy (E_A) obtained for this reaction (105.2 kJ/mol) is in the range of the reported values at acid pH (110-116 kJ/mol) [41]. On the contrary, the CBZ degradation reaction (Reactions 5) resulted in the highest kinetic parameters. E_A of CBZ was found to be 26.1 kJ/mol. This E_A is about 5 times lower than the values reported for some other pharmaceuticals such as ibuprofen (168 kJ/mol) [38], naproxen (155 kJ/mol) [23], ketoprofen (157 kJ/mol) [22] or bisoprolol (120 kJ/mol) [42].

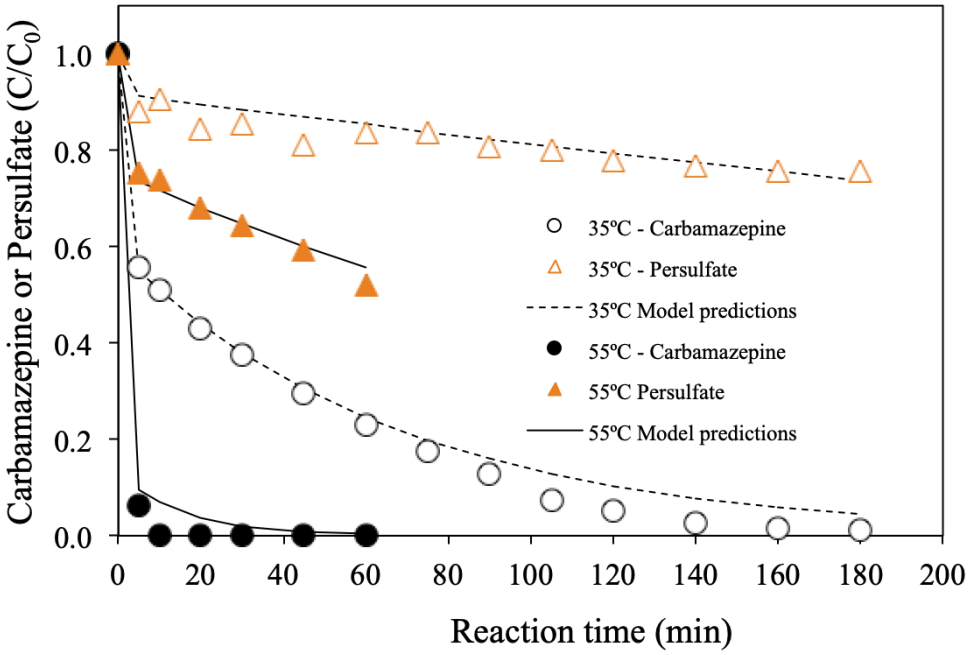

Figure 2. Comparison between experimental data (CBZ –dots- and PS –triangles-) and model predictions (lines) for the heat-activation experiments carried out at 35ºC and 55ºC. Experimental conditions: $[CBZ]_0$= 0.0025 mM and $[PS]_0$= 1 mM.

Table 2. Kinetic parameters resulting from the calibration of the heat-activated PS model at the different temperatures and the corresponding activation energy of the Arrhenius fitting.

		25ºC	35ºC	45ºC	55ºC	65ºC	E_A kJ/mol	r^2
k_1	min^{-1}	$(0.1\pm0.1)\cdot10^{-3}$	$(1.2\pm0.1)\cdot10^{-3}$	$(3.0\pm0.1)\cdot10^{-3}$	$(5.1\pm0.2)\cdot10^{-3}$	$(25.2\pm0.8)\cdot10^{-3}$	105.2	0.9496
k_2	$mM^{-1} min^{-1}$	0.069±0.001	0.089±0.002	0.147±0.006	0.326±0.014	0.404±0.026	40.4	0.9608
k_5		1.99±0.10	3.30±0.13	4.14±0.39	5.38±0.57	-	26.1	0.9722
k_6		0.141±0.006	0.150±0.007	0.156±0.011	0.159±0.005	-	3.2	0.9477

3.2 Iron-activation of PS

Sulfate radical can also be formed through the reaction of PS and metals in which one electron is transferred [30]. In this context, the use of iron has been widely studied because it presents low toxicity and low cost [43]. Furthermore, the use of its zero valent form in monometallic and multimetallic heterogeneous systems has been also evaluated presenting advantages on homogeneous systems mainly improving RSE with less iron sludge generation [28-29]. Based on the above considerations, in the next part of the study, the removal of CBZ (0.0025 mM) by Fe(II)-activated PS (1mM) under six different iron concentrations in the range from 0.009 mM to 0.18 mM (equivalent to 0.5 - 10 mg/L) at constant temperature (25ºC) was evaluated and modeled. In general, an important initial degradation of the pollutant is again observed and later the process is extremely slowed down due to the formation of Fe(III) (Figure 3). After 2 hours, the complete CBZ removal was not achieved in any case though, when 0.09 mM of Fe(II) or higher concentrations were used, about 90% oxidation was obtained within the first 5 min. Negligible differences in terms of CBZ removal were found between the experiments carried out with 0.09, 0.13 and 0.18 mM of Fe(II). This behavior, in which there is fast pollutant degradation at initial stages but, subsequently, asymptotic values of pollutant and oxidant agent are observed, is

in agreement with some other published works. Rodriguez et al. 2017 [35] reported similar process performance. Additionally, the authors indicated that an undesired reaction occurs that consumes both Fe(II) and PS if iron excess is added in the reaction bulk, which can justify the similarity between the experiments above 0.09 mM of iron. Minimizing this undesirable reaction (Reaction 7) is required to increase the efficiency of the oxidant, which could be obtained for instance by employing zero valent iron that allows a slow release of Fe(II). This was demonstrated by Ghauch and co-workers, who reported the superiority of ZVI particles in activating PS while keeping high performance of the system, especially because that reaction was accompanied with pH slight decrease favoring the continuous generation of iron species and iron corrosion products, which help PS activation in a controlled manner [27, 28]. Slight differences were also found between the experiments carried out with 0.009 and 0.018 mM of iron. For both concentrations, about 60% initial degradation was observed. Under these conditions, the process is probably initiated (mainly) by the above-mentioned acid-activation mechanism instead of iron-activation. Although it is not the objective of this work to optimize operating conditions, the effect of Fe:PS molar ratio on the final % CBZ degradation has been analyzed. The best result was obtained for 1:11 molar ratio (0.09 mM of iron and 1 mM of PS). The use of higher iron concentrations corresponding to 1:9 and 1:6 molar ratios did not improve CBZ degradation while the use of lower iron concentrations corresponding to 1:22, 1:56 and 1:111 molar ratios resulted in lower CBZ degradation percentages. This is in accordance with the results obtained by Amasha et al. 2018 [22], who studied the degradation of ketaprofen comparing different Fe:PS molar ratios at different PS initial concentrations. At the same PS initial concentration than the one used in this work (1 mM), it was found that 1:10 molar ratio was the most adequate value to obtain the highest pollutant degradation. The main difference

with the present work is that the final ketaprofen degradation did not remain constant but decreased when Fe:PS molar ratio was changed to 1:5 and 1:1 by increasing iron concentration. In this sense, it seems that quenching reactions cause a more negative effect on process performance when the pollutant concentration is in the range of mg/L than when it is in the range of µg/L, as in the latter the amount of radicals needed to achieve the complete pollutant degradation is much lower.

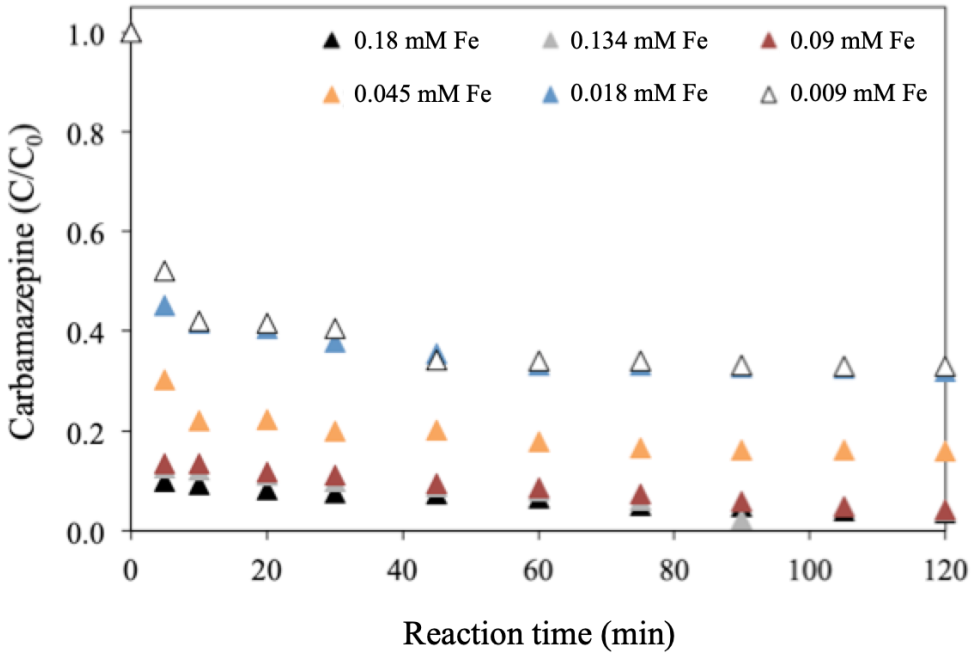

(a)

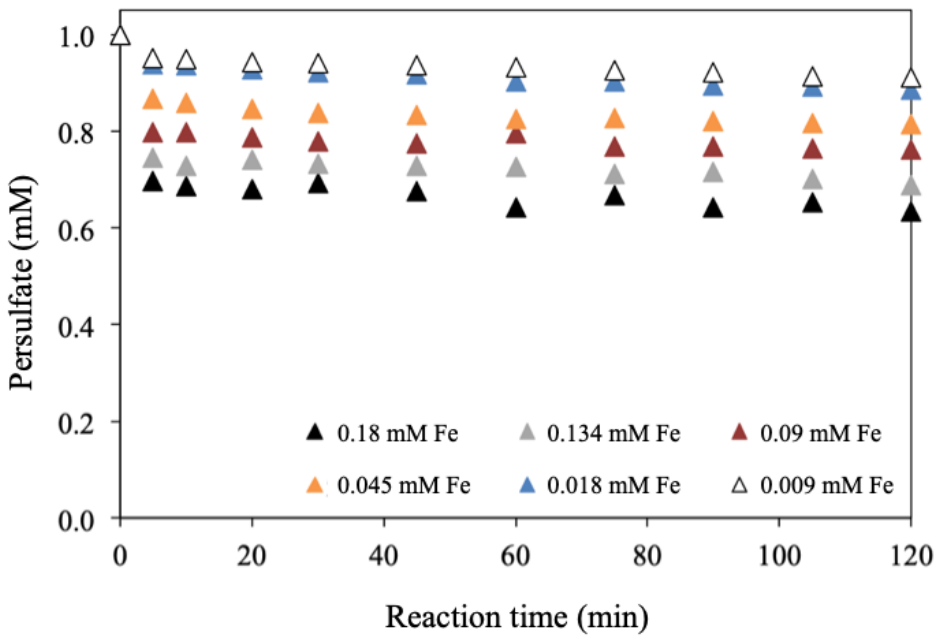

(b)

Figure 3. Effect of iron concentration on CBZ degradation (a) and PS decomposition (b) for the assays carried out at 25ºC. Experimental conditions: $[CBZ]_0$= 0.0025 mM, $[CBZ]_0$= 0.0025 mM, $[Fe]_0$= 0.009 mM/0.018 mM/0.045 mM/0.09 mM/0.134 mM/0.18 mM and $[PS]_0$= 1 mM.

In the next experimental series, the same iron concentrations were used but increasing the operation temperature to 35ºC (Figure 4). In all the cases, reaction kinetics improved with respect to the previous experimental series carried out at 25ºC. The complete degradation of CBZ was achieved in approximately 40 min when iron concentrations of 0.09 mM or higher were used. Again, negligible differences between the experiments with 0.09, 0.13 and 0.18 mM of iron were found. In the case of the experiment with 0.045 mM of iron, the pollutant could be also completely degraded after 100 min. In contrast, the assays with 0.009 and 0.018 mM of iron only allowed reaching ≈70% and ≈80% degradation,

respectively, after 120 min. With respect to Fe:PS molar ratio, a similar trend than the one obtained for the set of experiments carried out at 25ºC was found, being again 1:11 molar ratio the most adequate option.

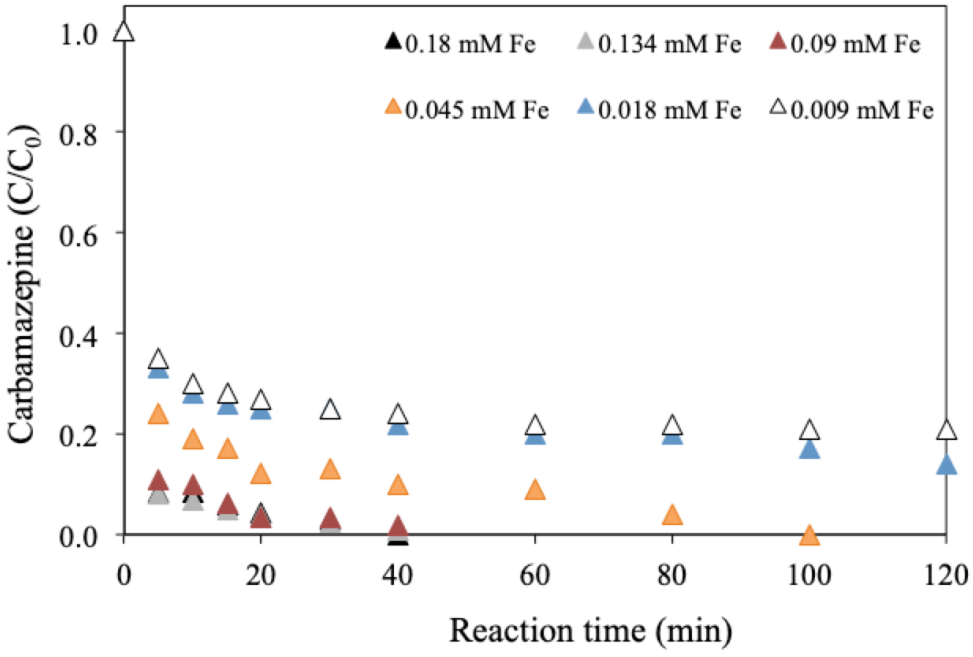

(a)

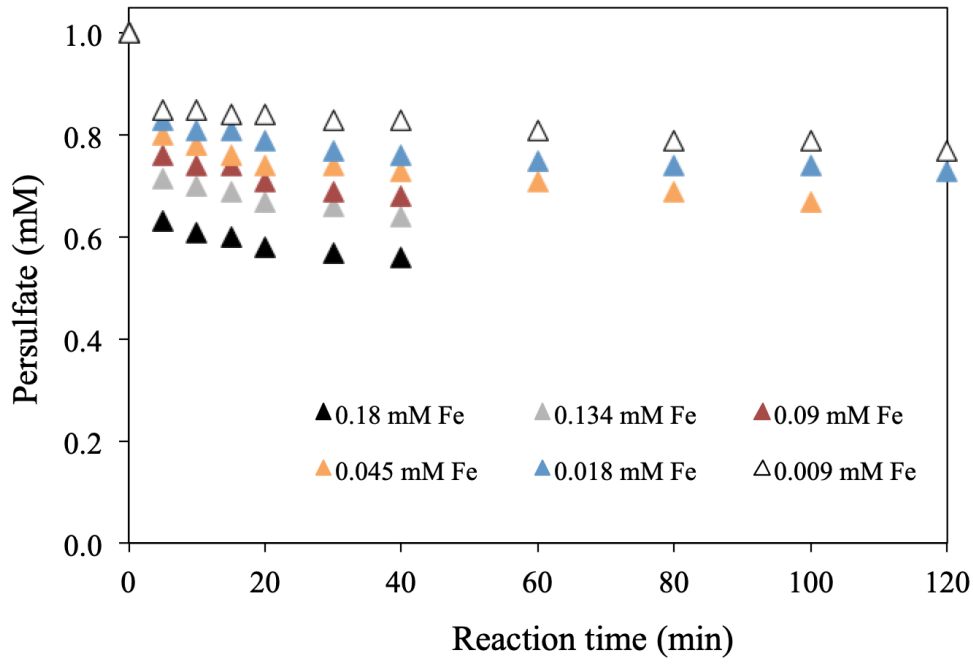

(b)

Figure 4. Effect of iron concentration on CBZ degradation (a) and PS decomposition (b) for the assays carried out at 35ºC. Experimental conditions: $[CBZ]_0$= 0.0025 mM, $[Fe]_0$= 0.009 mM/0.018 mM/0.045 mM/0.09 mM/0.134 mM/0.18 mM and $[PS]_0$= 1 mM.

The semi-empirical model proposed in the previous section was modified in order to include the activation of PS by iron species. In this way, Fe(II) and Fe(III) activation reactions (Reactions 3 and 4) were added in the mechanism and the model was again calibrated. In the first calibration step, only PS decomposition data was used to determine the kinetic constants of both Fe(II) and Fe(III) activation reactions, using the already obtained model parameters in the temperature experimental series (Table 3) for acid and heat activation (k_1 and k_2). This option left to acceptable predictions, however, a better agreement between simulated and experimental profiles of PS decomposition was obtained after model fine-tuning. The calibration process showed that, in the range from 25ºC to 35ºC, the model prediction capability improves if heat-activation is not considered in the model. Probably, this happens because it presents a small effect on process performance that can be implicitly included in the iron-activation reactions. On the contrary, this did not happen with acid-activation, which still showed an important effect on process performance. The next step was to include CBZ oxidation and scavenging reactions into the model and to simulate also the pollutant degradation profile. In addition, Fe(II) scavenging of radicals reaction (Reaction 7) was also included in the model to describe the negative effect of iron excess on process performance. Again, the values of the kinetic constants already available from the temperature experimental series (k_5 and k_6) were initially used determining only the kinetic parameter of Fe(II) scavenging reaction. As in the previous calibration stage, although model prediction was acceptable, it improved after model fine-

tuning. The comparison between experimental data and model predictions for the assays carried out with 5 mg/L of iron at 25ºC and 35ºC is shown in Figure 5. As it can be seen in the simulated profiles, the model prediction capability is high in both cases.

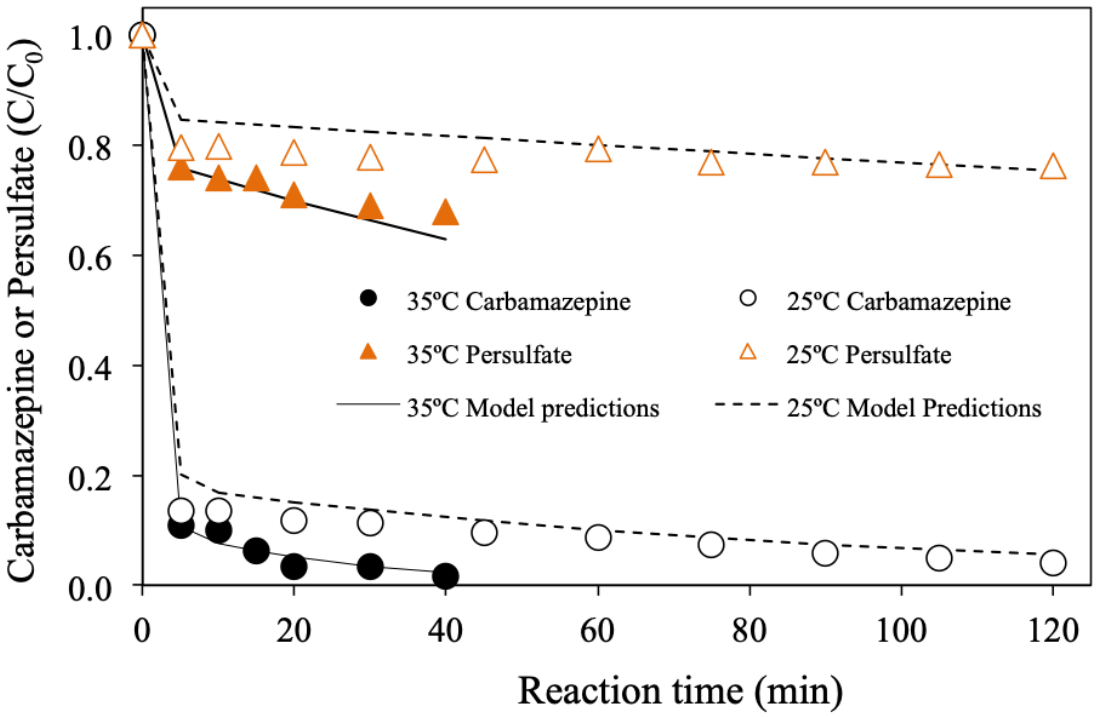

Figure 5. Comparison between experimental data (CBZ –dots- and PS –triangles-) and model simulations (lines) for the experiments carried out with $[CBZ]_0$= 0.0025 mM, $[Fe]_0$= 0.09 mM, $[PS]_0$= 1 mM and T=25ºC/35ºC.

Therefore, the final proposed model includes 3 reactions related to radical formation and 3 reactions related to radical consumption. PS can be activated to produce (mainly) sulfate radicals by acid conditions (Reaction 2), Fe(II) (Reaction 3) and Fe(III) (Reaction 4). With respect to heat-activation, it is not necessary to implicitly consider this mechanism in the model because it seems to be included through iron-activation reactions. With respect to

radicals consumption, their reactions with CBZ, organic matter and Fe(II) were considered. The kinetic parameters obtained by model fitting are presented in Table 3. This table shows that Fe(II) is the main responsible of PS activation with an small contribution of acid-activation. After the oxidation of Fe(II) to Fe(III), there is also PS activation by Fe(III), although it is extremely slow. The fastest reaction of the whole model was CBZ oxidation followed by Fe(II) oxidation by sulfate radical. Again, Fe(II)-activation of PS was the most important activation mechanism, with an initial contribution of acid-activation that has to be considered in the model and a very slow Fe(III) impact.

Table 3. Kinetic parameters for the iron concentration experimental series resulting from model fine-tuning.

	k_2	k_3	k_4	k_5	k_6	k_7
	$mM^{-1}\ min^{-1}$					
25ºC	2.04±0.16	0.0056±0.0009	0.016±0.008	16.42±0.96	0.46±0.11	8.25±0.92
35ºC	5.37±0.87	0.030±0.008	0.037±0.010	23.01±1.34	0.77±0.20	18.92±2.3

3.3 Model Validation

One assay from each experimental series (heat-activation, Fe(II)-activation at 25 and 35ºC) was not used for model calibration so that these could be used for model validation. In the case of the heat-activation experimental series, the assay carried out at 45ºC was the one selected for model validation. As it can be observed in Figure 6a, good agreement between experimental data and model simulations was obtained for both CBZ oxidation and PS decomposition profiles, validating the model proposed, which includes heat-activation plus acid-activation. In the case of the Fe(II)-activation model, the validation experiments are

presented in Figure 6b. Again, the model showed great prediction accuracy validating the semi-empirical approach in which only Fe(II)-activation and acid-activation are considered.

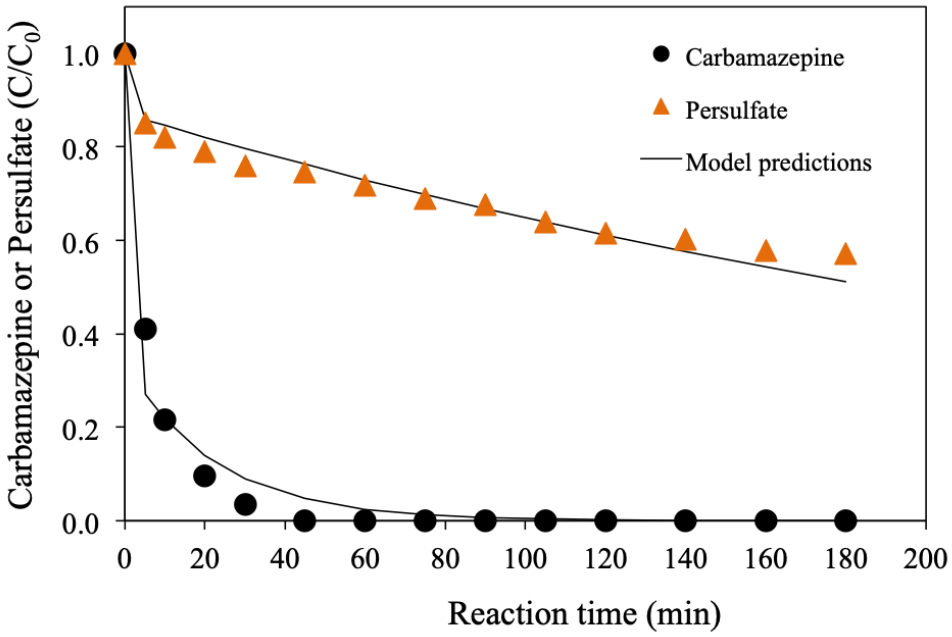

(a)

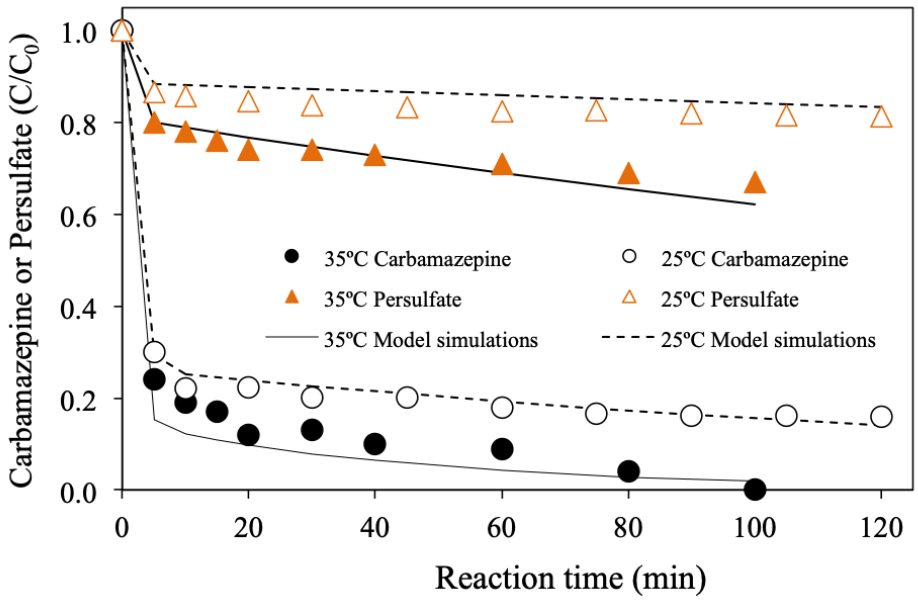

(b)

Figure 6. Comparison between experimental data (CBZ –dots- and PS –triangles-) and model predictions (lines) for the heat-activation experiment validation (a) and the iron

activation experiments validation (b). Experimental conditions: (a) $[CBZ]_0$= 0.0025 mM, $[PS]_0$= 1 mM and T=45ºC (b) $[CBZ]_0$= 0.0025 mM, $[Fe]_0$= 0.045 mM, $[PS]_0$= 1 mM and T=25ºC/35ºC.

Finally, two new validation experiments were carried out. In the first one, the removal of CBZ (0.0025 mM) using PS (1 mM) activated by different and low Fe(II) additions (0.018 mM each at 0, 10 and 20 min) was studied. Three steps can be clearly identified in the decontamination process corresponding to each one of the iron additions (Figure 7a). Initially, an important degradation is produced and, then, the process is almost stopped. The CBZ oxidation steps diminished with each one of the iron additions resulting in 60%, 20% and 10%. The model adequately predicts this process behavior; nevertheless, the prediction capability for CBZ removal diminished after the first addition. The initial CBZ concentration in all the experimental series used to develop the model was constant at 0.0025 mM. Consequently, the model has not been trained for concentrations lower than 0.0025 mM, as ≈0.001 mM and ≈0.0005 mM, concentrations measured when the second and third additions were done. A similar trend can be observed for PS decomposition. While the simulation for the first addition is adequate, in the second and third ones the PS concentration is overestimated. In the last validation experiment, the removal of CBZ (0.0025 mM) using 0.09 mM of Fe(II) and three PS additions (0.17 mM each at 0, 10 and 20 min) was studied. In this case, it is difficult to identify the additions in the CBZ oxidation curve, which is indeed extremely similar to the curves obtained in the Fe(II)-activation experimental series. After the first addition, almost 60% CBZ oxidation was obtained, then, 5% oxidation was achieved in the second one and, finally, the third addition resulted in only 2% degradation. This process behavior is well predicted by the model,

indeed, model simulation shows that almost all the Fe(II) present initially in solution is already oxidized to Fe(III) (see Figure 7b) after the first PS addition. Consequently it can be said that the model is able to successfully simulate both CBZ oxidation process and PS decomposition, showing that it can be used as a predictive tool.

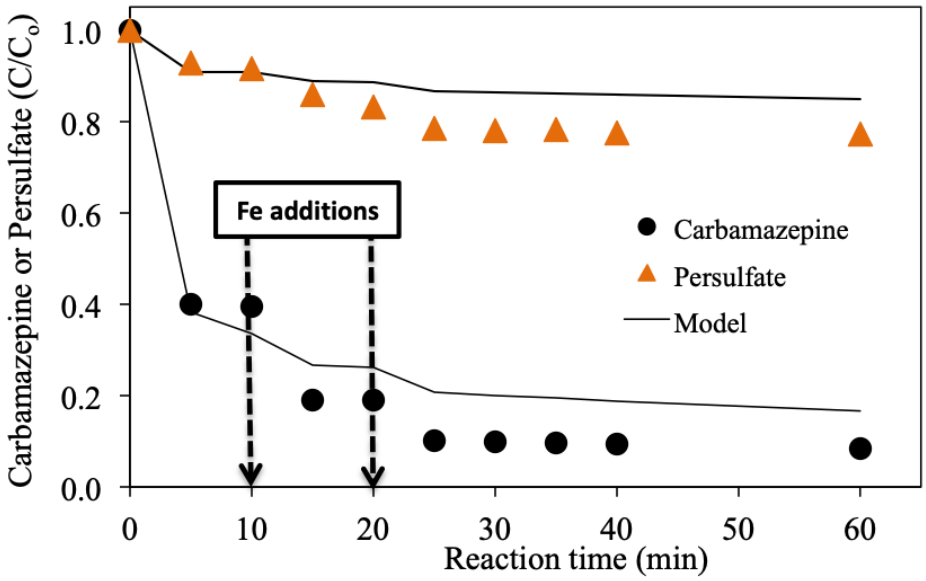

(a)

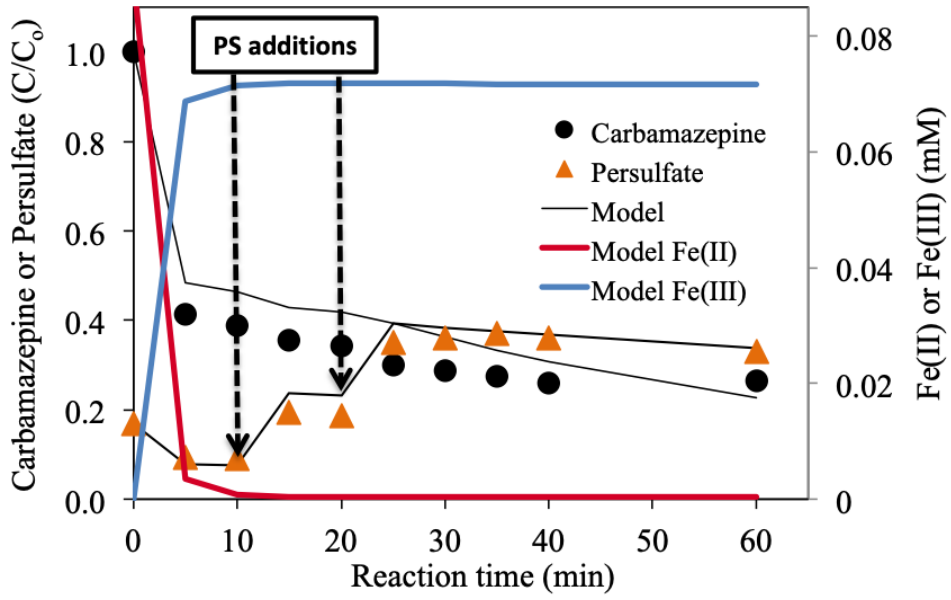

(b)

Figure 7. Comparison between experimental data (dots) and model predictions (lines) for

the experiment validation carried out with iron additions (a) and PS additions (b). Experimental conditions: (a) $[CBZ]_0$= 0.0025 mM, $[PS]_0$= 1mM, $[Fe]_0$= 0.018 mM, $[Fe]_{additions}$= 0.018 mM and T=25ºC (b) $[CBZ]_0$= 0.0025 mM, $[Fe]_0$= 0.09 mM, $[PS]_0$= 0.17 mM, $[PS]_{additions}$= 0.17 mM and T=25ºC.

4. Conclusions

A semi-empirical mathematical model of the heat-activated and iron-activated PS processes applied to the removal of CECs in water using CBZ as model pollutant has been proposed and validated.

In the heat-activated experimental series, the selected temperature range was 25ºC-65ºC. The CBZ degradation reached 20% at 25ºC after 120 min while, from 35ºC; the complete degradation of the pollutant was always achieved. Kinetics always improved with temperature. The obtained RSE was very low, in the range of 0.017 at 25ºC to 0.007 at 65ºC, which seems to be related to acidic conditions and the low initial concentration of CBZ. The highest model prediction capability was obtained when heat and acid activation of PS were considered in the reaction mechanism, which included also CBZ degradation reaction and TOC scavenging reaction. Very good agreement between experimental results and model predictions were obtained both for CBZ and PS time-concentration profiles for the complete range of temperatures studied.

In the next experimental series, six different Fe(II) concentrations in the range from 0.009 to 0.18 mM at 25ºC and 35ºC were evaluated. At the lowest temperature, the complete CBZ removal was not achieved in any case, although about 90% degradation in the first 5 min was obtained when 0.09 mM of Fe(II) or higher concentrations were used. The fast pollutant degradation at initial stages and the asymptotic values of pollutant and oxidant

agent obtained subsequently suggest that undesired reactions that consume both Fe(II) and PS^{-} are favored if iron excess is added in the reaction bulk. At 35ºC, the complete degradation of CBZ was obtained in about 40 min when Fe(II) concentration was 0.09 mM or higher, finding again negligible differences between the experiments with 0.09, 0.13 and 0.18 mM of iron. The best results in terms of final pollutant degradation and degradation rate were obtained for 1:11 Fe:PS molar ratio at both temperatures. With respect to model reaction mechanism for this part of the study, the calibration process showed that the model prediction capability improves if PS heat activation is not considered. Probably, this is due to its small effect on process performance, which can be included in the iron-activation reactions. On the contrary, this did not happen with acid-activation, which still showed an important contribution to the process. Thus, the model reaction mechanism that showed the highest prediction accuracy includes: acid, Fe(II) and Fe(III) PS activation, CBZ degradation and both TOC and Fe(II) scavenging reactions.

Finally, the model was validated using one assay from each experimental series (heat-activation, iron-activation at 25ºC and iron-activation at 35ºC) and two additional assays, one using Fe(II) additions (0.018 mM each at 0, 10 and 20 min) and another one using PS additions (0.17 mM each at 0, 10 and 20 min) with satisfactory results.

In conclusion, a predictive tool for the use of PS in the removal of contaminants of emerging concern has been developed. This type of studies are needed in order to get the process closer to actual application, as models allow simulating the process, optimizing operation conditions or scaling-up reactors, among others. Further studies are needed in order to improve the model so that the effect of some other important variables such as sun-light and matrix content can be also considered.

5. Acknowledgments

A. Cabrera-Reina wants to thank FONDECYT 11160680 for the financial support of his research stay at Plataforma Solar de Almería and SERC Chile (FONDAP 15110019). The authors wish to thank CONICYT (International Cooperation Program, REDES 180149), FONDECYT 11170122 and the Spanish Ministry of Science, Innovation and Universities for funding under the CalypSol Project (Reference: RTI2018-097997-B-C32).

6. References

[1] Krzeminski, P., Tomei, M.C., Karaolia, P., Langenhoff, A., Almeida, C.M.A., Felis, E., Gritten, F., Andersen, H.R., Fernandes, T., Manaia, C.M., Rizzo, L., Fatta-Kassinos, D., Performance of secondary wastewater treatment methods for the removal of contaminants of emerging concern implicated in crop uptake and antibiotic resistance spread: a review. Sci. Total Environ. Volume 648, (2019) Pages 1052–1081 https://doi.org/10.1016/j.scitotenv.2018.08.130

[2] Petrie, B., Barden, R., Kasprzyk-Hordern B., A review on emerging contaminants in wastewaters and the environment: Current knowledge, understudied areas and recommendations for future monitoring, Water Res., Volume 72, (2015) Pages 3-27, https://doi.org/10.1016/j.watres.2014.08.053

[3] Sousa J.C.G., Ribeiro, A.R., Barbosa, M., Pereira, F., Silva, A.M.T., A review on environmental monitoring of water organic pollutants identified by EU guidelines, J. Hazard., Volume 344, (2018) Pages 146-162, https://doi.org/10.1016/j.jhazmat.2017.09.058

[4] Grassi, M., Rizzo, L., Farina, A., Endocrine disruptors compounds, pharmaceuticals and personal care products in urban wastewater: implications for agricultural reuse and their

removal by adsorption process. Environ. Sci. Pollut. R., Volume 20, (2013) Pages 3616-3628, https://doi.org/10.1007/s11356-013-1636-7

[5] Roig, B., Pharmaceuticals in the Environment: Current knowledge and need assessment to reduce presence and impact, IWA Publishing, (2010) ISBN: 9781843393146

[6] Zhang, Y., Geiben, S., Gal, C., Carbamazepine and diclofenac: Removal in wastewater treatment plants and occurrence in water bodies, Chemosphere, Volume 73, (2008) Pages 1151-1161 https://doi.org/10.1016/j.chemosphere.2008.07.086

[7] Yang, Y., Sik Ok, Y., Kim, K., Kwon, E.E., Fai Tsang, Y., Occurrences and removal of pharmaceuticals and personal care products (PPCPs) in drinking water and water/sewage treatment plants: A review, Sci. Total Environ., Volumes 596–597, (2017) Pages 303-320, https://doi.org/10.1016/j.scitotenv.2017.04.102

[8] Wood, T.P., Duvenage, C.S.J., Rohwer, E., The occurrence of anti-retroviral compounds used for HIV treatment in South African surface water, Environ. Pollut., Volume 199, (2015) Pages 235-243, https://doi.org/10.1016/j.envpol.2015.01.030

[9] Hernando, M.D., Mezcua, M., Fernández-Alba, A.R., Barceló, D., Environmental risk assessment of pharmaceutical residues in wastewater effluents, surface waters and sediments, Talanta, Volume 69 (2), (2006) Pages 334-342, https://doi.org/10.1016/j.talanta.2005.09.037

[10] Kleywegt, S., Pileggi, V., Chunyan Hao, P.Y., Zhao, X., Rocks, C., Thach, S., Cheung, P., Whitehead, B., Pharmaceuticals, hormones and bisphenol A in untreated source and finished drinking water in Ontario, Canada — Occurrence and treatment efficiency, Sci. Total Environ., Volume 409 (8), (2011) Pages 1481-1488, https://doi.org/10.1016/j.scitotenv.2011.01.010

[11] Costa, E., Roccamante, M., Amorim, C., Oller, I., Sánchez Pérez, J.A., Malato, S., New trend on open solar photoreactors to treat micropollutants by photo-Fenton at circumneutral pH: Increasing optical pathway, Chem. Eng. J., Volume 385, (2020) 123982, https://doi.org/10.1016/j.cej.2019.123982

[12] Du, S., Bai, X., Xu, L., Yang, L., Jin, P., Visible-light activation of persulfate by TiO_2/g-C_3N_4 photocatalyst toward efficient degradation of micropollutants, Chem. Eng. J., Volume 384 (2020) 123245, https://doi.org/10.1016/j.cej.2019.123245

[13] Gauch, A., Baydoun, H., Dermesropian, P., Degradation of aqueous carbamazepine in ultrasonic/Fe^0/H_2O_2 systems, Chem. Eng. J. Volume 172 (1), (2011) Pages 18-27 https://doi.org/10.1016/j.cej.2011.04.002

[14] Wacławek, S., Lutze, H.V., Grübel, K., Padil, V.V.T., Černík, M., Dionysiou, D.D., Chemistry of persulfates in water and wastewater treatment: A review, Chem. Eng. J., Volume 330, (2017) Pages 44-62, https://doi.org/10.1016/j.cej.2017.07.132

[15] Miralles-Cuevas, S., Darowna, D., Wanag, A., Mozia, S., Malato, S., Oller, I., Comparison of UV/H_2O_2, UV/$S_2O_8^{2-}$, solar/Fe(II)/H_2O_2 and solar/Fe(II)/$S_2O_8^{2-}$ at pilot plant scale for the elimination of micro-contaminants in natural water: An economic assessment, Chem. Eng. J., Volume 310 (2), (2017) Pages 514-524, https://doi.org/10.1016/j.cej.2016.06.121

[16] Matzek, L., Carter, K.E., Activated persulfate for organic chemical degradation: A review, Chemosphere, Volume 151, (2016) Pages 178-188, https://doi.org/10.1016/j.chemosphere.2016.02.055

[17] Rodriguez, S., Vasquez, L., Costa, D., Romero, A., Santos, A. Oxidation of Orange G by persulfate activated by Fe(II), Fe(III) and zero valent iron (ZVI) Chemosphere, Volume 101, (2014) Pages 86-92 https://doi.org/10.1016/j.chemosphere.2013.12.037

[18] Zhang, R., Sun, P., Boyer, T.H., Zhao, L., Huang, C.H., Degradation of pharmaceuticals and metabolite in synthetic human urine by UV, UV/H_2O_2, and UV/PDS Environ. Sci. Technol., Volume 49 (5), (2015) Pages 3056-3066. https://doi.org/10.1021/es504799n

[19] Ghauch, A., Baalbaki, A., Amasha, M., El Asmar, R., Tantawi, O., Contribution of persulfate in UV-254 nm activated systems for complete degradation of chloramphenicol antibiotic in water Chem. Eng. J. Volume 317, (2017) Pages 1012-1025 https://doi.org/10.1016/j.cej.2017.02.133

[20] Al Hakim, S., Jaber, S., Eddine, N., Baalbaki, A., Ghauch, A., Degradation of theophylline in a UV254/PS system: Matrix effect and application to a factory effluent, Chem. Eng. J., Volume 380, (2020) 122478, https://doi.org/10.1016/j.cej.2019.122478

[21] Tan, C., Gao, N., Deng, Y., An, N., Deng, J., Heat-activated persulfate oxidation of diuron in water, Chem. Eng. J., Volume 203, (2012) Pages 294-300, https://doi.org/10.1016/j.cej.2012.07.005

[22] Amasha, M., Baalbaki, A., Ghauch, A., A comparative study of the common persulfate activation techniques for the complete degradation of an NSAID: The case of ketoprofen, Chem. Eng. J., Volume 350, (2018) Pages 395-410, https://doi.org/10.1016/j.cej.2018.05.118

[23] Ghauch, A., Tuqan A.M., Kibbi, N., Naproxen abatement by thermally activated persulfate in aqueous systems, Chem. Eng. J., Volume 279, (2015) Pages 861-873 https://doi.org/10.1016/j.cej.2015.05.067

[24] Ji, Y., Dong, C., Kong, D., Lu, J., Zhou, Q., Heat-activated persulfate oxidation of atrazine: Implications for remediation of groundwater contaminated by herbicides, Chem. Eng. J., Volume 263, (2015) Pages 45-54, https://doi.org/10.1016/j.cej.2014.10.097

[25] Zhao, L., Hou, H., Fujii, A., Hosomi, M., Li, F. Degradation of 1,4-dioxane in water with heat- and Fe^{2+}-activated persulfate oxidation, Environ. Sci. Pollut. R., Volume 21 (12), (2014) Pages 7457-7465. https://doi.org/10.1007/s11356-014-2668-3

[26] Miralles-Cuevas, S., Oller, I., Ruíz-Delgado, A., Cabrera-Reina, A., Cornejo-Ponce, L., Malato, S., EDDS as complexing agent for enhancing solar advanced oxidation processes in natural water: Effect of iron species and different oxidants, J. Hazard. Mater., Volume 372, (2019) Pages 129-136 https://doi.org/10.1016/j.jhazmat.2018.03.018

[27] Ghauch, A., Ayoub, G., Naim, S., Degradation of sulfamethoxazole by persulfate assisted micrometric Fe^0 in aqueous solution, Chem. Eng. J., Volume 228, (2013) Pages 1168-1181 https://doi.org/10.1016/j.cej.2013.05.045

[28] Ayoub, G., Ghauch, A., Assessment of bimetallic and trimetallic iron-based systems for persulfate activation: application to sulfamethoxazole degradation, Chem. Eng. J., Volume 256, (2014) Pages 280-292 https://doi.org/10.1016/j.cej.2014.07.002

[29] Naim, S., Ghauch, A., Ranitidine abatement in chemically activated persulfate systems: assessment of industrial iron waste for sustainable applications Chem. Eng. J., Volume 288, (2016) Pages 276-288 https://doi.org/10.1016/j.cej.2015.11.101

[30] Lominchar, M.A., Rodríguez, S., Lorenzo, D., Santos, N., Romero, A., Santos, A. Phenol abatement using persulfate activated by nZVI, H2O2 and NaOH and development of a kinetic model for alkaline activation, Environ. Techn. (United Kingdom), Volume 39 (1), (2018) Pages 35-43 https://doi.org/10.1080/09593330.2017.1294203

[31] Vicente, F., Santos, A., Romero, A., Rodriguez, S. Kinetic study of diuron oxidation and mineralization by persulphate: Effects of temperature, oxidant concentration and iron dosage method Chem. Eng. J., Volume 170 (1), (2011) Pages 127-135 https://doi.org/10.1016/j.cej.2011.03.042

[32] Ji, Y., Ferronato, C., Salvador, A., Yang, X., Chovelon, J.-M. Degradation of ciprofloxacin and sulfamethoxazole by ferrous-activated persulfate: Implications for remediation of groundwater contaminated by antibiotics, Sci. Total Environ., Volume 472, (2014) Pages 800-808 https://doi.org/10.1016/j.scitotenv.2013.11.008

[33] Kusic, H., Peternel, I., Ukic, S., Koprivanac, N., Bolanca, T., Papic, S., Loncaric Bozic, A. Modeling of iron activated persulfate oxidation treating reactive azo dye in water matrix. Chem. Eng. J., Volume 172, (2011) Pages 109–121 https://doi.org/10.1016/j.cej.2011.05.076

[34] Bu, L., Shi, Z., Zhou, S., Modeling of Fe(II)-activated persulfate oxidation using atrazine as a target contaminant, Sep. Purif. Technol., Volume 169, (2016) Pages 59–65 https://doi.org/10.1016/j.seppur.2016.05.037

[35] Rodriguez, S., Santos, A., Romero, A., Oxidation of priority and emerging pollutants with persulfate activated by iron: Effect of iron valence and particle size, Chem. Eng. J., Volume 318, (2017) Pages 197-205, https://doi.org/10.1016/j.cej.2016.06.057

[36] Kolthoff, I.M., Miller, I.K., 1951. The chemistry of persulfate 1. The kinetics and mechanism of the decomposition of the persulfate ion in aqueous medium. J. Am. Chem. Soc., Volume 73, (1951), Pages 3055-3059, https://doi.org/10.1021/ja01151a024

[37] Liang, C., Wang Z-S., Bruell, C.J., Influence of pH on persulfate oxidation of TCE at ambient temperatures, Chemosphere, Volume 66, Issue 1, (2007) Pages 106-113, https://doi.org/10.1016/j.chemosphere.2006.05.026

[38] Ghauch, A., Tuqan A.M., Kibbi, N., Ibuprofen removal by heated persulfate in aqueous solution: A kinetics study, Chem. Eng. J., Volume 197, (2012) Pages 483–492 http://dx.doi.org/10.1016/j.cej.2012.05.051

[39] Soriano-Molina, P., García Sánchez, J.L., Malato, S., Plaza-Bolaños, P., Agüera, A., Sánchez Pérez, J.A., On the design and operation of solar photo-Fenton open reactors for the removal of contaminants of emerging concern from WWTP effluents at neutral pH, Appl. Catal. B Environ., Volume 256, (2019) 117801 https://doi.org/10.1016/j.apcatb.2019.117801

[40] Bourgin, M., Beck, B., Boehler, M., Borowska, E., Fleiner, J., Salhi, E., Teichler, R., von Gunten, U., Siegrist, H., McArdell, C.S., Evaluation of a full-scale wastewater treatment plant upgraded with ozonation and biological post-treatments: abatement of micropollutants, formation of transformation products and oxidation by-products. Water Res. Volume 129, (2018) Pages 486–498 https://doi.org/10.1016/j.watres.2017.10.036

[41] House, D.A., Kinetics and mechanism of oxidations by peroxydisulfate. Chem. Rev., Volume 62 (3), (1962) Pages 185-203, https://doi.org/10.1021/cr60217a001

[42] Ghauch, A., Tuqan, A.M., Oxidation of bisoprolol in heated persulfate/H_2O systems: kinetics and products, Chem. Eng. J., Volume 183, (2012) Pages 162–171 https://doi.org/10.1016/j.cej.2011.12.048

[43] Zhang, M., Chen, X., Zhou, H., Murugananthan, M., Zhang, Y., Degradation of p-nitrophenol by heat and metal ions co-activated persulfate, Chem. Eng. J., Volume 264, (2015) Pages 39-47, https://doi.org/10.1016/j.cej.2014.11.060

Modeling persulfate activation by iron and heat for the removal of contaminants of emerging concern using carbamazepine as model pollutant

Cabrera-Reina, A.[1], Miralles-Cuevas, S.[2,3], Oller, I.[3,4], Sánchez-Pérez, J.A.[2,3], Malato, S.[3,4]

[1] Engineering Faculty, University of Tarapacá, Avda. General Velásquez, Arica, Chile
[2] Chemical Engineering Department, University of Almería, Ctra. Sacramento s/n, Almería, Spain
[3] CIESOL, Joint Centre of the University of Almería-CIEMAT, Ctra. Sacramento s/n, Almería Spain
[4] Plataforma Solar de Almeria-CIEMAT, Carretera de Senés, km 4, Tabernas, Spain

Corresponding authors: Cabrera-Reina, A. (acabrera@limza.cl)

Oller, I. (isabel.oller@psa.es)

Abstract

A semi-empirical model of heat-activated and iron-activated persulfate (PS) processes applied to the removal of carbamazepine (CBZ) in water at low concentration (0.0025 mM) has been proposed and validated. In heat-activation systems, carried out at pH 3, temperature was varied from 25ºC to 65ºC, and acid-activation of PS showed an important initial role in the process. In iron-activated experimental series, iron concentration was changed from 0.009 mM to 0.18 mM at two different temperatures (25ºC and 35ºC), heat-activation was negligible with iron being the main activation mechanism and acid-activation showing also an important initial effect on process performance. High model prediction capability for both CBZ degradation and PS decomposition profiles was obtained in each case. Finally, the model was validated including supplementary experiments based on Fe(II) additions (0.018 mM each) and PS additions (0.17 mM) throughout the treatment. Developed model in this work is a powerful predictive tool for the application of PS in the removal of contaminants of emerging concern in water.

Keywords: modelling, microcontaminants, tertiary treatment, kinetics, wastewater

1. Introduction

Contaminants of emerging concern (CECs) are unregulated substances that enter the environment at low concentrations, among others, through municipal wastewater treatment plants (MWWTP) because biological systems were not designed for their removal [1]. Their properties make CECs highly risky for the environment and human health as they are bio-accumulative substances, very persistent in the environment and, at the same time, show a great capacity for transformation, generating intermediate products, such as metabolites, which, in many occasions, are more toxic than the parent compounds [2]. Personal care products, antiseptics, detergents and their metabolites, gasoline additives and industrial agents, among others, are considered as CECs [3]. Nevertheless, the ones that are possibly causing the greatest concern are the pharmaceutical products and, in particular, antibiotics [4]. The use of pharmaceutical products in European Union countries has been estimated of thousands of tons per year, and the majority of the most consumed, including antibiotics, are used in amounts similar to those of pesticides. Indeed, the presence of more than 3,000 pharmaceuticals in the aquatic environment has been already reported by Roig 2010 [5]. In this study, the carbamazepine (CBZ) was selected as CEC model because it is a bio-recalcitrant microcontaminant that is not efficiently removed by MWWTPs and usually reaches water bodies. According to Zhang et al. 2008 [6], CBZ has been detected in MWWTP effluents and surface waters around the world, as happens in Germany where it has been found at concentrations of around 3 µg/L in MWWTP effluents and 0.5 µg/L in surface waters. Moreover, according to several researchers, this pollutant is frequently detected in surface water, groundwater and even in drinking water at ng/L- µg/L levels [3, 7-10]. Therefore, it is a good indicator for following the performance of an advanced tertiary treatment to polish the effluent from conventional MWWTPs and it has been

widely used for AOPs applications research, e.g. in solar photo-Fenton [11], PS/TiO_2 [12] or improved methods such as the combination of ultrasonication, zero valent iron and hydrogen peroxide [13].

To prevent the entry of these CECs into the environment and also to achieve good water-reuse quality, an advanced tertiary treatment must be proposed and carried out as a final step in the treatment of MWWTP effluents. In recent years, sulfate radical-based advanced oxidation processes ($SO_4^{\bullet-}$-AOPs) applied to the removal of CECs are being investigated as an alternative to AOPs only based on the generation of hydroxyl radicals [14]. Sulfate radical, which has an oxidation potential similar to the one of hydroxyl radical, is very efficient to degrade CECs at low concentrations and environmentally friendly [15-17]. PS activation to form highly reactive species can be achieved by many different mechanisms in homogeneous as well as in heterogeneous media: UV light [18-20], thermal energy [21-23], acidic and alkaline conditions [24] or transition metals, e.g. silver, iron, copper, zinc. These transition metals can be in the form of dissolved salts in solution [25, 26] or zero valent metals being monometallic or bi/trimetallics iron based systems (commercial or scrap waste collected from the car industry) [27-29]. The feasibility of $SO_4^{\bullet-}$ based-AOPs for CECs abatement has already been proven, furthermore, several investigations about kinetics, degradation mechanism of different contaminants and the effect of water matrix on process performance have been reported [17, 30-32]. Therefore, considering that the basic knowledge of the PS oxidation process is high, new research focused on pilot plant scale studies, economic assessments, modelling, etc. is needed in order to favor the appearance of PS actual applications. Few studies about PS modelling can be found in the literature. Kusic et al. 2011 [33] developed a first principle mathematical model to predict decolorization of Reactive Red 45 and mineralization using PS activated via zerovalent iron

and ferrous sulfate both under dark and UV light conditions. Besides, PS was compared to H_2O_2 addition using 80 mg/L of Reactive Red 45 as initial pollutant load (≈32 mg/L of total organic carbon -TOC-). The reaction scheme included 12 bulk Fenton reactions, 14 surface Fenton reactions, 11 inorganic bulk reactions related to H_2O_2, 3 bulk iron/PS reactions, 5 surface iron/PS reactions, 6 inorganic bulk reactions related to PS, 6 photo-induced reactions and 8 pollutant degradation reactions. Selecting the corresponding reactions from this group, different models for direct UV photolysis, UV/H_2O_2, UV/$S_2O_8^{2-}$, Fe^{2+}/H_2O_2, UV/Fe^{2+}/H_2O_2, Fe^0/H_2O_2, UV/Fe^0/H_2O_2, UV/Fe^{2+}/$S_2O_8^{2-}$, Fe^{2+}/$S_2O_8^{2-}$, Fe^0/$S_2O_8^{2-}$ and UV/Fe^0/$S_2O_8^{2-}$ were proposed. Bu et al., 2017 [34] reported the modelling of Fe(II)-activated PS for the removal of atrazine at different initial concentrations. A first principle model based on 26 reactions including the influence of tertiary butanol, methanol and natural organic matter on process performance was used. Lominchar et al. 2018 [30] proposed a simplified reaction mechanism to model phenol abatement by alkaline-activated (pH 12) PS. Good agreement between experimental data and model simulations was found, being the model able to accurately predict the evolution of phenol, PS, hydroquinone and catechol. Another modelling work was carried out by Rodriguez et al. 2017 [35], who studied the removal of diuron, caffeine and ibuprofen at concentrations in the range from 0.086 mM to 0.129 mM by zerovalent iron-activated PS. An interesting semi-empirical modelling approach based only on 7 general reactions was proposed, capable of describing the evolution of pollutant, oxidant agent, iron concentrations and mineralization. All the reported studies considered an extremely higher concentration of target pollutants compared to the actual concentration of microcontaminants that can be found in MWWTP effluents.

The aim of the present work was to develop a general mathematical model under a semi-empirical approach of the heat-activated and iron-activated PS processes when these are applied to the removal of CECs. In this sense, CBZ dissolved in water at very low concentration (0.0025 mM), closer to actual conditions, was used as model pollutant. In a first experimental series, a heat-activation PS model was proposed for a temperature range from 25ºC to 65ºC. In the second part of the study, a complementary model was implemented for PS activated by iron in concentrations from 0.009 mM to 0.18 mM at 25ºC and 35ºC. Finally, the model was validated including supplementary experiments based on iron and PS additions carried out throughout the treatment.

2. Materials and Methods

2.1 Chemicals and reagents

CBZ (standard quality, 99%), acetonitrile (HPLC-grade), ferrous sulfate heptahydrate ($FeSO_4 \cdot 7H_2O$), 1,10-phenantroline (99% w/w), acetic acid (99.7% w/v), ascorbic acid (99%, w/w), formic acid (95%, w/v) were supplied by Sigma-Aldrich. Sodium persulfate, $Na_2S_2O_8$ was provided by Merck Millipore (Darmstadt, Germany). Ultrapure water was produced with a Millipore (Direct-Q® Ultrapure Water System, Bedford, MA, USA).

2.2 Analytical methods

CBZ concentration was quantified by ultra-performance liquid chromatography (UPLC, Agilent 1260) coupled to UV/DAD detector. The column selected was C18 (1.8 µm, 50 x 4.6 mm). The initial conditions of 10% AcN and 90% of Milli-Q water acidified with formic acid (25mM w/v) progressed to 100% AcN in 15 min. 3 min post-time was selected: time elapsed before the next injection for the method to stabilize in the selected initial condition. Flow rate was 1 mL/min and the injection volume was 100 µL. Wavelength for CBZ quantification was 267 nm. Each sample was previously filtered (0.22 µm –

Milipore). Additionally, the filter was washed with AcN, added to the sample so that proportion between sample and AcN was the same than the one of the HPLC solvents at the start of the method (10% AcN – 90% sample). The AcN addition also allows quenching the radicals present in the samples.

PS concentration was quantified by evaluating the sulfate anion concentration generated during the reaction by ion chromatography with a Metrohm 872 Extension Module 1 and 2 ion chromatograph (IC) system configured for gradient analysis. Samples stability was confirmed after long time storing. To determine the total iron concentration, the 1,10-phentranoline method was used (ISO 6332).

2.3 Experimental procedure

Experiments were carried out in an opaque-wall reaction vessel (1L) placed under dark conditions. Temperature was manually controlled using a heater that also provided agitation in order to work under perfect mixing conditions. In a typical run, pH of the deionized water was adjusted to 2.7-2.9, then CBZ (0.0025 mM equivalent to 500 µg/L) was added and, finally, PS was added marking the start of the experiment. CBZ stock solution (4 g/L) was prepared in methanol. To achieve the initial concentration, 0.125 mL of stock solution was added to the reactor providing 37 mg/L of total organic carbon (TOC) to the solution due to methanol content. This amount is similar to the natural organic content found in MWWTP effluents. In the iron-activation experimental series, Fe(II) (as $FeSO_4 \cdot 7H_2O$) was added before PS.

2.4 Reaction kinetic model

To develop a PS model (first principle model) considering all the possible interactions between CECs, inorganic salts, natural organic matter (NOM) and oxidizing species present in actual MWWTP effluents is not possible. The opposite approach relies on a completely

empirical view of the process and the use of response surface platform. This option is simpler, however, it is only valid under exactly the same conditions applied for model development. Thus, its application is also very limited. To face up these problems, this work proposes an intermediate solution, semi-empirical modelling. With this aim, PS oxidation process is described by means of a small group of simple reactions (usually known as "pseudo-reactions") where each one represents what is actually occurring through many elementary steps.

In this work, PS reaction mechanism is represented in the model by a limited number of reactions that can be grouped in three classes: (i) PS activation reactions, which are related to radicals production, (ii) reactions in which radicals are efficiently consumed, i.e. reactions related to CBZ oxidation and (iii)reactions in which radicals are inefficiently consumed, i.e. reactions related to mineralization (total organic carbon degradation) which is not the objective of tertiary treatments. Therefore, although the proposed model is simple due to the low number of reactions used, it still represents the overall process. Semi-empirical dynamic model is based on mass balances of the most relevant components of the process obtained under batch mode operation and considering perfect mixing conditions in the reactor.

In the case of heat-activated PS process, the model assumes 4 reactions and 5 model components (Table 1), these being $S_2O_8^{2-}$ (PS), $SO_4^{\bullet-}$ (SRs), H^+ (H), carbamazepine (CBZ) and TOC. With respect to reactions, the activation of PS by heat (Reaction 1) and acidic conditions (Reaction 2), CBZ oxidation (Reaction 5) and mineralization (Reaction 6) are the interactions between model components considered. As no equilibrium reactions were included in the model in order to follow the parsimony principle, the acid-activation reaction was only considered within the first 5 min of the process.

In the iron-activated PS process, the model assumes 7 reactions and model components (Table 1), including the 5 components of the heat-activated PS process plus Fe(II) and Fe(III). With respect to reactions, Reactions 1, 2, 5 and 6 are complemented with the activation of PS by Fe(II) (Reaction 3) and Fe(III) (Reaction 4) and the oxidation of Fe(II) by SRs (Reaction 7).

A summary of the reactions and the corresponding kinetics equations are presented in Table 1.

Table 1. Reactions and kinetics equations included in the semi-empirical model proposed.

Reaction		**Rate law equation**	
$PS + heat \rightarrow 2\,SRs$	(Reaction 1)	$r_1 = k_1\,[PS]$	(Equation 1)
$PS + H \rightarrow SRs$	(Reaction 2)	$r_2 = k_2\,[PS]\,[H]$	(Equation 2)
$PS + Fe(II) \rightarrow SRs + Fe(III)$	(Reaction 3)	$r_3 = k_3\,[PS]\,[Fe(II)]$	(Equation 3)
$PS + Fe(III) \rightarrow SRs + Fe(II)$	(Reaction 4)	$r_4 = k_4\,[PS]\,[Fe(III)]$	(Equation 4)
$CBZ + SRs \rightarrow Products$	(Reaction 5)	$r_5 = k_5\,[CBZ]\,[SRs]$	(Equation 5)
$TOC + SRs \rightarrow Products$	(Reaction 6)	$r_6 = k_6\,[TOC]\,[SRs]$	(Equation 6)
$Fe(II) + SRs \rightarrow Fe(III)$	(Reaction 7)	$r_7 = k_7\,[Fe(II)]\,[SRs]$	(Equation 7)

2.5. Numerical issues and assays

The experiments carried out in this study were divided into two groups for parameter identification and model validation. One experiment from the heat-activation experimental series and two experiments from the iron-activated experimental series were used for model validation plus another two specific assays, one based on iron additions (0.018 mM) and another based on PS additions (0.17 mM).

In a first step of the model calibration procedure, only PS decomposition data was taken into account in the construction of the objective function, so that the kinetic constants of the PS activation reactions could be obtained. The remaining parameters were obtained in a

second step where the objective function was augmented with CBZ oxidation profiles. The searching procedure was carried out until trapped in local minima for some combinations of kinetic parameters with no improvement of the defined objective function.

The model parameters were obtained by implementing a Monte Carlo approach in MATLAB® in which the objective was the minimization of the function presented in Equation 8.

$$J = \sum_{n} \left[\sum_{m} \frac{\left| X_{e,n,m} - X_{p,n,m} \right|}{X_{e,m}} \right] \quad \text{(Equation 8)}$$

Where the subscript "e" represents the experimental measurement and the subscript "p" the model prediction of the variable X (CBZ and/or PS concentrations); being the subscript "m" the total number of samples of the "n" experiments carried out.

When only model fine-tuning was carried out, MATLAB® optimization toolbox with a weighted quadratic objective function was used.

In order to calculate uncertainties of the kinetic constants, new groups of simulated experiments were generated by random modification of the experimental data based on the errors of PS and CBZ measurement methods. For each new data set, model fine-tuning procedure was carried out so that a new group of model parameters was obtained. Finally, the standard deviation of each model parameter was calculated.

3. Results and discussion

3.1 Heat-activation of PS

PS can form two $SO_4^{\bullet-}$ through scission of the peroxide bond as a result of heat energy absorption [36]. In this part of the study, the degradation of CBZ (0.0025 mM) by using PS

(1mM) as oxidant agent at temperatures in the range from 25ºC to 65ºC and pH 3 was evaluated (Figure 1). This pH was selected in order to know heat-activation contribution when PS is also activated by dissolved iron (notice that acidic pH is needed to keep iron in solution). At the lowest temperature (25ºC), about 30% CBZ degradation was achieved after 20 min remaining the pollutant concentration almost constant from this moment until the end of the assay (180 min). From 35ºC, the complete removal of CBZ was always achieved. Increasing the temperature always resulted in faster kinetics till attaining complete polluant removal in less than 5 min at 65ºC. These results show that there is an initial degradation non-related to heat-activation, as the latter should be characterized by a continuous decomposition of PS, as occurs at 35ºC (see Figure 1a). This phenomenom could be caused by acid-catalyzed decomposition of PS, which has been reported by several authors [32, 37]. At this point, the number of CBZ moles degraded over the number of PS moles consumed was calculated for each experiment. This parameter is known as the reaction stoichiometric efficiency (RSE). As it can be seen in the inset of Figure 1a, RSE decreased with temperature from 0.017 at 25ºC to 0.007 at 65ºC. These values are rather low in comparison to the ones reported in similar works related to heat activation of PS. Gauch et al. 2015 [23], who studied Naproxen degradation at circumneutral pH, obtained RSE values ≈0.70 when working at 70ºC. This important difference seems to be mainly caused by pH. Gauch et al. 2012 [38] reported that the RSE value for the removal of ibuprofen by PS heat activation decreases from 0.65 at pH 7 to 0.25 at pH 9 and to 0.09 at pH 4. Although this RSE value for acidic pH is still higher than the range of values obtained in this work, this difference can be justified since the ibuprofen initial concentration (20.3 μM equivalent to ≈4 mg/L) was considerably higher than the CBZ initial concentration used in this research (2.5 μM equivalent to ≈0.5 mg/L). Such low

concentration of contaminant favors the appearance of reactions different from pollutant degradation such as radical-to-radical reactions or reaction between radicals and organic matter and so, RSE diminishes.

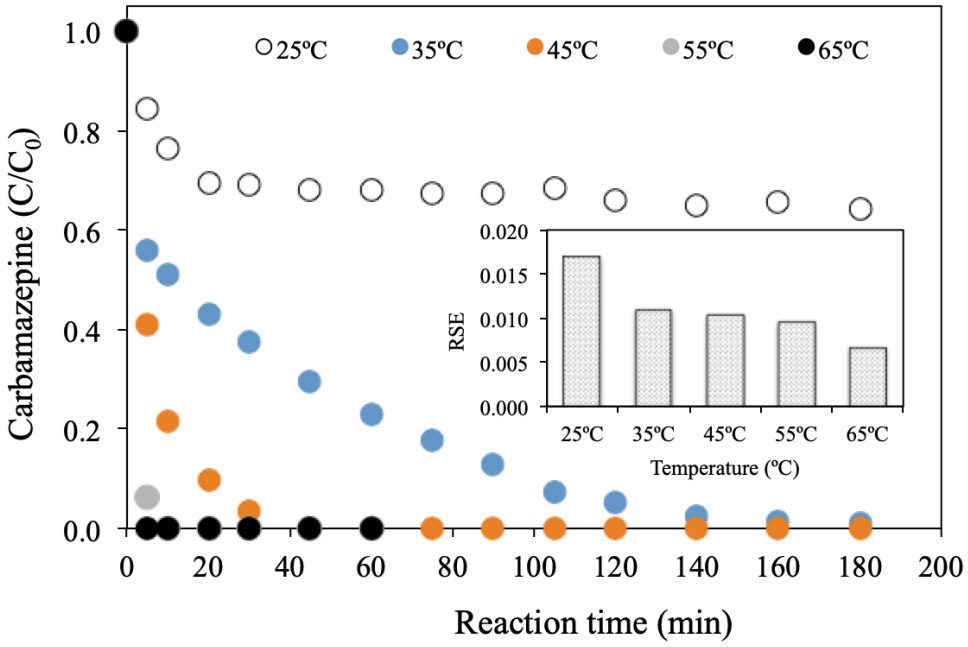

(a)

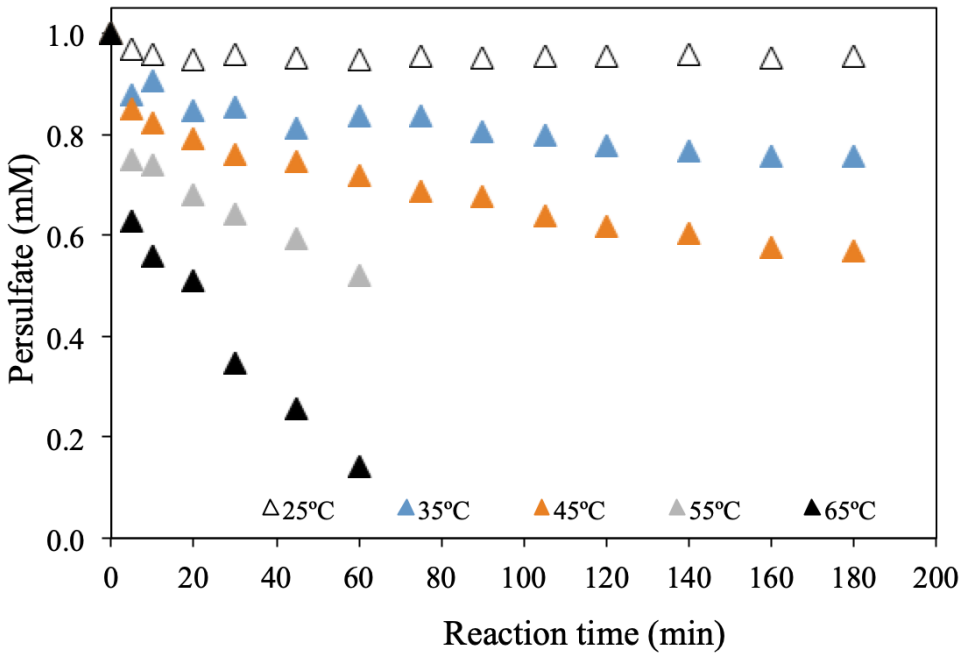

(b)

Figure 1. Effect of temperature on CBZ degradation (a) and PS decomposition (b). Experimental conditions: $[CBZ]_0$= 0.0025 mM, $[PS]_0$= 1 mM and T=25ºC/35ºC/45ºC/55ºC/65ºC.

The above explanation is also in accordance with model structure resulting from calibration process. If only heat-activation of PS is considered in the model, the agreement between experimental data and model prediction profiles is good only for 45, 55 and 65ºC experiments, i.e. once temperature is high enough to be the main activation mechanism. Including acid-catalyzed decomposition of PS in the reaction mechanism improved model accuracy allowing also an accurate prediction of the low temperature experiments. Another important aspect to enhance model predictions was to include a radical scavenging reaction, as the CBZ stock solution was prepared in methanol, which provides additional TOC (37 mg/L) in the reaction bulk affecting process performance. This situation is similar to the one found in natural surface waters and municipal WWTP secondary effluents, where similar TOC values are also found in the matrix. Mineralization was not selected as prediction objective because it is not a concern when dealing with CECs dissolved in real aqueous matrices, in which TOC concentration is in the order of several tens of mg/L, while the concentration of CECs is typically in the order of µg/L. Therefore, the mineralization of CECs cannot be detected in actual wastewater treatment conditions [39] and degradation of harmless TOC is not an objective of any advanced tertiary treatment designed to polish the effluent from conventional WWTPs [40].

As it can be seen in Figure 2, very good agreement between experimental results and model predictions were obtained both for CBZ and PS time-concentration profiles for the complete range of temperatures studied. The kinetic parameters of the proposed model are

shown in Table 2. The slowest reactions were those responsible of radical production (Reactions 1 and 2) being the lowest values obtained for PS heat-activation reaction (Reaction 1). The corresponding activation energy (E_A) obtained for this reaction (105.2 kJ/mol) is in the range of the reported values at acid pH (110-116 kJ/mol) [41]. On the contrary, the CBZ degradation reaction (Reactions 5) resulted in the highest kinetic parameters. E_A of CBZ was found to be 26.1 kJ/mol. This E_A is about 5 times lower than the values reported for some other pharmaceuticals such as ibuprofen (168 kJ/mol) [38], naproxen (155 kJ/mol) [23], ketoprofen (157 kJ/mol) [22] or bisoprolol (120 kJ/mol) [42].

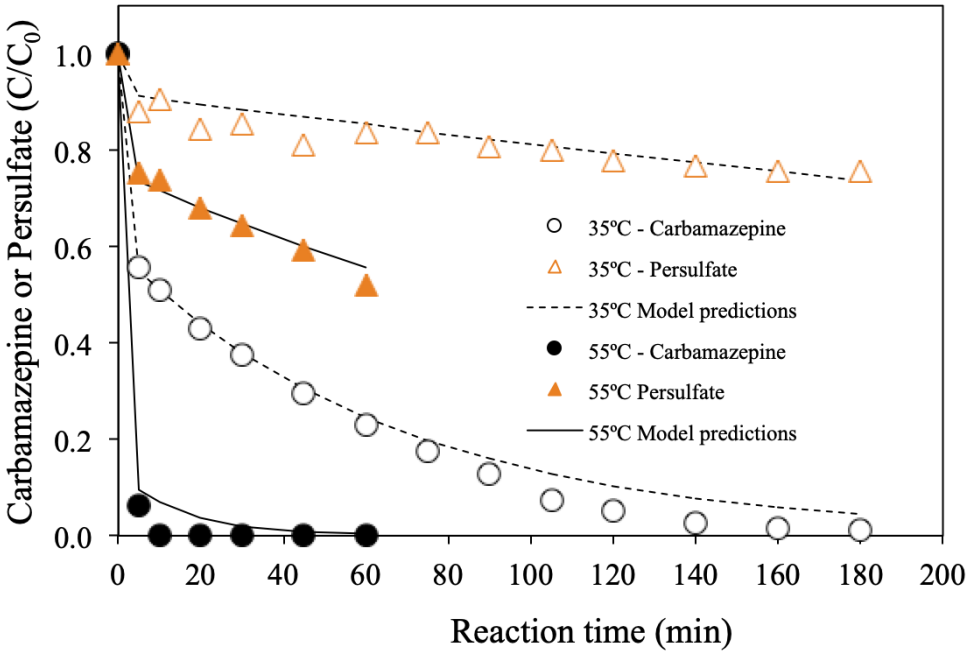

Figure 2. Comparison between experimental data (CBZ –dots- and PS –triangles-) and model predictions (lines) for the heat-activation experiments carried out at 35ºC and 55ºC. Experimental conditions: $[CBZ]_0$= 0.0025 mM and $[PS]_0$= 1 mM.

Table 2. Kinetic parameters resulting from the calibration of the heat-activated PS model at the different temperatures and the corresponding activation energy of the Arrhenius fitting.

		25ºC	35ºC	45ºC	55ºC	65ºC	E_A kJ/mol	r^2
k_1	min^{-1}	$(0.1\pm0.1)\cdot10^{-3}$	$(1.2\pm0.1)\cdot10^{-3}$	$(3.0\pm0.1)\cdot10^{-3}$	$(5.1\pm0.2)\cdot10^{-3}$	$(25.2\pm0.8)\cdot10^{-3}$	105.2	0.9496
k_2	$mM^{-1}min^{-1}$	0.069±0.001	0.089±0.002	0.147±0.006	0.326±0.014	0.404±0.026	40.4	0.9608
k_5		1.99±0.10	3.30±0.13	4.14±0.39	5.38±0.57	-	26.1	0.9722
k_6		0.141±0.006	0.150±0.007	0.156±0.011	0.159±0.005	-	3.2	0.9477

3.2 Iron-activation of PS

Sulfate radical can also be formed through the reaction of PS and metals in which one electron is transferred [30]. In this context, the use of iron has been widely studied because it presents low toxicity and low cost [43]. Furthermore, the use of its zero valent form in monometallic and multimetallic heterogeneous systems has been also evaluated presenting advantages on homogeneous systems mainly improving RSE with less iron sludge generation [28-29]. Based on the above considerations, in the next part of the study, the removal of CBZ (0.0025 mM) by Fe(II)-activated PS (1mM) under six different iron concentrations in the range from 0.009 mM to 0.18 mM (equivalent to 0.5 - 10 mg/L) at constant temperature (25ºC) was evaluated and modeled. In general, an important initial degradation of the pollutant is again observed and later the process is extremely slowed down due to the formation of Fe(III) (Figure 3). After 2 hours, the complete CBZ removal was not achieved in any case though, when 0.09 mM of Fe(II) or higher concentrations were used, about 90% oxidation was obtained within the first 5 min. Negligible differences in terms of CBZ removal were found between the experiments carried out with 0.09, 0.13 and 0.18 mM of Fe(II). This behavior, in which there is fast pollutant degradation at initial stages but, subsequently, asymptotic values of pollutant and oxidant agent are observed, is

in agreement with some other published works. Rodriguez et al. 2017 [35] reported similar process performance. Additionally, the authors indicated that an undesired reaction occurs that consumes both Fe(II) and PS if iron excess is added in the reaction bulk, which can justify the similarity between the experiments above 0.09 mM of iron. Minimizing this undesirable reaction (Reaction 7) is required to increase the efficiency of the oxidant, which could be obtained for instance by employing zero valent iron that allows a slow release of Fe(II). This was demonstrated by Ghauch and co-workers, who reported the superiority of ZVI particles in activating PS while keeping high performance of the system, especially because that reaction was accompanied with pH slight decrease favoring the continuous generation of iron species and iron corrosion products, which help PS activation in a controlled manner [27, 28]. Slight differences were also found between the experiments carried out with 0.009 and 0.018 mM of iron. For both concentrations, about 60% initial degradation was observed. Under these conditions, the process is probably initiated (mainly) by the above-mentioned acid-activation mechanism instead of iron-activation. Although it is not the objective of this work to optimize operating conditions, the effect of Fe:PS molar ratio on the final % CBZ degradation has been analyzed. The best result was obtained for 1:11 molar ratio (0.09 mM of iron and 1 mM of PS). The use of higher iron concentrations corresponding to 1:9 and 1:6 molar ratios did not improve CBZ degradation while the use of lower iron concentrations corresponding to 1:22, 1:56 and 1:111 molar ratios resulted in lower CBZ degradation percentages. This is in accordance with the results obtained by Amasha et al. 2018 [22], who studied the degradation of ketaprofen comparing different Fe:PS molar ratios at different PS initial concentrations. At the same PS initial concentration than the one used in this work (1 mM), it was found that 1:10 molar ratio was the most adequate value to obtain the highest pollutant degradation. The main difference

with the present work is that the final ketaprofen degradation did not remain constant but decreased when Fe:PS molar ratio was changed to 1:5 and 1:1 by increasing iron concentration. In this sense, it seems that quenching reactions cause a more negative effect on process performance when the pollutant concentration is in the range of mg/L than when it is in the range of µg/L, as in the latter the amount of radicals needed to achieve the complete pollutant degradation is much lower.

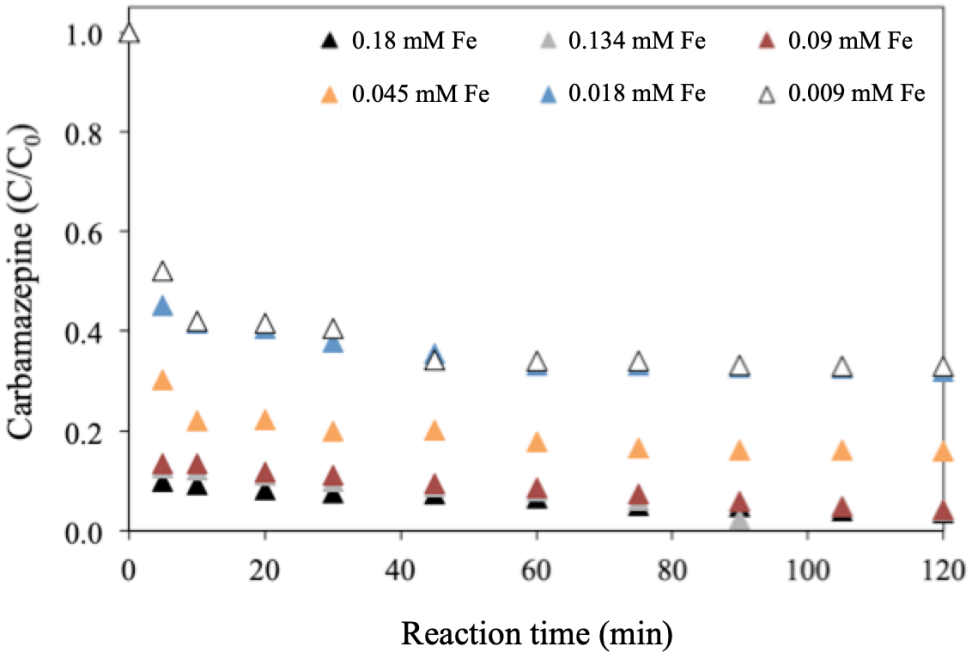

(a)

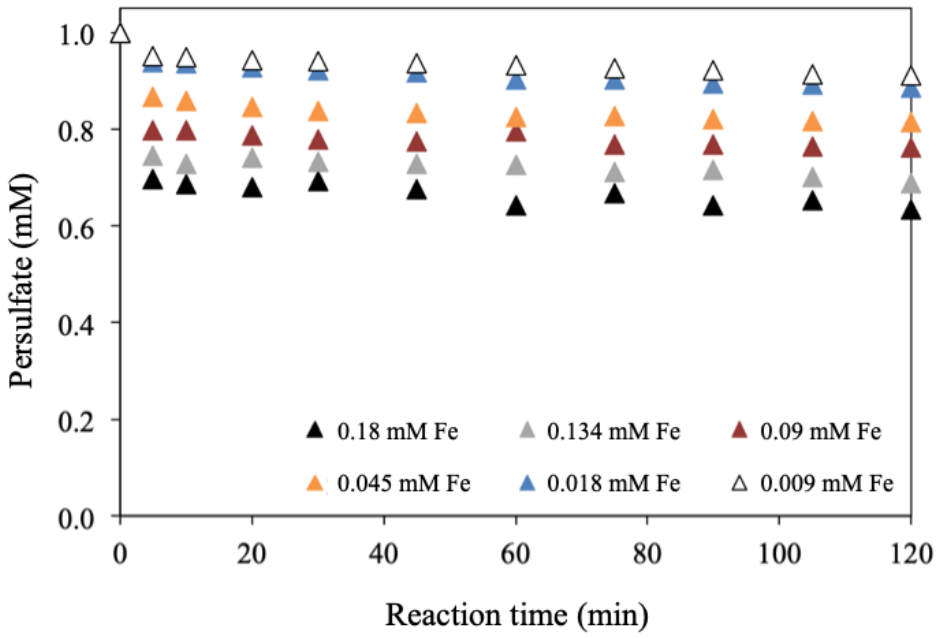

(b)

Figure 3. Effect of iron concentration on CBZ degradation (a) and PS decomposition (b) for the assays carried out at 25ºC. Experimental conditions: $[CBZ]_0$= 0.0025 mM, $[CBZ]_0$= 0.0025 mM, $[Fe]_0$= 0.009 mM/0.018 mM/0.045 mM/0.09 mM/0.134 mM/0.18 mM and $[PS]_0$= 1 mM.

In the next experimental series, the same iron concentrations were used but increasing the operation temperature to 35ºC (Figure 4). In all the cases, reaction kinetics improved with respect to the previous experimental series carried out at 25ºC. The complete degradation of CBZ was achieved in approximately 40 min when iron concentrations of 0.09 mM or higher were used. Again, negligible differences between the experiments with 0.09, 0.13 and 0.18 mM of iron were found. In the case of the experiment with 0.045 mM of iron, the pollutant could be also completely degraded after 100 min. In contrast, the assays with 0.009 and 0.018 mM of iron only allowed reaching ≈70% and ≈80% degradation,

respectively, after 120 min. With respect to Fe:PS molar ratio, a similar trend than the one obtained for the set of experiments carried out at 25ºC was found, being again 1:11 molar ratio the most adequate option.

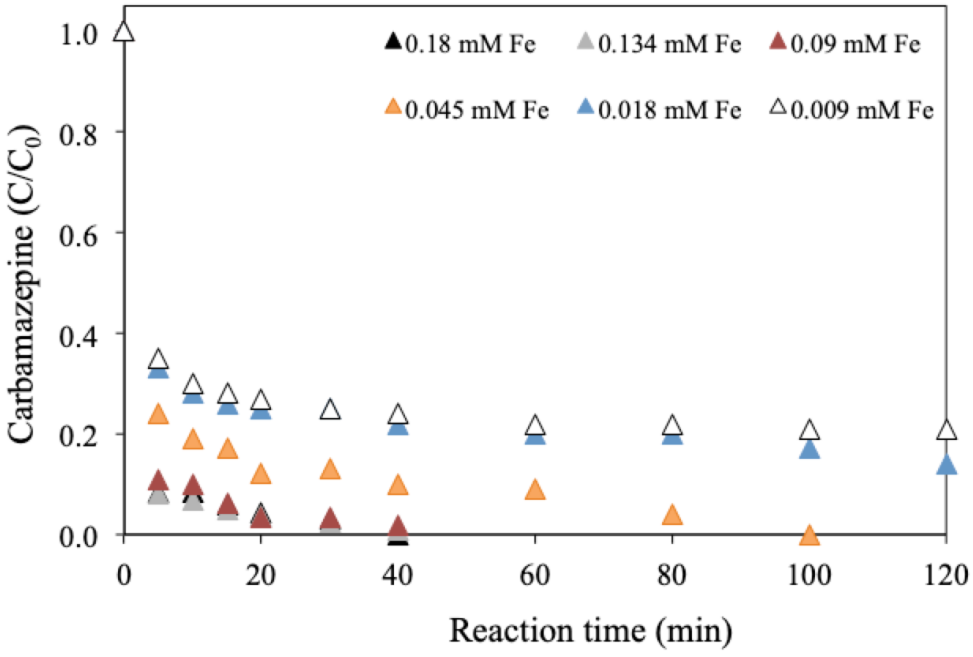

(a)

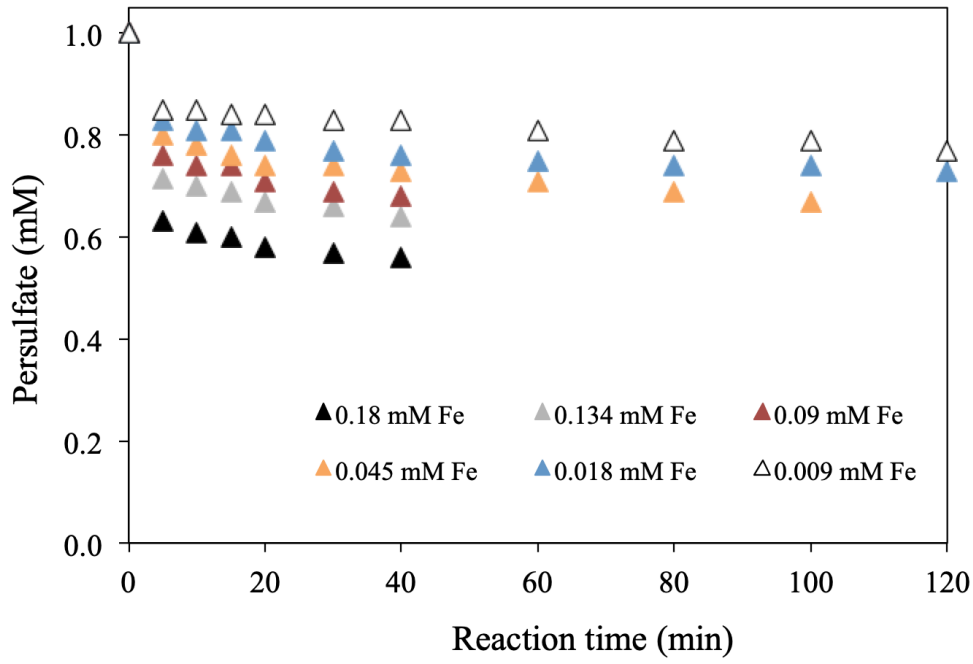

(b)

Figure 4. Effect of iron concentration on CBZ degradation (a) and PS decomposition (b) for the assays carried out at 35ºC. Experimental conditions: $[CBZ]_0$= 0.0025 mM, $[Fe]_0$= 0.009 mM/0.018 mM/0.045 mM/0.09 mM/0.134 mM/0.18 mM and $[PS]_0$= 1 mM.

The semi-empirical model proposed in the previous section was modified in order to include the activation of PS by iron species. In this way, Fe(II) and Fe(III) activation reactions (Reactions 3 and 4) were added in the mechanism and the model was again calibrated. In the first calibration step, only PS decomposition data was used to determine the kinetic constants of both Fe(II) and Fe(III) activation reactions, using the already obtained model parameters in the temperature experimental series (Table 3) for acid and heat activation (k_1 and k_2). This option left to acceptable predictions, however, a better agreement between simulated and experimental profiles of PS decomposition was obtained after model fine-tuning. The calibration process showed that, in the range from 25ºC to 35ºC, the model prediction capability improves if heat-activation is not considered in the model. Probably, this happens because it presents a small effect on process performance that can be implicitly included in the iron-activation reactions. On the contrary, this did not happen with acid-activation, which still showed an important effect on process performance. The next step was to include CBZ oxidation and scavenging reactions into the model and to simulate also the pollutant degradation profile. In addition, Fe(II) scavenging of radicals reaction (Reaction 7) was also included in the model to describe the negative effect of iron excess on process performance. Again, the values of the kinetic constants already available from the temperature experimental series (k_5 and k_6) were initially used determining only the kinetic parameter of Fe(II) scavenging reaction. As in the previous calibration stage, although model prediction was acceptable, it improved after model fine-

tuning. The comparison between experimental data and model predictions for the assays carried out with 5 mg/L of iron at 25ºC and 35ºC is shown in Figure 5. As it can be seen in the simulated profiles, the model prediction capability is high in both cases.

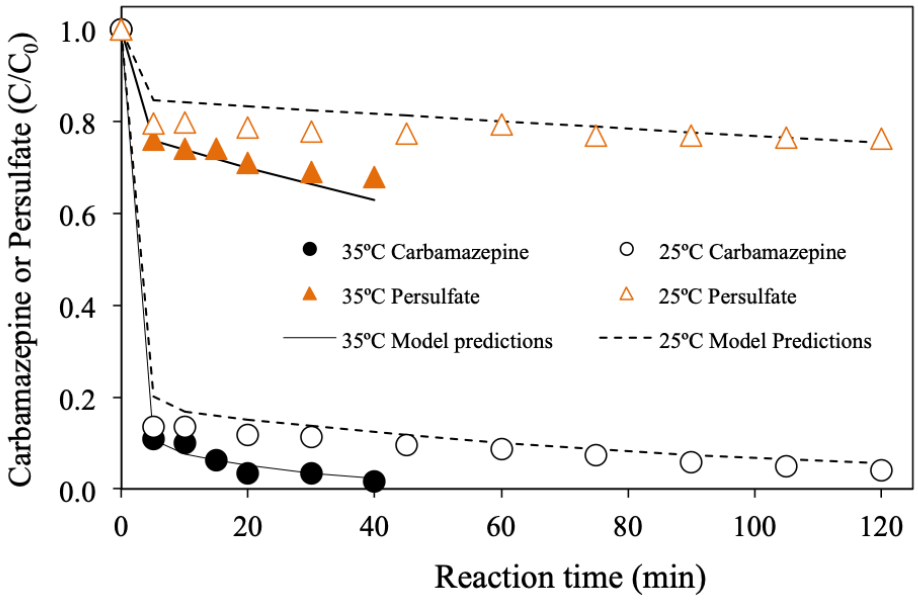

Figure 5. Comparison between experimental data (CBZ –dots- and PS –triangles-) and model simulations (lines) for the experiments carried out with $[CBZ]_0$= 0.0025 mM, $[Fe]_0$= 0.09 mM, $[PS]_0$= 1 mM and T=25ºC/35ºC.

Therefore, the final proposed model includes 3 reactions related to radical formation and 3 reactions related to radical consumption. PS can be activated to produce (mainly) sulfate radicals by acid conditions (Reaction 2), Fe(II) (Reaction 3) and Fe(III) (Reaction 4). With respect to heat-activation, it is not necessary to implicitly consider this mechanism in the model because it seems to be included through iron-activation reactions. With respect to

radicals consumption, their reactions with CBZ, organic matter and Fe(II) were considered. The kinetic parameters obtained by model fitting are presented in Table 3. This table shows that Fe(II) is the main responsible of PS activation with an small contribution of acid-activation. After the oxidation of Fe(II) to Fe(III), there is also PS activation by Fe(III), although it is extremely slow. The fastest reaction of the whole model was CBZ oxidation followed by Fe(II) oxidation by sulfate radical. Again, Fe(II)-activation of PS was the most important activation mechanism, with an initial contribution of acid-activation that has to be considered in the model and a very slow Fe(III) impact.

Table 3. Kinetic parameters for the iron concentration experimental series resulting from model fine-tuning.

	k_2	k_3	k_4	k_5	k_6	k_7
	$mM^{-1}\ min^{-1}$					
25ºC	2.04±0.16	0.0056±0.0009	0.016±0.008	16.42±0.96	0.46±0.11	8.25±0.92
35ºC	5.37±0.87	0.030±0.008	0.037±0.010	23.01±1.34	0.77±0.20	18.92±2.3

3.3 Model Validation

One assay from each experimental series (heat-activation, Fe(II)-activation at 25 and 35ºC) was not used for model calibration so that these could be used for model validation. In the case of the heat-activation experimental series, the assay carried out at 45ºC was the one selected for model validation. As it can be observed in Figure 6a, good agreement between experimental data and model simulations was obtained for both CBZ oxidation and PS decomposition profiles, validating the model proposed, which includes heat-activation plus acid-activation. In the case of the Fe(II)-activation model, the validation experiments are

presented in Figure 6b. Again, the model showed great prediction accuracy validating the semi-empirical approach in which only Fe(II)-activation and acid-activation are considered.

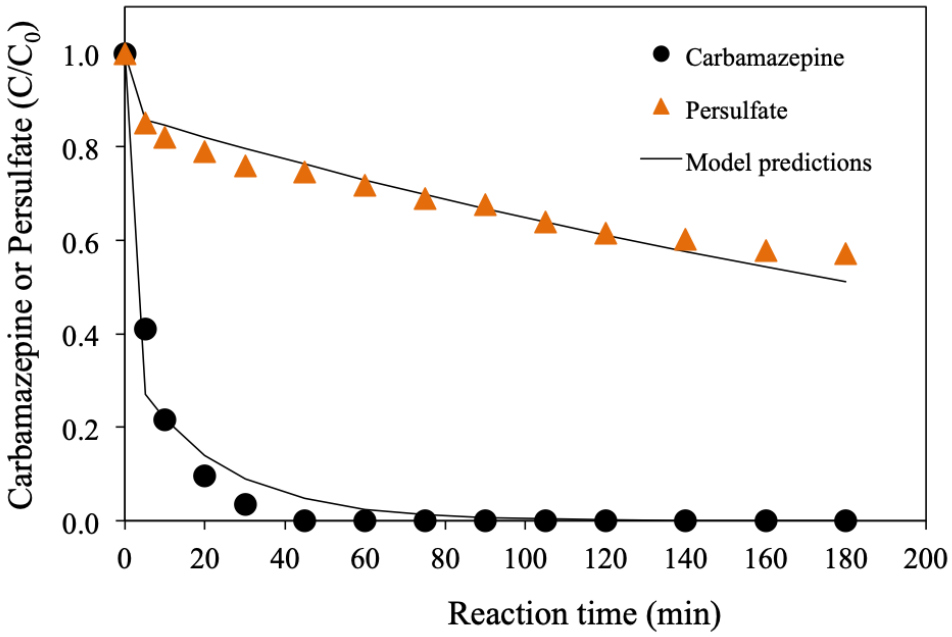

(a)

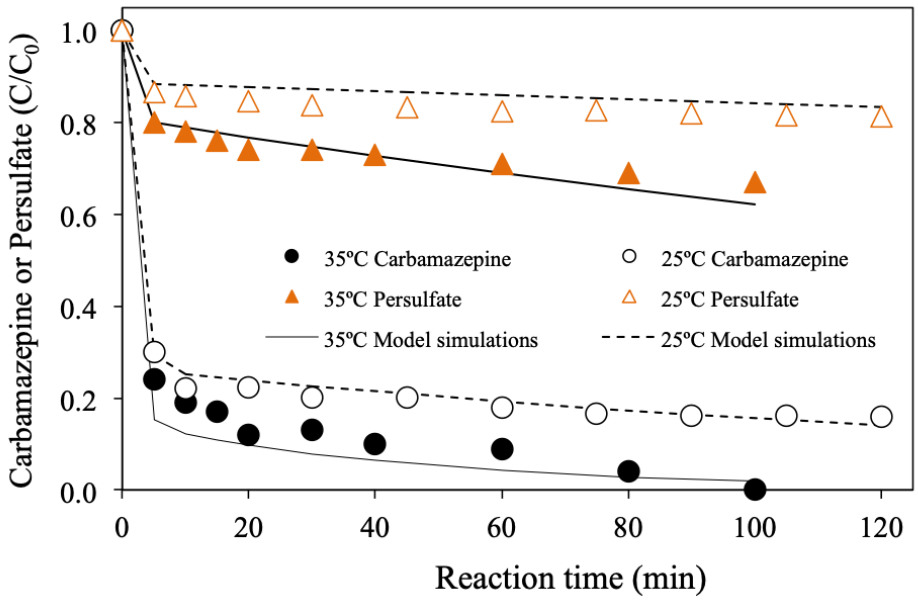

(b)

Figure 6. Comparison between experimental data (CBZ –dots- and PS –triangles-) and model predictions (lines) for the heat-activation experiment validation (a) and the iron

activation experiments validation (b). Experimental conditions: (a) $[CBZ]_0$= 0.0025 mM, $[PS]_0$= 1 mM and T=45ºC (b) $[CBZ]_0$= 0.0025 mM, $[Fe]_0$= 0.045 mM, $[PS]_0$= 1 mM and T=25ºC/35ºC.

Finally, two new validation experiments were carried out. In the first one, the removal of CBZ (0.0025 mM) using PS (1 mM) activated by different and low Fe(II) additions (0.018 mM each at 0, 10 and 20 min) was studied. Three steps can be clearly identified in the decontamination process corresponding to each one of the iron additions (Figure 7a). Initially, an important degradation is produced and, then, the process is almost stopped. The CBZ oxidation steps diminished with each one of the iron additions resulting in 60%, 20% and 10%. The model adequately predicts this process behavior; nevertheless, the prediction capability for CBZ removal diminished after the first addition. The initial CBZ concentration in all the experimental series used to develop the model was constant at 0.0025 mM. Consequently, the model has not been trained for concentrations lower than 0.0025 mM, as ≈0.001 mM and ≈0.0005 mM, concentrations measured when the second and third additions were done. A similar trend can be observed for PS decomposition. While the simulation for the first addition is adequate, in the second and third ones the PS concentration is overestimated. In the last validation experiment, the removal of CBZ (0.0025 mM) using 0.09 mM of Fe(II) and three PS additions (0.17 mM each at 0, 10 and 20 min) was studied. In this case, it is difficult to identify the additions in the CBZ oxidation curve, which is indeed extremely similar to the curves obtained in the Fe(II)-activation experimental series. After the first addition, almost 60% CBZ oxidation was obtained, then, 5% oxidation was achieved in the second one and, finally, the third addition resulted in only 2% degradation. This process behavior is well predicted by the model,

indeed, model simulation shows that almost all the Fe(II) present initially in solution is already oxidized to Fe(III) (see Figure 7b) after the first PS addition. Consequently it can be said that the model is able to successfully simulate both CBZ oxidation process and PS decomposition, showing that it can be used as a predictive tool.

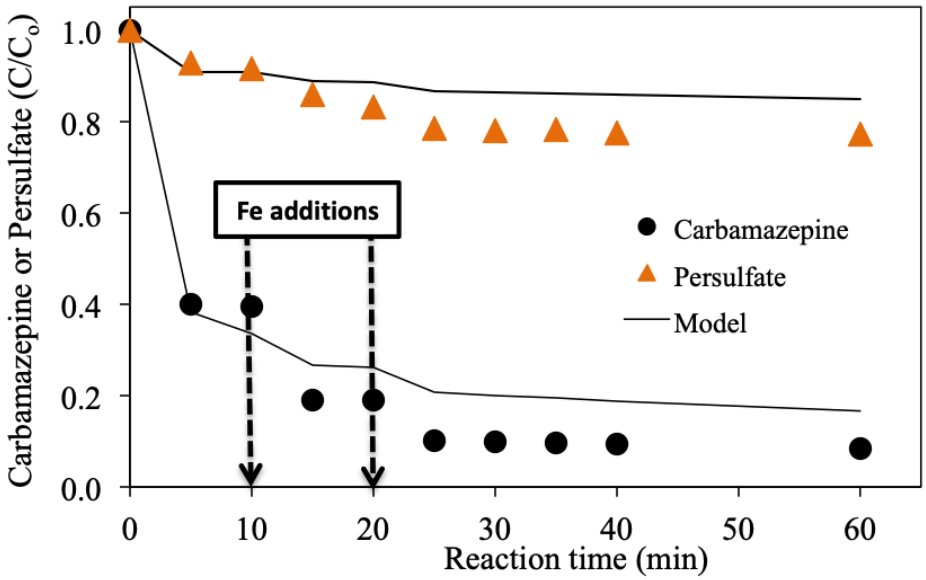

(a)

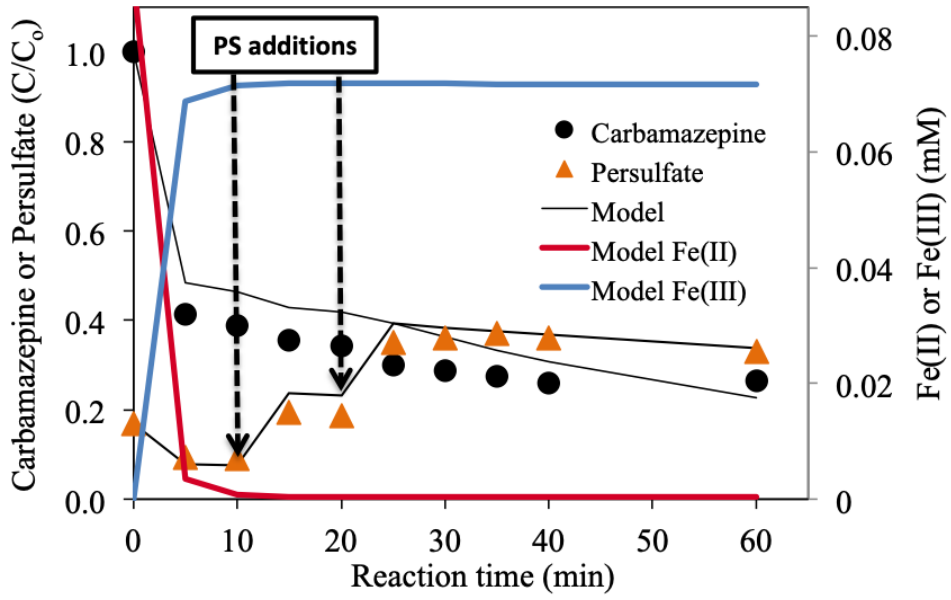

(b)

Figure 7. Comparison between experimental data (dots) and model predictions (lines) for

the experiment validation carried out with iron additions (a) and PS additions (b). Experimental conditions: (a) $[CBZ]_0$= 0.0025 mM, $[PS]_0$= 1mM, $[Fe]_0$= 0.018 mM, $[Fe]_{additions}$= 0.018 mM and T=25ºC (b) $[CBZ]_0$= 0.0025 mM, $[Fe]_0$= 0.09 mM, $[PS]_0$= 0.17 mM, $[PS]_{additions}$= 0.17 mM and T=25ºC.

4. Conclusions

A semi-empirical mathematical model of the heat-activated and iron-activated PS processes applied to the removal of CECs in water using CBZ as model pollutant has been proposed and validated.

In the heat-activated experimental series, the selected temperature range was 25ºC-65ºC. The CBZ degradation reached 20% at 25ºC after 120 min while, from 35ºC; the complete degradation of the pollutant was always achieved. Kinetics always improved with temperature. The obtained RSE was very low, in the range of 0.017 at 25ºC to 0.007 at 65ºC, which seems to be related to acidic conditions and the low initial concentration of CBZ. The highest model prediction capability was obtained when heat and acid activation of PS were considered in the reaction mechanism, which included also CBZ degradation reaction and TOC scavenging reaction. Very good agreement between experimental results and model predictions were obtained both for CBZ and PS time-concentration profiles for the complete range of temperatures studied.

In the next experimental series, six different Fe(II) concentrations in the range from 0.009 to 0.18 mM at 25ºC and 35ºC were evaluated. At the lowest temperature, the complete CBZ removal was not achieved in any case, although about 90% degradation in the first 5 min was obtained when 0.09 mM of Fe(II) or higher concentrations were used. The fast pollutant degradation at initial stages and the asymptotic values of pollutant and oxidant

agent obtained subsequently suggest that undesired reactions that consume both Fe(II) and PS^{-} are favored if iron excess is added in the reaction bulk. At 35ºC, the complete degradation of CBZ was obtained in about 40 min when Fe(II) concentration was 0.09 mM or higher, finding again negligible differences between the experiments with 0.09, 0.13 and 0.18 mM of iron. The best results in terms of final pollutant degradation and degradation rate were obtained for 1:11 Fe:PS molar ratio at both temperatures. With respect to model reaction mechanism for this part of the study, the calibration process showed that the model prediction capability improves if PS heat activation is not considered. Probably, this is due to its small effect on process performance, which can be included in the iron-activation reactions. On the contrary, this did not happen with acid-activation, which still showed an important contribution to the process. Thus, the model reaction mechanism that showed the highest prediction accuracy includes: acid, Fe(II) and Fe(III) PS activation, CBZ degradation and both TOC and Fe(II) scavenging reactions.

Finally, the model was validated using one assay from each experimental series (heat-activation, iron-activation at 25ºC and iron-activation at 35ºC) and two additional assays, one using Fe(II) additions (0.018 mM each at 0, 10 and 20 min) and another one using PS additions (0.17 mM each at 0, 10 and 20 min) with satisfactory results.

In conclusion, a predictive tool for the use of PS in the removal of contaminants of emerging concern has been developed. This type of studies are needed in order to get the process closer to actual application, as models allow simulating the process, optimizing operation conditions or scaling-up reactors, among others. Further studies are needed in order to improve the model so that the effect of some other important variables such as sun-light and matrix content can be also considered.

5. Acknowledgments

A. Cabrera-Reina wants to thank FONDECYT 11160680 for the financial support of his research stay at Plataforma Solar de Almería and SERC Chile (FONDAP 15110019). The authors wish to thank CONICYT (International Cooperation Program, REDES 180149), FONDECYT 11170122 and the Spanish Ministry of Science, Innovation and Universities for funding under the CalypSol Project (Reference: RTI2018-097997-B-C32).

6. References

[1] Krzeminski, P., Tomei, M.C., Karaolia, P., Langenhoff, A., Almeida, C.M.A., Felis, E., Gritten, F., Andersen, H.R., Fernandes, T., Manaia, C.M., Rizzo, L., Fatta-Kassinos, D., Performance of secondary wastewater treatment methods for the removal of contaminants of emerging concern implicated in crop uptake and antibiotic resistance spread: a review. Sci. Total Environ. Volume 648, (2019) Pages 1052–1081 https://doi.org/10.1016/j.scitotenv.2018.08.130

[2] Petrie, B., Barden, R., Kasprzyk-Hordern B., A review on emerging contaminants in wastewaters and the environment: Current knowledge, understudied areas and recommendations for future monitoring, Water Res., Volume 72, (2015) Pages 3-27, https://doi.org/10.1016/j.watres.2014.08.053

[3] Sousa J.C.G., Ribeiro, A.R., Barbosa, M., Pereira, F., Silva, A.M.T., A review on environmental monitoring of water organic pollutants identified by EU guidelines, J. Hazard., Volume 344, (2018) Pages 146-162, https://doi.org/10.1016/j.jhazmat.2017.09.058

[4] Grassi, M., Rizzo, L., Farina, A., Endocrine disruptors compounds, pharmaceuticals and personal care products in urban wastewater: implications for agricultural reuse and their

removal by adsorption process. Environ. Sci. Pollut. R., Volume 20, (2013) Pages 3616-3628, https://doi.org/10.1007/s11356-013-1636-7

[5] Roig, B., Pharmaceuticals in the Environment: Current knowledge and need assessment to reduce presence and impact, IWA Publishing, (2010) ISBN: 9781843393146

[6] Zhang, Y., Geiben, S., Gal, C., Carbamazepine and diclofenac: Removal in wastewater treatment plants and occurrence in water bodies, Chemosphere, Volume 73, (2008) Pages 1151-1161 https://doi.org/10.1016/j.chemosphere.2008.07.086

[7] Yang, Y., Sik Ok, Y., Kim, K., Kwon, E.E., Fai Tsang, Y., Occurrences and removal of pharmaceuticals and personal care products (PPCPs) in drinking water and water/sewage treatment plants: A review, Sci. Total Environ., Volumes 596–597, (2017) Pages 303-320, https://doi.org/10.1016/j.scitotenv.2017.04.102

[8] Wood, T.P., Duvenage, C.S.J., Rohwer, E., The occurrence of anti-retroviral compounds used for HIV treatment in South African surface water, Environ. Pollut., Volume 199, (2015) Pages 235-243, https://doi.org/10.1016/j.envpol.2015.01.030

[9] Hernando, M.D., Mezcua, M., Fernández-Alba, A.R., Barceló, D., Environmental risk assessment of pharmaceutical residues in wastewater effluents, surface waters and sediments, Talanta, Volume 69 (2), (2006) Pages 334-342, https://doi.org/10.1016/j.talanta.2005.09.037

[10] Kleywegt, S., Pileggi, V., Chunyan Hao, P.Y., Zhao, X., Rocks, C., Thach, S., Cheung, P., Whitehead, B., Pharmaceuticals, hormones and bisphenol A in untreated source and finished drinking water in Ontario, Canada — Occurrence and treatment efficiency, Sci. Total Environ., Volume 409 (8), (2011) Pages 1481-1488, https://doi.org/10.1016/j.scitotenv.2011.01.010

[11] Costa, E., Roccamante, M., Amorim, C., Oller, I., Sánchez Pérez, J.A., Malato, S., New trend on open solar photoreactors to treat micropollutants by photo-Fenton at circumneutral pH: Increasing optical pathway, Chem. Eng. J., Volume 385, (2020) 123982, https://doi.org/10.1016/j.cej.2019.123982

[12] Du, S., Bai, X., Xu, L., Yang, L., Jin, P., Visible-light activation of persulfate by TiO_2/g-C_3N_4 photocatalyst toward efficient degradation of micropollutants, Chem. Eng. J., Volume 384 (2020) 123245, https://doi.org/10.1016/j.cej.2019.123245

[13] Gauch, A., Baydoun, H., Dermesropian, P., Degradation of aqueous carbamazepine in ultrasonic/Fe^0/H_2O_2 systems, Chem. Eng. J. Volume 172 (1), (2011) Pages 18-27 https://doi.org/10.1016/j.cej.2011.04.002

[14] Wacławek, S., Lutze, H.V., Grübel, K., Padil, V.V.T., Černík, M., Dionysiou, D.D., Chemistry of persulfates in water and wastewater treatment: A review, Chem. Eng. J., Volume 330, (2017) Pages 44-62, https://doi.org/10.1016/j.cej.2017.07.132

[15] Miralles-Cuevas, S., Darowna, D., Wanag, A., Mozia, S., Malato, S., Oller, I., Comparison of UV/H_2O_2, UV/$S_2O_8^{2-}$, solar/Fe(II)/H_2O_2 and solar/Fe(II)/$S_2O_8^{2-}$ at pilot plant scale for the elimination of micro-contaminants in natural water: An economic assessment, Chem. Eng. J., Volume 310 (2), (2017) Pages 514-524, https://doi.org/10.1016/j.cej.2016.06.121

[16] Matzek, L., Carter, K.E., Activated persulfate for organic chemical degradation: A review, Chemosphere, Volume 151, (2016) Pages 178-188, https://doi.org/10.1016/j.chemosphere.2016.02.055

[17] Rodriguez, S., Vasquez, L., Costa, D., Romero, A., Santos, A. Oxidation of Orange G by persulfate activated by Fe(II), Fe(III) and zero valent iron (ZVI) Chemosphere, Volume 101, (2014) Pages 86-92 https://doi.org/10.1016/j.chemosphere.2013.12.037

[18] Zhang, R., Sun, P., Boyer, T.H., Zhao, L., Huang, C.H., Degradation of pharmaceuticals and metabolite in synthetic human urine by UV, UV/H_2O_2, and UV/PDS Environ. Sci. Technol., Volume 49 (5), (2015) Pages 3056-3066. https://doi.org/10.1021/es504799n

[19] Ghauch, A., Baalbaki, A., Amasha, M., El Asmar, R., Tantawi, O., Contribution of persulfate in UV-254 nm activated systems for complete degradation of chloramphenicol antibiotic in water Chem. Eng. J. Volume 317, (2017) Pages 1012-1025 https://doi.org/10.1016/j.cej.2017.02.133

[20] Al Hakim, S., Jaber, S., Eddine, N., Baalbaki, A., Ghauch, A., Degradation of theophylline in a UV254/PS system: Matrix effect and application to a factory effluent, Chem. Eng. J., Volume 380, (2020) 122478, https://doi.org/10.1016/j.cej.2019.122478

[21] Tan, C., Gao, N., Deng, Y., An, N., Deng, J., Heat-activated persulfate oxidation of diuron in water, Chem. Eng. J., Volume 203, (2012) Pages 294-300, https://doi.org/10.1016/j.cej.2012.07.005

[22] Amasha, M., Baalbaki, A., Ghauch, A., A comparative study of the common persulfate activation techniques for the complete degradation of an NSAID: The case of ketoprofen, Chem. Eng. J., Volume 350, (2018) Pages 395-410, https://doi.org/10.1016/j.cej.2018.05.118

[23] Ghauch, A., Tuqan A.M., Kibbi, N., Naproxen abatement by thermally activated persulfate in aqueous systems, Chem. Eng. J., Volume 279, (2015) Pages 861-873 https://doi.org/10.1016/j.cej.2015.05.067

[24] Ji, Y., Dong, C., Kong, D., Lu, J., Zhou, Q., Heat-activated persulfate oxidation of atrazine: Implications for remediation of groundwater contaminated by herbicides, Chem. Eng. J., Volume 263, (2015) Pages 45-54, https://doi.org/10.1016/j.cej.2014.10.097

[25] Zhao, L., Hou, H., Fujii, A., Hosomi, M., Li, F. Degradation of 1,4-dioxane in water with heat- and Fe^{2+}-activated persulfate oxidation, Environ. Sci. Pollut. R., Volume 21 (12), (2014) Pages 7457-7465. https://doi.org/10.1007/s11356-014-2668-3

[26] Miralles-Cuevas, S., Oller, I., Ruíz-Delgado, A., Cabrera-Reina, A., Cornejo-Ponce, L., Malato, S., EDDS as complexing agent for enhancing solar advanced oxidation processes in natural water: Effect of iron species and different oxidants, J. Hazard. Mater., Volume 372, (2019) Pages 129-136 https://doi.org/10.1016/j.jhazmat.2018.03.018

[27] Ghauch, A., Ayoub, G., Naim, S., Degradation of sulfamethoxazole by persulfate assisted micrometric Fe^0 in aqueous solution, Chem. Eng. J., Volume 228, (2013) Pages 1168-1181 https://doi.org/10.1016/j.cej.2013.05.045

[28] Ayoub, G., Ghauch, A., Assessment of bimetallic and trimetallic iron-based systems for persulfate activation: application to sulfamethoxazole degradation, Chem. Eng. J., Volume 256, (2014) Pages 280-292 https://doi.org/10.1016/j.cej.2014.07.002

[29] Naim, S., Ghauch, A., Ranitidine abatement in chemically activated persulfate systems: assessment of industrial iron waste for sustainable applications Chem. Eng. J., Volume 288, (2016) Pages 276-288 https://doi.org/10.1016/j.cej.2015.11.101

[30] Lominchar, M.A., Rodríguez, S., Lorenzo, D., Santos, N., Romero, A., Santos, A. Phenol abatement using persulfate activated by nZVI, H2O2 and NaOH and development of a kinetic model for alkaline activation, Environ. Techn. (United Kingdom), Volume 39 (1), (2018) Pages 35-43 https://doi.org/10.1080/09593330.2017.1294203

[31] Vicente, F., Santos, A., Romero, A., Rodriguez, S. Kinetic study of diuron oxidation and mineralization by persulphate: Effects of temperature, oxidant concentration and iron dosage method Chem. Eng. J., Volume 170 (1), (2011) Pages 127-135 https://doi.org/10.1016/j.cej.2011.03.042

[32] Ji, Y., Ferronato, C., Salvador, A., Yang, X., Chovelon, J.-M. Degradation of ciprofloxacin and sulfamethoxazole by ferrous-activated persulfate: Implications for remediation of groundwater contaminated by antibiotics, Sci. Total Environ., Volume 472, (2014) Pages 800-808 https://doi.org/10.1016/j.scitotenv.2013.11.008

[33] Kusic, H., Peternel, I., Ukic, S., Koprivanac, N., Bolanca, T., Papic, S., Loncaric Bozic, A. Modeling of iron activated persulfate oxidation treating reactive azo dye in water matrix. Chem. Eng. J., Volume 172, (2011) Pages 109–121 https://doi.org/10.1016/j.cej.2011.05.076

[34] Bu, L., Shi, Z., Zhou, S., Modeling of Fe(II)-activated persulfate oxidation using atrazine as a target contaminant, Sep. Purif. Technol., Volume 169, (2016) Pages 59–65 https://doi.org/10.1016/j.seppur.2016.05.037

[35] Rodriguez, S., Santos, A., Romero, A., Oxidation of priority and emerging pollutants with persulfate activated by iron: Effect of iron valence and particle size, Chem. Eng. J., Volume 318, (2017) Pages 197-205, https://doi.org/10.1016/j.cej.2016.06.057

[36] Kolthoff, I.M., Miller, I.K., 1951. The chemistry of persulfate 1. The kinetics and mechanism of the decomposition of the persulfate ion in aqueous medium. J. Am. Chem. Soc., Volume 73, (1951), Pages 3055-3059, https://doi.org/10.1021/ja01151a024

[37] Liang, C., Wang Z-S., Bruell, C.J., Influence of pH on persulfate oxidation of TCE at ambient temperatures, Chemosphere, Volume 66, Issue 1, (2007) Pages 106-113, https://doi.org/10.1016/j.chemosphere.2006.05.026

[38] Ghauch, A., Tuqan A.M., Kibbi, N., Ibuprofen removal by heated persulfate in aqueous solution: A kinetics study, Chem. Eng. J., Volume 197, (2012) Pages 483–492 http://dx.doi.org/10.1016/j.cej.2012.05.051

[39] Soriano-Molina, P., García Sánchez, J.L., Malato, S., Plaza-Bolaños, P., Agüera, A., Sánchez Pérez, J.A., On the design and operation of solar photo-Fenton open reactors for the removal of contaminants of emerging concern from WWTP effluents at neutral pH, Appl. Catal. B Environ., Volume 256, (2019) 117801 https://doi.org/10.1016/j.apcatb.2019.117801

[40] Bourgin, M., Beck, B., Boehler, M., Borowska, E., Fleiner, J., Salhi, E., Teichler, R., von Gunten, U., Siegrist, H., McArdell, C.S., Evaluation of a full-scale wastewater treatment plant upgraded with ozonation and biological post-treatments: abatement of micropollutants, formation of transformation products and oxidation by-products. Water Res. Volume 129, (2018) Pages 486–498 https://doi.org/10.1016/j.watres.2017.10.036

[41] House, D.A., Kinetics and mechanism of oxidations by peroxydisulfate. Chem. Rev., Volume 62 (3), (1962) Pages 185-203, https://doi.org/10.1021/cr60217a001

[42] Ghauch, A., Tuqan, A.M., Oxidation of bisoprolol in heated persulfate/H_2O systems: kinetics and products, Chem. Eng. J., Volume 183, (2012) Pages 162–171 https://doi.org/10.1016/j.cej.2011.12.048

[43] Zhang, M., Chen, X., Zhou, H., Murugananthan, M., Zhang, Y., Degradation of p-nitrophenol by heat and metal ions co-activated persulfate, Chem. Eng. J., Volume 264, (2015) Pages 39-47, https://doi.org/10.1016/j.cej.2014.11.060

***Declaration of Interest Statement**

Declaration of interests

X The authors declare that they have no known competing financial interests or personal relationships that could have appeared to influence the work reported in this paper.